Aus dem Institut für Mikrobiologie und Hygiene
der Medizinischen Fakultät Charité – Universitätsmedizin Berlin

DISSERTATION

Die Rolle mykobakterieller Nukleotid-Erkennung im Allgemeinen und des SNPs TLR8 A1G im Besonderen bei der humanen angeborenen Immunantwort auf *M. tuberculosis* und deren Einfluss auf Suszeptibilität und Verlauf einer Tuberkulose

zur Erlangung des akademischen Grades
Doctor medicinae (Dr. med.)

vorgelegt der Medizinischen Fakultät
Charité – Universitätsmedizin Berlin

von

Sanne Burkert

aus Rostock

Datum der Promotion: 04.03.2022

Inhaltsverzeichnis

Tabellenverzeichnis

Abbildungsverzeichnis

Abstract

Ein Viertel der Weltbevölkerung ist latent mit *Mycobacterium tuberculosis* infiziert. Trotz dieser hohen Krankheitslast und jahrzehntelanger Forschung ist unser Wissen über die Pathogenese einer aktiven Tuberkulose (TB) noch immer unzureichend. Das angeborene Immunsystem übernimmt eine wichtige Rolle in der Initiierung und Bahnung der Immunantwort, wodurch sich Ansatzpunkte für Diagnostik sowie modifizierende Therapeutika ergeben können. In dieser Arbeit wird der Einfluss von Nukleotidrezeptoren, insbesondere des Toll-like Rezeptors (TLR)8, auf die Suszeptibilität zur Entwicklung einer aktiven TB untersucht. Die Erkennung von endosomaler RNA durch TLR8 in Antigen-präsentierenden Zellen führt über Interleukin (IL)-12, Tumornekrosefaktor α, Interferon (IFN)γ und Typ-I IFN zur Initiierung einer T-Helferzellen (Th)1-Antwort, sowie über IL-21 zur Induktion follikulärer Th (Tfh)-Zellen, welche die humorale Immunantwort unterstützen. Analysen von Single-Nucleotid Polymorphismen (SNPs) in einer indischen TB-Kohorte zeigten, dass Träger des A-Alles von TLR8-A1G eine höhere Suszeptibilität aufwiesen, an TB zu erkranken (*OR* = 1,72 [1,10-2,70], *p* = ,010), sowie ein Rezidiv zu erleiden (*OR* = 2,01 [1,04-3,89], *p* = ,032). Es fand sich eine Interaktion der Bacillus Calmette-Guérin (BCG)-Impfung mit dem SNP, sodass sich im Vergleich der TB-Patienten mit ihren gesunden Haushaltsangehörigen nur unter BCG-Geimpften eine signifikant unterschiedliche Verteilung von TLR8-A1G aufwiesen ließ (*OR* = 2,36 [1,25-4,44], *p* = ,007). Funktionelle Studien ergaben, dass TLR8-1G eine hypermorphe Mutation darstellte, welche zu erhöhten nuclear factor kappa-light-chain-enhancer of activated B-cells (NFκB)-Spiegeln nach TLR8-Stimulation führt. Eine verminderte Zytokinantwort nach endosomaler RNA-Erkennung durch TLR8 scheint damit nachteilig für die Immunantwort zu sein, insbesondere bei BCG-Geimpften.

Weitere statistische Auswertungen der TB-Kohorte erbrachten Evidenz für eine Suszeptibilität für TB vermittelt durch TLR4-399T (*OR* = 1.57 [1.04–2.36], *p* = ,027) durch die Hemmung einer potentiellen Heterodimerisation von TLR4 und -8 an der Position TLR4-C399T, mit der Folge einer verminderten Induktion von Typ-I IFN und Th1-Anwort. Des Weiteren erhöhte das G-Allel des SNP rs311686 des zytosolischen DNA-Rezeptors cyclische GMP-AMP-Synthase (cGAS) die Chance, ein Rezidiv zu erleiden (*OR* = 0,35 [0,20-0,61], *p* < ,001), welcher funktionell ebenfalls den Typ-I IFN-Signalweg affektiert.

Somit lässt sich schlussfolgern, dass die mykobakterielle Nukleotiderkennung eine wichtige Rolle in der Initiierung einer effektiven Immunantwort durch die Stimulation einer Th1-Antwort spielt. Diese wird unterstützt von Typ-I IFN und der Stimulation von Tfh-Zellen, welche daher über die Zell-vermittelte und humorale Immunantwort auch eine Verbindung zum Immungedächtnis darstellen. Durch die hier zusammengefassten Ergebnisse lassen sich potentielle, neue Ansätze für zukünftige Vakzine und Therapeutika ableiten.

Abstract (English)

One quarter of the world's population has latent tuberculosis (TB) caused by asymptomatic infection with *Mycobacterium tuberculosis*. Despite this high burden of disease and research for decades, our knowledge about the pathophysiology remains insufficient. The innate immune system plays a crucial role in the initiation of the immune response, which can be used for diagnostic tools and modifying drugs. This thesis investigates the impact of nucleotide receptors, specifically Toll-like receptor (TLR)8, on the susceptibility to the development of active TB. Recognition of endosomal RNA by TLR8 in antigen-presenting cells leads via interleukin (IL)-12, tumour necrosis factor α, interferon (IFN)γ and type I IFN to the initiation of a T-helper cell (Th)1-response, and via IL-21 to an induction of T follicular helper (Tfh) cells, supporting the humoral immune response. Single-nucleotide polymorphism (SNP) analyses of an Indian cohort showed that individuals carrying TLR8-1A have a higher susceptibility to develop both primary TB (*OR* = 1.72 [1.10-2.70], *p* = .010) and a relapse (*OR* = 2.01 [1.04-3.89], *p* = .032). There was evidence for an interaction with the Bacillus Calmette-Guérin (BCG)-vaccination, as only among BCG-vaccinated individuals there was a difference in the allele distribution between TB patients and their healthy household contacts (*OR* = 2.36 [1.25-4.44], *p* = .007). Functional studies revealed that TLR8-1G was a hypermorphic mutation, leading to higher levels of nuclear factor kappa-light-chain-enhancer of activated B-cells (NFκB) after TLR8-stimulation. Lower cytokine levels after endosomal RNA-recognition therefore seemed to be detrimental for the immune defence against TB, especially in BCG-vaccinated individuals.

Further statistical analyses showed evidence for a susceptibility to TB conveyed by TLR4-399T (*OR* = 1.57 [1.04–2.36], *p* = .027) through inhibition of the potential heterodimerisation of TLR4 and -8, leading to a reduced induction of type I IFNs and a Th1-response. Furthermore, the odds to suffer

from a relapse were higher for the G-allele of the cyclic GMP-AMP-synthase (cGAS)-SNP rs311686 (*OR* = 0.35 [0.20-0.61], $p < .001$), also affecting the type I IFN pathway.

In conclusion, mycobacterial nucleotide recognition seems to play an important role in the initiation of an effective defence against TB by promotion of a Th1-response, supported by type I IFNs, as well as the induction of Tfh-cells, thus linking the immune response both to the cell-mediated and humoral immune system and thereby the immunological memory. The results summarised in this thesis can hence lead to potentially new approaches for vaccinations and future drugs.

1. Einführung

Laut der Weltgesundheitsorganisation sind 2019 1,2 Millionen Menschen weltweit an Tuberkulose (TB) gestorben, womit sie zu den zehn häufigsten Todesursachen weltweit zählt [1]. Der Erreger der TB, *Mycobacterium tuberculosis* (MTB), wurde bereits 1882 von Robert Koch entdeckt. Trotz langjähriger, intensiver Erforschung dieser Erkrankung ist unser Wissen hinsichtlich Pathogenese, Diagnostik und Therapie immer noch unzureichend, sodass in den aktuellen „Sustainable Developement Goals“ der Vereinten Nationen ein besonderes Augenmerk auf TB gesetzt wurde und als explizites Ziel das Ende der TB-Epidemie bis 2030 angestrebt wird [2].

Es wird geschätzt, dass ca. ein Viertel der Weltbevölkerung zwar mit MTB infiziert ist, jedoch keine Krankheitssymptome zeigt, in welchem Fall man von einer latenten TB spricht [3]. In etwa 5-10% entwickelt sich aus einer latenten eine symptomatische Erkrankung. Gründe für diese individuell unterschiedliche Progredienz sind nur unzureichend bekannt, aber neben Umweltfaktoren, Komorbiditäten und Bakterien-spezifischer Virulenzfaktoren scheint die genetische Disposition des Wirts eine wichtige Rolle zu spielen [4].

Für die Generierung einer Immunantwort ist die spezifische Erkennung des Erregers essenziell. Mit dieser Aufgabe sind initial sogenannte Pattern Recognition Receptors (PRR) betraut, zu welchen unter anderem die Toll-like Rezeptoren (TLRs) zählen, die sich durch N-terminalen leucinreichen (LRR)-Sequenzen und die Toll/IL-1R homology domain (TIR)-Domain auszeichnen. TLR8 erkennt endosomal Guanin-Uracil-reiche Einzelstrang (ss)-RNA und ist hauptsächlich in Monozyten und myelotischen Dendritischen Zellen (mDCs) exprimiert. Die Aktivierung des Rezeptors führt zu einer Signalkaskade, an dessen Ende durch den Transkriptionsfaktor nuclear factor kappa-light-chain-

enhancer of activated B-cells (NFκB)-getriggert Tumornekrosefaktor (TNF)-α und Interleukin (IL)-12 stehen, sowie Interferon (IFN) regulatory factor (IFR)-7 vermittelt IFNγ [5]. Durch die Expression in mDCs spielt TLR8 eine Schlüsselrolle in der Verlinkung des angeborenen mit dem erworbenen Immunsystems, da diese Zellen zu den Antigen-Präsentierenden Zellen (APCs) gehören und nach ihrer Aktivierung in die drainierenden Lymphknoten wandern, um dort T-Zellen zu aktivieren.

Seit der Entschlüsselung des menschlichen Genoms lässt die Analyse von Einzelpunkt-Mutationen (single-nucleotide polymorhisms (SNPs)), welche spontan in der Bevölkerung vorkommen und zu leichten Unterschieden in der Funktionsweise der kodierten Proteine führen, Rückschlüsse auf die Bedeutung der jeweiligen Gene in Bezug auf bestimmte Erkrankungen zu. Dieser Ansatz wurde in der vorliegenden Dissertation genutzt, um Erkenntnisse über den Einfluss bestimmter Rezeptoren des angeborenen Immunsystems auf die Pathogenese von TB zu gewinnen. In Bezug auf TB sind bereits mehrere SNPs von TLRs gefunden worden, welche Einfluss auf die Suszeptibilität für eine aktive Erkrankung haben: TLR1, -2, -8, und -9, sowie TIR-Adaptorprotein (TIRAP) [6]. Die vorgelegte Dissertation beschäftigt sich hauptsächlich mit TLR8.

Der SNP rs3764880 von TLR8 führt durch die Mutation von Alanin (A) zu Guanin (G) an der ersten Position der DNA in der Transkription zum Austausch von Valin zu Methionin, und somit zum Fehlen des Start-Codons, wodurch sich der Transkriptionsstart auf das nächste Exon verschiebt und das Protein sich um 3 Aminosäuren verkürzt [7]. TLR8 A1G ist ungleich auf der Welt verteilt: Während in Deutschland laut des Hap-Map-Projektes ca. 30-35% der Bevölkerung die verkürzte Variante (TLR8-1G) tragen, kommt es zu einer progressiven Zunahme von TLR8-1G gen Osten bis hin zu einem 80%igem Anteil von TLR8-1G in Japan. TLR8-1G wurde zuerst in einer indonesischen und russischen, männlichen Kohorte mit einer geringen Suszeptibilität für TB assoziiert [8], sowie mit einer geringeren Progressionsrate einer humanen Immundefizienz-Virus (HIV)-Erkrankung [7]. Des Weiteren wurde es indirekt durch komplettes Linkage Disequilibrium mit dem Promotor-SNP -129 G>C (rs3764879) mit einer geringeren Suszeptibilität für Hepatitis C [9] und anderen intrazellulären Infektionen wie *Helicobacter pylori* [10] und *Borrelia burgdorferi* assoziiert [11]. In einer pakistanischen TB-Kohorte hingegen war TLR8-1G mit einer höheren Suszeptibilität für TB assoziiert [12].

Aus der Identifikation relevanter SNPs von Nukleotid-Rezeptoren für die individuelle TB-Suszeptibilität und Rückschlüssen aus den sich anschließenden funktionellen Analysen wurden in dieser Arbeit wichtige Erkenntnisse über die Pathogenese der TB gewonnen, welche im Folgenden dargestellt sind.

2. Material und Methodik

Zur Erforschung oben genannter Problematik wurden verschiedene Ansätze gewählt: I) die statistische Auswertung epidemiologisch-genetischer Daten einer Kohorte indischer Tuberkulose-Patienten II) die Analyse experimentell gewonnener Daten durch Stimulation von Primärzellen aus dem Blut gesunder Freiwilliger (GF) und III) die Analyse experimentell gewonnener Daten durch Stimulation von Zelllinien nach selektiver Überexpression.

2.1. Genotypisierung und SNP-Analyse der indischen Kohorte

Die Generierung der indischen Kohorte erfolgte als Gemeinschaftsarbeit im Rahmen der internationalen Kooperation des Graduiertenkollegs im Mahavir Hospital. Dies erfolgte unter Zustimmung der Ethikkommission des Mahavir Hospitals in Hyderabad, sowie gemäß der ethischen Prinzipien der Helsinki-Erklärung, und diente bereits als Grundlage verschiedener Publikationen der Mitglieder des Graduiertenkollegs [13–15]. Von eingeschlossenen TB-Patienten wurden nach aufgeklärtem Einverständnis Basis-Charakteristika dokumentiert und Blut vor Beginn der antituberkulösen Therapie gewonnen. Als Einschlusskriterium diente die Diagnose einer pulmonalen (PTB) oder extrapulmonalen TB (EPTB), welche mittels klinischer Untersuchung, Röntgen-Thorax und mikroskopischer Sputumanalyse bzw. einer entsprechenden Biopsie mit histopathologischer Begutachtung gestellt wurde. HIV galt als Ausschlusskriterium. Rezidivfälle wurden als solche gekennzeichnet. Als Kontrollgruppe dienten zum einen die begleitenden Angehörigen der Patienten (gesunde Haushaltsangehörige(GH)), zum anderen eine Gruppe gesunder, nicht dem Haushalt angehöriger Freiwilliger (GNH) aus dem Großraum Hyderabad. Die DNA-Isolierung aus Vollblut erfolgte mittels FlexiGene DNA Kit (Qiagen, India) gemäß dem Hersteller-Protokoll.

Um die SNP-Verteilung zwischen TB-Patienten, GH und GNH zu vergleichen, erfolgte eine Genotypisierung mittels LightCycler Assays (Roche), welcher auf Grundlage einer Polymerase-Kettenreaktion (PCR) floureszensbasierte Schmelzpunktanalysen des Sensor-Anker-Komplexes eine

zielsichere Unterscheidung der Genotypen erlaubt. Anschließend erfolgte die statistische Analyse unter Verwendung von STATA (Version 16). *p*-Werte kleiner 0,05 galten als statistisch signifikant. 95% Konfidenzintervalle der Effektgrößen sind in eckigen Klammern dargestellt, bzw. Interquartilsabstände (IQR) falls indiziert. Basis-Charakteristika wurden mittels *t*-Test trotz einer nicht-normalen Verteilung auf Grundlage des zentralen Grenzwerttheorems mit ausreichend hohen Stichprobenanzahl analysiert. Für kategorische Daten wurde ein χ^2-Test verwendet. Zur Evaluation des Zusammenhangs des Allels- und des Krankheitsstatus wurde ein logistisches Regressionsmodel mit einer *a priori* Adjustierung für Alter und Geschlecht verwendet, in welchem rezessive Genotypen zusammengefasst gegen den dominanten Genotyp verglichen wurden. Mögliche unabhängige Risikofaktoren wurden mit Hilfe des Wald-Tests evaluiert. Potenzielle „Confounder" wurden durch den Vergleich des basalen und des adjustierten Odds Ratios (*OR*) analysiert. Identifizierte „Confounder" und unabhängige Risikofaktoren wurden in das adjustierte Model mit aufgenommen, welches auf kausales Modelling intendierte. Effekt-Modifizierung wurde mittels Likelihood Ratio Tests (LRTs) evaluiert, wie auch die finale Signifikanztestung der untersuchten Einflussfaktoren [16]. Potenzielle Multikollinearität wurde mittels Vergleiches der Standardfehler evaluiert.

2.2.Zellkulturexperimente mit PBMCs

Für funktionelle *in-vitro* Analysen des angeborenen Immunsystems eignen sich Experimente mit einkernigen peripheren Blutzellen, sogenannten PBMCs (periphere blood mononuclear cells), dessen größter Anteil Monozyten, die Vorläuferzellen von Makrophagen, darstellen. Unter der Zustimmung der Ethikkommission der Charité wurden aus Wangenabstrichen von Freiwilligen in Berlin entsprechend des Herstellerprotokolls des DNA blood mini kit (Qiagen, Deutschland) DNA isoliert und anschließend per LightCycler Assay genotypisiert. Auf Grundlage des entsprechenden Genotyps von TLR8 A1G wurden PBMCs aus Vollblut mittels Lymphozyten Seperationsmedium (LSM 1077, GE Healthcare, Deutschland), basierend auf einer Dichtezentrifugation, isoliert und auf Zellkulturplatten übertragen. Die Stimulation erfolgte mit dem TLR8-Agonisten CLO75 (1µg/ml), Lipopolysaccharid (LPS, 10ng/µl) oder mykobakterieller RNA (1µg/ml), welche aus gamma-bestrahlten Zellen von MTB H37Rv (BEI Resources, USA, NR-14819) mittels InnuPrep RNA Mini Kit (Analytik Jena, Deutschland) extrahiert und mit dem liposomalen Transfektionsreagenz DOTAP (Roche, Deutschland) nach Herstellerprotokoll 1:5 komplexiert wurde, um einen endosomalen

Transport sicher zu stellen. Für eine Hemmung der endosomalen Azidifikation wurden Zellen ggf. 1h mit Bafilomycin vorbehandelt. In den Stimulationsüberständen wurde nach 4h mit Hilfe eines Enzyme-linked Immunosorbent Assay (ELISA) mit spezifischen Antikörpern für TNFα (BD Pharmingen, Deutschland: 551220, 554511), sowie nach 24h für Il12p40 (BD Pharmingen: 551227, 554660) die Reaktivität bestimmt. Die statistische Auswertung der unterschiedlich stark exprimierten Zytokine erfolgte unter Nutzung von R (Version 4.0.1) mittels eines Mann-Whitney-U-Tests, sofern keine gruppenspezifische Normalverteilung (beurteilt mit dem Shapiro-Wilk Test) und keine Homogenität der Varianz (beurteilt anhand der *F*-Statistik) vorlag, in welchem Fall ein *t*-Test angewandt wurde. Die graphische Auswertung erfolgte mit GraphPad PRISM (Version 5.01).

2.3.Zellkulturexperimente mit HEK Zellen

Human embryonic kidney (HEK)-Blue Null-1-Reporter Zellen (Invivogen, Deutschland) gehören zu einer humanen Zelllinie aus embryonalen Nierenzellen, welche sich durch die Abstinenz von TLRs auszeichnet, wodurch sich die Erforschung derselben durch spezifische Transfektion und Überexpression ermöglicht. Zur genaueren Analyse der funktionellen Auswirkung des SNPs TLR8-A1G erfolgte eine entsprechende Mutagenese des Plasmids hTLR8-pUno3 (Invivogen, Deutschland) mittels des QuikChange II XL Site-Directed Mutagenesis Kit (Agilent Genes, Deutschland) nach Herstellerangaben unter der Verwendung folgender Primer, die mit dem PrimerX-Programm generiert wurden: vorwärts (GAGATCACCGGTCACCGTGGAAAACATGTTC), rückwärts (GGAACATGTT-TTCCACGGTGACCGGTGATCTC). Hierauf folgte der Maxi Prep beider Plasmid-Varianten mittels des Plasmid Maxi Kit (Qiagen, Deutschland) und DH5α *E. coli* (Promega, Deutschland) und deren Überprüfung durch DNA-Sequenzierung (Eurofins, Deutschland) unter Verwendung des Primers CTGTAGTCGACGATTGCTGC, entworfen mit Primer3 (Version 0.3.1). Im Anschluss erfolgte eine stabile Transfektion der HEK-Blue-Zellen durch Selektion mittels Blastizidin. Diese selektiv TLR8-überexprimierenden Zellen wurden mit TLR8-Agonisten oder LPS stimuliert und die Reaktion durch die intrinsische Kopplung der sezernierten Alkalischen Phosphatase (SEAP) an eine NFκB-Aktivierung mittels einer Farbreaktion des HEK Blue Detection Mediums (Invivogen, Deutschland) quantifiziert. Nach Normalisierung gegen die Stimulation mit Medium erfolgte die statistische Auswertung nach Testung auf Normalverteilung mittels des Shapiro-Wilks-Testes mit *t*-Tests, unter Nutzung von R (Version 4.0.1.). Die graphische Auswertung erfolgte mit GraphPad PRISM (Version 5.01). Die

etablierte Zelllinie HEK-Blue Null-1 mit dem SEAP-Reporter-Gene-Assay wurde ebenfalls erfolgreich für funktionelle Studien an TLR1 [13] und TLR4 [14,17] genutzt.

3. Ergebnisse

3.1. TLR8 A1G

3.1.1. TLR8 A1G-Verteilungsanalysen der indischen Kohorte

Die indische Kohorte wurde zu verschiedenen Zeitpunkten analysiert, sodass assoziierte publizierte Ergebnisse unterschiedliche Fallzahlen aufweisen. Die hier verwendete Kohorte umfasste 722 Individuen, wovon 282 GF waren (101 GNH und 181 GH), 345 TB-Primärfälle (224 PTB- und 121 EPTB-Patienten) und 95 Rezidiv-Fälle. Die TB-Patienten waren im Median (*Mdn*) jünger (23 Jahre) als die GF (32 Jahre, $t(574) = 8{,}72$, $p < {,}001$) und Rezidivfälle (28 Jahre, $t(398) = -4{,}07$, $p < {,}001$; Tabelle 1). Der Frauenanteil überwog sowohl unter den primären TB-Fällen (61,45 %), als auch unter den Rezidivfällen (52,63 %) und den GH (58,56 %), während sich unter den GNH mehr Männer fanden (54,46 %). Der Unterschied in der Geschlechterverteilung war nicht signifikant zwischen den TB-Patienten und ihren GH ($\chi^2(1) = 0{,}41$, $p = {,}520$) oder den Rezidivfällen ($\chi^2(1) = 0{,}41$, $p = {,}520$). Primäre TB-Patienten hatten im *Mdn* einen niedrigeren Body-Mass-Index (BMI) als die GF (16,9 mg/kg² vs. 23,9 mg/kg², $t(571) = 17{,}08$, $p < {,}001$), und PTB-Patienten einen niedrigeren BMI als EPTB-Patienten (15,9 mg/kg² vs. 20,0 mg/kg², $t(301) = 7.61$, $p < {,}001$). Rezidiv-Fälle zeigten einen medianen BMI ähnlich der PTB-Fälle (16,1 mg/kg², $t(259) = 0.19$, $p = {,}850$). Hinsichtlich der BCG-Impfung waren die primären TB-Patienten seltener geimpft (48,84 %) als ihre Verwandten (73,86 %, ($\chi^2(1) = 28{,}61$, $p < {,}001$). Die GNH waren zu 100 % geimpft. Patienten mit PTB im Vergleich zu EPTB wiesen einen nicht signifikant geringeren Anteil an Geimpften auf (44,4 % vs. 51,6 %, $\chi^2(1) = 1{,}48$, $p = {,}224$). Bei den Rezidiv-Fällen war der Anteil im Vergleich zu primären TB-Fällen ebenfalls nicht signifikant geringer (36,92 %, $\chi^2(1) = 3{,}06$, $p = {,}080$).

In Bezug auf die Verteilung des SNPs TLR8 A1G zeigte sich, dass TB-Patienten eine signifikant höhere Frequenz des A-Allels (Allelfrequenz p(A) = ,44) im Vergleich zu GF aufwiesen ($p(A) = {,}35$, $\chi^2(1) = 9{,}59$, $p = {,}002$). Auch der Vergleich von TB-Patienten und ihren GH ($p(A) = 0{,}34$) ergab ähnliche Ergebnisse

Tabelle 1. Basis-Charakteristika der generierten Kohorte aus primären Tuberkulose (1° TB)-Patienten, bestehend aus Fällen von pulmonaler (PTB) und extrapulmonaler (EPTB) TB, sowie gesunden Freiweilligen (GF), bestehend aus gesunden Haushaltangehörigen (GH) und gesunden, nicht dem Haushalt angehörigen Freiwilligen (GNH), sowie TB-Rezidiv-Fälle (2° TB). *N* = Stichprobenanzahl (prozentualer Spaltenanteil)

Variable (*N*)		**GF (*N* in %)**	**GNH (*N* in %)**	**GH (*N* in %)**	**1° TB (*N* in %)**	**PTB (*N* in %)**	**EPTB (*N* in %)**	**2° TB (*N* in %)**
***N* (722)**		282	101	181	345	224	121	95
Alter (668)	[Jahre]*	32 [26-40]	32 [24-37]	32 [27-40]	23 [18-30]	23 [18-30]	24 [17-30]	28 [22-39]
BMI (648)	[mg/kg²]*	23,9 [21,0-27,2]	25,3 [22,0-29,0]	23,3 [20,3-26,4]	16,9 [15,01-19,4]	15,9 [14,4-18,1]	19,0 [16,6-22,7]	16,1 [14,7-18,3]
Geschlecht (722)	weiblich	152 (53,90)	46 (45,54)	106 (58,56)	212 (61,45)	130 (58,04)	82 (67,77)	50 (52,63)
	männlich	129 (46,1)	55 (54,46)	75 (41,44)	134 (38,73)	94 (41,96)	39 (32,23)	45 (47,37)
BCG-Status (637)	nicht geimpft	46 (17,10)	0 (0)	46 (26,14)	155 (51,16)	90 (48,39)	65 (55,56)	41 (63,08)
	geimpft	223 (82,90)	93 (100)	130 (73,86)	148 (48,84)	96 (51,61)	52 (44,44)	24 (36,92)
TLR8 A1G (705)	A/AA	62 (22,71)	27 (27,00)	35 (20,23)	96 (28,32)	60 (27,40)	36 (30,25)	46 (48,94)
	AG	66 (24,18)	20 (20,00)	46 (26,59)	103 (30,38)	64 (29,22)	39 (32,77)	22 (23,40)
	G/GG	145 (53,11)	53 (53,00)	92 (53,18)	140 (41,30)	95 (43,38)	44 (36,97)	26 (27,66)

*für Alter und BMI sind der Median [IQR] dargestellt.

Tabelle 2. Logistisches Regressionsmodell für TB-Primärfälle im Vergleich zu gesunden Freiwilligen (Stichprobenanzahl *N* = 556). *OR* = Odds Ratio, CI = Konfidenzintervall, *SE* = Standardfehler

Variable	***OR* [95% CI]**	***SE***	***p***
TLR8 A1G	1,72 [1,10-2,70]	0,40	,017
Alter	0,98 [0,96-1,00]	0,01	,101
BMI	0,76 [0,72-0,8]	0,02	<,001
Geschlecht	0,75 [0,47-1,18]	0,17	,214
BCG-Status	0,36 [0,23-0,58]	0,09	<,001

Tabelle 3. Effektmodifikation der BCG-Impfung auf den Einfluss von TLR8 A1G auf den Tuberkulose (TB)-Status im logistischten Regressionsmodel zwischen TB-Patienten und ihren gesunden Haushaltsangehörigen (GH), pulmonaler (PTB) und extrapulmonaler (EPTB) TB, sowie primären TB und Rezidiv-Fällen, adjustiert für Alter, BMI und Geschlecht. In Teilen Modifiziert aus [18] Supp. Tab. 4. *N* = Stichprobenanzahl, *OR* = Odds Ratio, CI = Konfidenzintervall, *SE* = Standardfehler

Untergruppen	**BCG-Status**	***OR* [95% CI] für TLR8-1A**	***SE***	***p***
GH vs. TB	alle	1,72 [1,06-2,78]	0,42	,027
	positiv (N=268)	2,36 [1,25-4,44]	0,76	,007
	negativ (N=196)	1,02 [0,45-2,11]	0,02	,947
PTB vs EPTB	alle	1,21 [0,70-2,10]	0,34	,500
	positiv (N=146)	0,55 [0,25-1,25]	0,23	,151
	negativ (N=150)	2,36]1,07-5,21]	0,95	,032
Primär-TB vs. Rezidiv	alle	2,01 [1,04-3,89]	0,68	,032
	positiv (N=168)	1,37 [0,50-3,78]	0,71	,536
	negativ (N=187)	2,67 [1,10-6,47]	1,20	,023

($\chi^2(1) = 9{,}50$, $p = ,002$). GNH ($p(A) = ,37$) und GH unterschieden sich in ihrer Allel-Frequenz von TLR8-1A nicht signifikant ($\chi^2(1) = 0{,}67$, $p = ,412$), wie sich auch pulmonale ($p(A) = ,42$) von extrapulmonalen ($p(A) = ,47$) TB-Patienten nicht unterschieden ($\chi^2(1) = 1{,}34$, $p = ,246$). Adjustiert für Alter, Geschlecht, BMI und BCG-Status zeigte sich mit guter Evidenz, dass Träger des A-Allels von TRL8-A1G eine 1,7-fach erhöhte Chance aufwiesen, an TB erkrankt zu sein (*OR* = 1,72 [1,10-2,70], $p = ,010$, Tabelle 2). Es gab schwache Evidenz für eine Effekt-Modifikation des BCG-Status und TLR8 A1G (*OR* = 0,46 [0,20-1,05], LRT = 3,42, $p = ,065$, Tabelle 3, in Teilen modifiziert aus [18] ‚Supplementary Table 4'). Um dies weiter zu untersuchen, wurden aufgrund unterschiedlicher Impfraten der GH und GNH nur die GH mit den TB-Patienten verglichen. Hierbei zeigte sich zunächst, dass auch in diesem Vergleich die Chance, als Träger des A-Allels an TB erkrankt zu sein, 1,7-fach erhöht war (*OR* = 1,72 [1,06-2,78], $p = ,027$). Betrachtete man ausschließlich BCG-Geimpfte, zeigten Träger des A-Alles von TLR8-A1G eine 2,4-fach erhöhte Chance, an TB zu erkranken (*OR* = 2,36 [1,25-4,44], $p = ,007$). Unter den Nicht-Geimpften fand sich kein signifikanter Einfluss der Punktmutation (*OR* = 1,02 [0,45-2,11], $p = ,947$).

Im Vergleich von PTB- mit EPTB-Fällen ließ sich, mit guter Evidenz, eine Interaktion zwischen der BCG-Impfung und TLR8-A1G nachweisen (*OR* = 4,07 [1,53-10,83], LRT = 8,02, $p = ,005$): Unter den Geimpften ergab sich kein signifikanter Unterschied, hingegen hatten unter den Nicht-Geimpften Träger des A-Allels ein höheres Risiko, an EPTB als an PTB zu erkranken (*OR* = 2,36 [1,07-5,21], $p = ,032$). In der Analyse der Rezidivfälle im Vergleich zu primären TB-Fällen zeigte sich, dass Träger des A-Allels eine höhere Chance hatten, ein Rezidiv erlitten zu haben (*OR* = 2,01 [1,04-3,89], $p = ,032$, Tabelle 4). Nicht BCG-geimpft zu sein war ein weiterer Risikofaktor (*OR* = 0,46 [0,24-0,87], $p = ,017$). Zwar gab es keinen Hinweis auf eine Interaktion zwischen der BCG-Impfung und TLR8 A1G im Vergleich zwischen primären und rezidivierten TB-Fällen (*OR* = 0,74 [0,22-2,54], LRT = 0,22, $p = ,636$), jedoch hatten unter den nicht-Geimpften ein höherer Anteil das A-Allel für TLR8 A1G als die Primärfälle (*OR* = 2,67 [1,10-6,47], $p = ,023$). Unter den Geimpften zeigten sich keine signifikanten Unterschiede (*OR* = 1,37 [0,50-3,78], $p = ,536$).

Somit lässt sich insgesamt hinsichtlich des Einflusses von TLR8 A1G auf TB ableiten, dass Träger des A-Allels eine höhere Suszeptibilität haben, an einer aktiven TB zu erkranken. Bei genauerer Betrachtung, galt dies jedoch nur für BCG-Geimpfte. Nicht-Geimpfte mit TLR8-1A hingegen wiesen eine höhere Chance für eine extrapulmonale Manifestation, sowie für ein Rezidiv auf.

Tabelle 4. Logistisches Regressionsmodell für TB-Rezidivfälle im Vergleich zu primären TB-Fällen (Stichprobenanzahl *N* = 355). *OR* = Odds Ratio, CI = Konfidenzintervall, *SE* = Standardfehler

Variable	*OR* [95% CI]	*SE*	*p*
TLR8 A1G	2,01 [1,04-3,89]	0,68	,032
Alter	1,06 [1,04-1,09]	0,02	<,001
BMI	0,82 [0,73-0,91]	0,05	<,001
Geschlecht	1,70 [0,89-3,28]	0,59	,110
BCG-Status	0,46 [0,24-0,87]	0,15	,017

3.1.2. Zellkulturexperimente mit PBMCs

Um den Einfluss von TLR8 A1G funktionell zu untersuchen, wurden PBMCs, welche sich hinsichtlich des Allel-Status von TLR8 A1G unterschieden (*N*(A/AA) = 18, *N*(AG) = 10, *N*(G/GG) = 24), mit dem TLR8-Agonisten CLO75, mykobakterieller RNA und LPS stimuliert. Der Vergleich der TNFα-Spiegel von PBMCs nach Stimulation mit CLO75 zeigte keine Evidenz für signifikante Unterschiede der Genotypen (Abb. 1A, exemplarisch für 0,3 µg/ml: *Mdn*(A/AA) = 764,4 pg/ml, IQR [615,1-,774,4] vs. *Mdn*(G/GG) = 245,8 pg/ml, IQR [215,9-624,2], *U* = 54,4, *p* = ,160), wie auch, wie erwartet, für LPS. Die Stimulation mit mykobakterieller RNA ergab eine schwache Evidenz, dass homozygote Träger des A-Allels mehr TNFα sezernierten (*Mdn* = 456,0 pg/ml, IQR [212,77-819,75]) als homozygote Träger des G-Alles (*Mdn* = 213,7 pg/ml, IQR [105,4-428,3], *U* = 242, *p* = ,053; Abb. 1C). Nach Hinzugabe von RNAse war keine Stimulation mehr nachweisbar. Zur Überprüfung der endosomalen Stimulation wurde der Endosomen-Inhibitor Bafilomycin eingesetzt, wonach ebenfalls keine TNFα-Induktion durch RNA und CLO75 mehr nachweisbar war. Als weiteres „Read-Out“ wurde Il12p40 gewählt, wonach sich keine signifikanten Unterschiede als Reaktion auf CLO75 (Abb. 1B modifiziert aus [18] ‚Supplementary Figure 8‘, exemplarisch für 0,3 µg/ml: (*Mdn*(A/AA) = 881,0 pg/ml, IQR [616,4-1094,6], *Mdn*(G/GG) = 655,7 pg/ml, IQR [483,0-867,0], *U*(A/AA vs. G/GG) = 26, *p* = ,699) oder komplexierte RNA (*Mdn*(A/AA) = 283,2 pg/ml, IQR [76,2-545,2], *Mdn*(G/GG) = 488,00 pg/ml, IQR [131,5-591,5], *U*(A/AA vs. G/GG)=17, *p* = ,519, Abb. 1D modifiziert aus [18] ‚Supplementary Figure 8‘) ergaben.

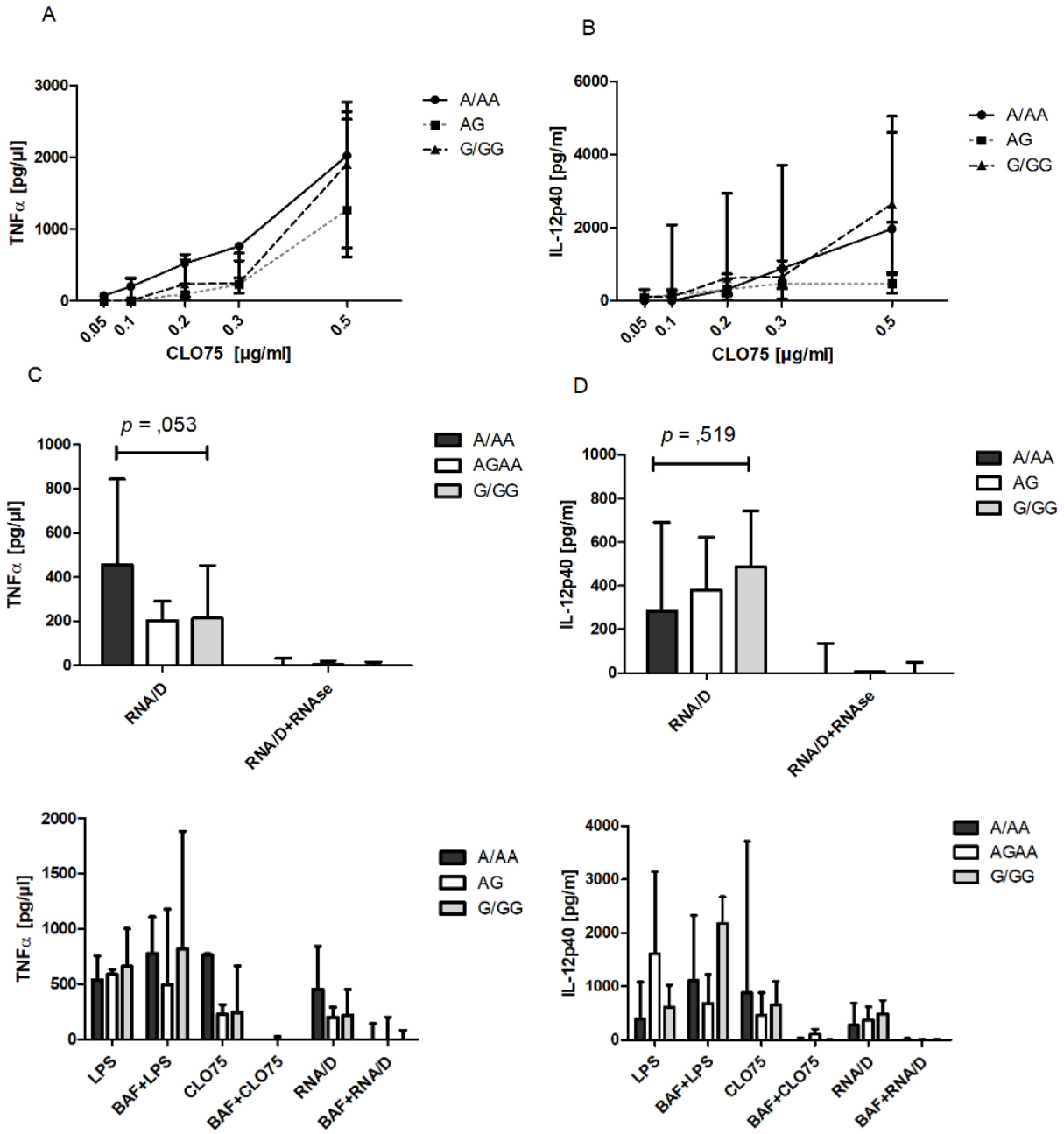

Abb. 1. Funktionelle Studien zu Toll-like Rezeptor (TLR)-8 A1G in mononukleären Zellen des peripehren Blutes (PBMCs, *N*(A/AA) = 18, *N*(AG) = 10, *N*(G/GG) = 24). **A,C,E** Konzentration von Tumornekrosefaktor (TNF)-α wurden 4h nach Stimulation gemessen. **B,D,F** Konzentrationen von Interleukin (IL)-12p40 wurden 24h nach Stimulation gemessen, modifiziert aus [18] ‚Supplementary Figure 8'. **A-B** Nach Stimulation mit verschiedenen Konzentrationen mit CLO75 unterschieden sich die unterschiedlichen Genotypen nicht signifikant in TNFα- (**A)** oder IL12p40-Spiegeln (**B**). **C-D** PBMCs mit TLR8 A/AA zeigten höhere TNFα-Spiegel nach RNA-Stimulation (1µg/ml komplexiert mit DOTAP (RNA/D) als GG/G (nach Stimulation mit verschiedenen Konzentrationen mit CLO75 **(C)**, jedoch keinen Unterschied in IL12p40 (**D**). Behandlung mit RNAse führte zum Verlust der TNFα- und IL12p40-Induktion. **E-F** Nach Bafilomycin (BAF)-Vorbehandlung zeigten PBMCs stimuliert mit 10ng/ml Lipopolysachharid (LPS) höhere TNFα-Spiegel als ohne, vor allem für Genotyp G/GG, (**E)**. TNFα-Induktion durch 0,3µg/ml CLO75 oder 1µg/ml RNA/D wurde durch Bafilomycin unterbunden. In Hinblick auf IL12p40 zeigten sich ebenfalls durch Vorbehandlung mit Bafilomycin vor allem für den Genotyp G/GG eine höhere Sekretion nach Stimulation mit LPS, jedoch eine Unterdrückung der Sekretion nach CLO75- oder RNA/D-Stimulation **(F**). Abbildungen zeigen Mittelwerte gemessener Zytokine +/- Standardabweichung.

3.1.3. Zellkulturexperimente mit HEK-Zellen

Im Vergleich zu PBMCs, welche eine Vielzahl von Zellen mit unterschiedlich exprimierten Immunrezeptoren darstellen, lässt sich im HEK-System ein reineres Signal des zu untersuchenden Rezeptors erwarten. Nach Etablierung des Reportersystems in der stabil transfizierten Zelllinie zeigte sich eine höhere NFκB-Aktivität (Abb. 2 modifiziert aus [18] ‚Supplementary Figure 8') in TLR8-1G transfizierten Zellen im Vergleich zu TLR8-1A nach Stimulation mit den TLR8-Agonisten CLO75 (Mittelwert (*M)* -1G = 3,20; Standardabweichung (*SD)* -1G = 0,32; *M*(A) = 2,23, *SD*(A) = 0,37; *t*(9) = -4,80, *p* < ,001) und R848 (*M*(G) = 3,02, *SD*(G) = 0,26; *M*(A) = 2,09, *SD*(A) = 0,29; *t*(9) = -5,95, *p* < ,001). Für LPS zeigte sich keine relevante NFκB-Induktion (*M* = 1,02, *SD* = 0,07). Nach Stimulation mit mykobakterieller RNA kam es zwar zu einer relevanten Expression von NFκB, Unterschiede zwischen den Genotypen waren jedoch nicht signifikant (*M*(G) = 2,10, *SD*(G) = 0,33; *M*(A) = 2,17, *SD* = 0,20; *t*(7) = 0,37, *p* = ,724).

3.2. Interaktion von TLR4 und -8

Durch die statistische Auswertung der TB-Kohorte ergaben sich weitere Ansatzpunkte zur Erforschung der Auswirkung angeborener Immunrezeptoren in der Pathogenese der TB. Es zeigte sich überraschenderweise, dass TLR4-399T mit einer Suszeptibilität für TB assoziiert was (*OR* = 1.57 [1.04–2.36], *p* = ,027), obwohl für MTB kein eindeutiger Agonist für TLR4 beschrieben ist [17]. Weitere Analysen ergaben, dass die Suszeptibilität von TLR8-1A nur für Individuen mit TLR4-399T nachzuweisen war (*OR* = 1,97 [1,15-3,37], *p* = ,013), aber nicht mit TLR4-399C (*OR* = 1,19 (0,52-2,72), *p* = ,681, Vergleich auch [17] Tabelle 1). Funktionelle Studien zeigten, dass es durch eine Hemmung von TLR8 mittels Bafilomycin zu einer stärkeren TLR4-Responsitvität gemessen an TNFα- (Abb. 1E, in der gesamten Kohorte: ohne Bafilomycin *Mdn* = 596,0 pg/ml, IQR [354,0-774,9], mit Bafilomycin *Mdn* = 777,5 pg/ml, IQR [408,6-1367,9], U = 344, *p* = ,001) und IL-12-Spiegeln (Abb. 1F modifiziert aus [18] ‚Supplementary Figure 8', in der gesamten Kohorte: ohne Bafilomycin *Mdn* = 554,8 pg/ml, IQR [346,4-978,7], mit Bafilomycin *Mdn* = 1241,0 pg/ml, IQR [690,1-2289,9], U = 66, *p* = ,020) kam. Somit lässt sich insgesamt ein indirekter Effekt von TLR4-C399T auf TB durch die Interaktion von TLR4 und -8 vermuten.

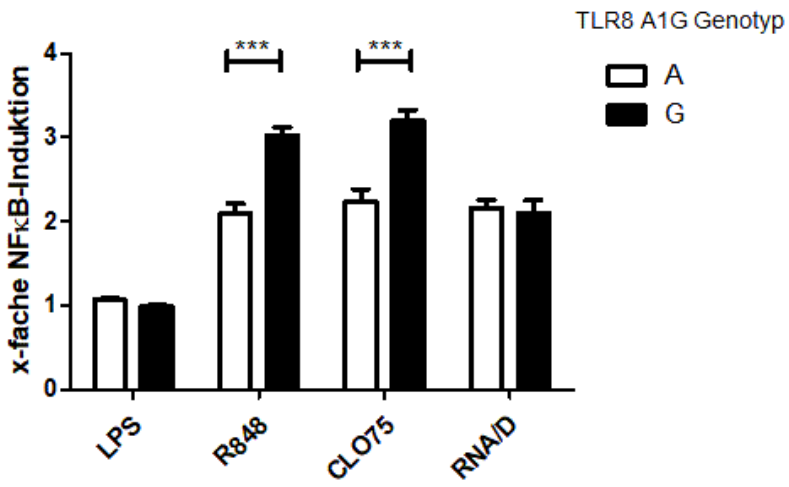

Abb. 2. **Funktionelle Studien von Human embryonic kidney (HEK)-Blue Null-1-Reporter Zellen**, welche sich im Genotyp von Toll-like Rezeptor (TLR)-8 A1G unterschieden (pro Genotyp *N* = 6). Nach Stimulation mit 100ng Lipopolysaccharid (LPS), 1µg/ml R848, 1µg/ml CLO75 oder 1µg/ml mykobakterieller RNA komplexiert mit DOTAP (RNA/D) wurde die NFκB-Induktion bestimmt, durch Division mit der Negativkontrolle normalisiert und deren Mittelwerte mit Standardfehler dargestellt. TLR8-1A zeigte eine geringere Induktion als -1G für synthetische TLR8-Agonisten. Abbildung modifiziert aus [18] ‚Supplementary Figure 8'. *** *p*<,001

3.3. Zytosolische DNA-Rezeptoren

Des Weiteren wurde die beschriebene indische TB-Kohorte genutzt, um Mutationen der zytosolischen DNA-Rezeptoren cyclische GMP-AMP-Synthase (cGAS) und Stimulator of interferon genes (STING) zu untersuchen, dessen statistische Auswertung Teil dieser Doktorarbeit war. Für die Mutation cGAS rs311686 (A>G) zeigte sich, dass Träger des G-Allels eine geringere Chance hatten, an einem Rezidiv zu erkranken (*OR* = 0,35 [0,20-0,61], *p* < ,001, adjustiert für Alter, Geschlecht, BMI und BCG-status)[14]. Es zeigte sich außerdem, dass Träger des G-Allels ein geringeres Risiko hatten, an einer EPTB zu leiden (*OR* = 0,55 [0,31-0,98], *p* = ,041; adjustiert für Alter, BMI, Geschlecht und BCG). In Bezug auf STING fand sich ein komplettes Linkage-Desequilibrium, sodass exemplarisch die Auswertung für STING-G230C (rs78233829) erfolgte, für welchen SNP sich eine schwache Evidenz dafür zeigte, dass weibliche TB Patienten häufiger das C-Allel aufwiesen als ihre gesunden Verwandten (*OR* = 1,55 [0,96-2,50], *p* = ,068; adjustiert für Alter, Geschlecht, BMI und BCG-Status).

4. Diskussion

Ziel dieser Arbeit war es, SNPs von Nukleotid-Rezeptoren im Allgemeinen und TLR8 im Besonderen hinsichtlich ihres Einflusses auf die Krankheitssuszeptibilität von TB zu untersuchen, um neue Erkenntnisse über die Pathogenese zu gewinnen. Durch das signifikant häufiger vorkommende TLR8-

1A-Allel bei TB-Patienten, welches zugleich die funktionell weniger responsive Variante darstellt, lässt sich ableiten, dass eine gesteigerte TLR8-Aktivität mit einem Vorteil gegenüber eine TB-Erkrankung einherzugehen scheint. Des Weiteren konnte Evidenz dafür gefunden werden, dass TLR4-399T über Interaktion mit TLR8 ebenfalls mit einer Suszeptibilität für TB assoziiert ist. Auch für die zytoplasmatische DNA-Erkennung ließ sich ein Unterschied in der SNP-Verteilung von cGAS rs311686 dahingehend finden, dass Rezidiv- und extrapulmonale TB-Fälle weniger häufig das G-Allel trugen. Somit lässt sich insgesamt eine wichtige Rolle der Nukleotiderkennung in der Immunabwehr gegen MTB annehmen.

Der hier berichtete Effekt des SNP TLR8-1A für eine TB-Suszeptibilitätstimmt mit Ergebnissen aus einer indonesischen und russischen Kohorte überein [8], welcher mittlerweile auch in moldawischen, türkischen und indischen Kohorten [19–21] bestätigt wurde. Konträr dazu wurde in einer pakistanischen und chinesischen Studie eine assoziierte Suszeptibilität für TLR8-1G berichtet [9,12], wofür sich momentan kein adäquater Erklärungsansatz findet. In HIV-Studien konnte bereits gezeigt werden, dass die kürzere Variante des Rezeptors funktionell zu einer stärkeren Immunantwort führt [7]. Dies konnte diese Arbeit mittels stabil transfizierter HEK-Zellen bestätigen, wenngleich auch nur für die synthetischen TLR8-Liganden CL075 und R848, aber nicht spezifisch für mykobakterielle RNA. Die Stimulation mit RNA verlangt jedoch zur endosomalen Stimulation ein weiteres Transfektionsmedium, was zusätzlichen Stress für die bereits transfizierten Zellen mit sich bringt und etwaige Unterschiede überschatten könnte. In PBMCs ließ sich im Gegensatz zu den HEK-Zellen und bisherigen publizierten Daten ein geringgradige Hyperreagibilität finden, gemessen an der NFκB-Aktivierung von TLR8-1A im Vergleich zu -1G nach Stimulation mit mykobakterieller RNA, jedoch nicht mit CL075. Dies kann ein falsch positives Ergebnis darstellen, möglicherweise verursacht durch zum einen andere, hier nicht untersuchte genetische Unterschiede zwischen den Spendern und zum anderen durch einen unterschiedlichen Anteil an Monozyten in den isolierten PBMCs, der bei Gesunden zwischen 2-6 % variieren kann. Dieser Anteil wurde in dieser Arbeit nicht quantifiziert, da Experimente mit isolierten Monozyten aufgrund der geringen Ausbeute aus PBMCs eine quantitative Herausforderung darstellen. Stattdessen wurde IL-12 als weiteres „read-out“ gewählt, dessen Ursprung in PBMCs Monozyten darstellen. Hier ließen sich keine signifikanten Unterschiede

zwischen den Genotypen finden. Insgesamt lässt sich auch ohne nachweisbaren Unterschied in PBMCs ein funktionaler Mehrgewinn von TLR8-1G gegenüber -1A annehmen.

Modelling kann als Erklärungsansatz für diesen funktionellen Unterschied dienen, da die Konformationsänderung von TLR8-1G zu einer Zunahme an freier Energie und Flexibilität führt, sowie zu größeren Bindungstaschen und damit möglicherweise zu einer besseren Ligandenbindung [18]. Des Weiteren gibt es Hinweise, dass TLR8-A1G mit einem Promoter-SNP gelinkt ist, welcher ebenfalls zu einer höheren Promoteraktivität führt kann [22].

Im Hinblick auf die sich anschließende Immunantwort konnte gezeigt werden, dass die Aktivierung von TLR8 in APCs einen wichtigen Unterschied in der ausgelösten Signalkaskade des angeborenen Immunsystems darstellt. Auf Grund der ubiquitär vorkommenden RNAsen dient das Vorhandensein bakterieller RNA in Endosomen als Indikator bakterieller Viabilität. RNA, wie auch zytosolische DNA, stellt somit ein wichtiges sogenanntes „Vita-PAMP“ dar, welches das angeborene Immunsystem dahingehend modifiziert, dass eine Aktivierung über die Stimulation von NFκB, IL-12 und Typ-I IFN zur Induktion der T Helferzellen (Th)-1 Antwort führt [6]. Dieser Mechanismus kann auch eine Erklärung für die bereits lang bekannten, aber bisher unzureichend verstandene höhere Effizienz von Lebend- gegenüber Totimpfstoffen liefern. Insbesondere IL-12 als Schlüsselzytokin nach endosomaler RNA-Erkennung spielt noch eine weitere wichtige Rolle, indem es konsekutiv über IL-21 follikuläre Th-Zellen (TfH)-Zellen stimuliert [18]. TfH-Zellen helfen B-Zellen im Antikörper-Switch von IgM zu IgG und unterstützen somit die humorale Immunantwort. Klassischerweise gilt die humorale Immunantwort gegen TB als vernachlässigbar, aber Mäuse, welche kein IL-21 oder IL-21-Rezeptor exprimieren können und somit eine geschwächte TfH-Antwort haben, wiesen eine höhere Mortalität für TB auf [23,24]. Des Weiteren wurde unter exponierten chinesischen Mitarbeitern des Gesundheitswesen protektive IgA-Antikörper gegen TB gefunden [25], sodass diese These zur Diskussion steht.

Die funktionale Verbindung von TLR8 und TfH-Zellen erklärt potentiell den in dieser Arbeit herausgearbeiteten Effekt, dass die TLR8-1A vermittelte Suszeptibilität für TB nur in der Subgruppe der BCG-geimpften statistisch signifikant blieb, sich also ein indirekter Effekt des Rezeptors auf TB über die Impfung ableiten lässt. BCG ist die weltweit am häufigsten angewandte Lebendimpfung, für

welche jedoch sehr unterschiedliche Effektivitätswerte angegeben wurden [26]. Neben den bisher postulierten Einflussfaktoren der allgemeinen Mykobakterienlast in der Umwelt können entsprechend der Ergebnisse dieser Arbeit eventuell auch populationsbasierte, genetische Unterschiede im Signalweg der mykobakteriellen RNA-Erkennung eine Rolle spielen. Eine weitere klinische Bedeutung der RNA-Erkennung als Trigger der Immunmodifikation lässt sich in der Überwindung des Nachteils der Totimpfstoffe durch Hinzunahme von TLR8-Agonisten als Adjuvans hypothesieren. IL-12 als Adjuvans beispielsweise hat allerdings bisher nicht zum Erfolg geführt, auch wenn die gemessene Th1-Antwort erhöht war [27].

Bezüglich der Pathogenese von pulmonaler oder extrapulmonaler Manifestationen einer TB ist neben einem jungen Alter und einer Immunsuppression, welches Letzteres begünstigt, wenig über Risikofaktoren oder immunologische Determinanten bekannt. In der in dieser Arbeit untersuchten Kohorte hatte sich gezeigt, dass konträr zur BCG-abhängigen TLR8-1A-Suszeptibilität für TB insgesamt, bezüglich einer EPTB im Vergleich zur PTB TLR8-1A nur mit einer Suszeptibilität in der Subgruppe der Ungeimpften assoziiert war. Selbiges Muster fand sich bei den Rezidivfällen. Geimpfte mit TLR8-1A hatten somit zwar primär ein erhöhtes Risiko, an TB zu erkranken, aber weder ein erhöhtes Risiko für extrapulmonale Manifestationen noch für ein Rezidiv, im Gegensatz zu Ungeimpften mit TLR8-1A. Der aktuelle Stand der Wissenschaft lässt nur Spekulation zu, auf welche Weise die BCG-Impfung sekundär in Zusammenspiel mit TLR8 und einer APC-getriggerten Antwort des angeborenen Immunsystems partiell vor EPTB und einem Rezidiv schützen kann.

In Bezug auf die Interaktion von TLR4 und -8 konnten Studien, welche auf den Ergebnissen dieser Arbeit aufbauten, zeigen, dass der SNP TLR4-C399T an der potentiellen Stelle liegt, welche über Ligandenbindung zu einer Heterodimerisation mit TLR8 führen könnte. Das T-Allel führt durch eine inhibierte Bindung zu einer geringeren Wahrscheinlichkeit der Heterodimerisation und kann daher als Erklärungsansatz für den hier gesehenen Unterschied in der TB-Suszeptibilität dienen. Eine simultane Stimulation von TLR4 und -8 führt zu einer stärkeren Aktivierung von IL-12, IRF3 und Typ-I IFN [6]. Auch der cGAS/STING-Signalweg führt zu einer Induktion von Typ-I Interferonen, sodass sich insgesamt aus den in dieser Arbeit einflussreichen SNPs für TB ableiten lässt, dass eine verringerte Expression von Typ-I IFN mit einer erhöhten Suszeptibilität einherzugehen scheint. Klassischerweise wurde Typ-I IFN in der TB-Immunantwort als nachteilig betrachtet, da es IL-12, TNFα und IFNγ

inhibiert [28]. Dies kann erklären, weshalb in dieser Arbeit gemessene TNFα-Spiegel nach LPS-Stimulation mit endosomaler Blockade durch Bafilomycin höher waren als ohne diese. Zuletzt erfolgte jedoch dennoch ein Umdenken in der Bedeutung von Typ-I IFN, da mehrere Studien einen positiven bzw. notwendigen Effekt selbiger in der initialen Krankheitsphase nahelegen: Typ-I IFN führt über ein Positive-Feedback Loop in Natural Killer (NK)-Zellen zu einer Steigerung von IFNγ und somit einer gesteigerten Th1-Antwort [5] und *in vitro* konnten höhere IFNγ-Werte gemessen werden, wenn zur Stimulation mit BCG Typ-I IFN hinzugegeben wurde [29]. Die in dieser Arbeit gezeigten Ergebnisse legen nahe, dass Typ-I IFN in der angeborenen Immunabwehr gegen TB eine wichtige Rolle spielt.

Die hier untersuchte TB-Kohorte umfasste mehr weibliche Patienten, was im Gegensatz zu den allgemein höheren Fallzahlen bei Männern steht, jedoch auch bei den GH zu finden war. Aufgrund der ähnlichen soziodemographischen Risikofaktoren der TB-Patienten und ihren GH ist der Vergleich der untersuchten SNPs zwischen diesen Gruppen besonders aussagekräftig, auch wenn Komorbiditäten wie z.B. Diabetes mellitus nicht erfasst wurden. Alkohol- und Nikotinabusus als wichtige Risikofaktoren für die Entwicklung einer aktiven TB wurden zwar anamnestisch erfasst, jedoch aus der statistischen Analyse bei einem hohen Anteil an Fehlwerten, sowie einer wahrscheinlichen Verzerrung der Antworten aufgrund sozialer Erwünschtheit, ausgeschlossen. Eine weitere Schwäche dieser epidemiologischen Studie stellt die Art des Ausschlusses einer TB-Erkrankung bei den GH dar, welche rein Symptom-basiert erfolgte. Die Feststellung der stattgefundenen BCG-Impfung erfolgte anamnestisch und anhand der charakteristischen Narbe, was ebenfalls eine Fehlerquelle durch eine potentielle Erinnerungsverzerrung darstellen kann. Die Impfrate der GNH von 100% lässt einen Stichproben-Bias vermuten. Letztendlich gewinnt die Studie jedoch dadurch an interner Validität, dass sich zwischen GH und GNH genetisch keine Unterschiede erkennen lassen, während sich TB-Patienten und GH in mehreren Punkten unterschieden.

5. Abkürzungsverzeichnis

APC – antigen presenting cell; BCG - Bacillus Calmette-Guérin; BMI – body mass index; cGAS - cyclische GMP-AMP-Synthase; DOTS – directly observed treatment, short-course; ELISA – enzyme-linked immunosorbent assay; EPTB – extrapulmonary tuberculosis; GF – gesunde Freiwillige; GNH – gesunde, nicht dem Haushalt angehörige Freiwilige; GH – gesunde Haushaltangehörige; HEK – human embryonic kidney cells; HIV – human immunodeficiency virus; IL – Interleukin; IQR – interquartile range; IRF – interferon

regulatory factor; LRR – leucin-rich repeats; LRT – likelihood ratio test; M – Mittelwer; mDC – myeloid dencdritic cells; Mdn – Median; MTB – Mycobacterium tuberculosis; NFκB - nuclear factor kappa-light-chain-enhancer of activated B-cells; NK– Natural Killer; *OR* – odds ratio; PCR – Polymerase-Kettenreaktion; PRR – pattern recognition receptor; PTB – pulmonary tuberculosis; SD – Standardabweichung; SE – Standardfehler; SEAP – secreted embryonic alkaline phosphatase; SNP – single nucleotid polymorphism; ss – single strand; STING - Stimulator of interferon genes; TB – Tuberkulose; TfH – follikuläre T-Helferzellen; Th – T-Helferzellen; TIR - Toll/IL-1R homology domain; TIRAP - Toll/IL-1R homology domain adaptor protein; TLR – Toll-like Rezeptor; TNFα – Tumor-Nekrosefaktor α

6. Literaturverzeichnis

1. World Health Organization. *Global Tuberculosis Report 2020*.; 2020.
2. United Nations. *Transforming Our World: The 2030 Agenda for Sustainable Development*.; 2015.
3. Cohen A, Mathiasen VD, Schön T, Wejse C. The global prevalence of latent tuberculosis: a systematic review and meta-analysis. *Eur Respir J*. 2019;54(3).
4. Ai J-W, Ruan Q-L, Liu Q-H, Zhang W-H. Updates on the risk factors for latent tuberculosis reactivation and their managements. *Emerg Microbes Infect*. 2016;5(1):1-8.
5. Keegan C, Krutzik S, Schenk M, Scumpia PO, Lu J, Pang YLJ, Russell BS, Lim KS, Shell S, Prestwich E, Su D, Elashoff D, Hershberg RM, Bloom BR, Belisle JT, Fortune S, Dedon PC, Pellegrini M, Modlin RL. Mycobacterium tuberculosis Transfer RNA Induces IL-12p70 via Synergistic Activation of Pattern Recognition Receptors within a Cell Network . *J Immunol*. 2018;200(9):3244-3258.
6. Burkert S, Schumann RR. RNA Sensing of Mycobacterium tuberculosis and Its Impact on TB Vaccination Strategies. *Vaccines*. 2020;8(1):67.
7. Oh D-Y, Taube S, Hamouda O, Kücherer C, Poggensee G, Jessen H, Eckert JK, Neumann K, Storek a, Pouliot M, Borgeat P, Oh N, Schreier E, Pruss a, Hattermann K, Schumann RR. A functional toll-like receptor 8 variant is associated with HIV disease restriction. *J Infect Dis*. 2008;198(5):701-709.
8. Davila S, Hibberd ML, Hari Dass R, Wong HEE, Sahiratmadja E, Bonnard C, Alisjahbana B, Szeszko JS, Balabanova Y, Drobniewski F, van Crevel R, van de Vosse E, Nejentsev S, Ottenhoff THM, Seielstad M. Genetic Association and Expression Studies Indicate a Role of Toll-Like Receptor 8 in Pulmonary Tuberculosis. Gojobori T, ed. *PLoS Genet*. 2008;4(10):e1000218.
9. Wang M-G, Zhang M-M, Wang Y, Wu S-Q, Zhang M, He J-Q. Association of TLR8 and TLR9 polymorphisms with tuberculosis in a Chinese Han population: a case-control study. *BMC Infect Dis*. 2018;18(1):561.
10. Gantier MP, Irving AT, Kaparakis-Liaskos M, Xu D, Evans VA, Cameron PU, Bourne JA, Ferrero RL, John M, Behlke MA, Williams BRG. Genetic modulation of TLR8 response following bacterial phagocytosis. *Hum Mutat*. 2010;31(9):1069-1079.
11. Cervantes JL, Vake CJ La, Weinerman B, Luu S, O 'connell C, Verardi PH, Salazar JC. Human TLR8 is activated upon recognition of Borrelia burgdorferi RNA in the phagosome of human monocytes. *J Leukoc Biol*. 2013;94(December):1231-1241.
12. Bukhari M, Aslam MA, Khan A, Iram Q, Akbar A, Naz AG, Ahmad S, Ahmad MM, Ashfaq UA, Aziz H, Ali M. TLR8 gene polymorphism and association in bacterial load in southern Punjab of Pakistan: an association study with pulmonary tuberculosis. *Int J Immunogenet*. 2015;42(1):46-51.
13. Dittrich N, Berrocal-Almanza LC, Thada S, Goyal S, Slevogt H, Sumanlatha G, Hussain A, Sur S, Burkert S, Oh D-Y, Valluri V, Schumann RR, Conrad ML. Toll-like receptor 1 variations influence susceptibility and immune response to Mycobacterium tuberculosis. *Tuberculosis (Edinb)*. 2015;95(3):328-335.
14. Thada S, Burkert S, Sivangala R, Hussain A, Sur S, Dittrich N, Conrad ML, Slevogt H, Latha Gaddam S, Schumann RR. A SNP upstream of the cyclic GMP-AMP synthase (cGAS) gene protects from relapse and extra-pulmonary TB and relates to BCG vaccination status in an Indian cohort. *Genes Immun*.

2020;21(1):13-26.
15. Berrocal-Almanza LC, Goyal S, Hussain A, Klassert TE, Driesch D, Grozdanovic Z, Sumanlatha G, Ahmed N, Valluri V, Conrad ML, Dittrich N, Schumann RR, Lala B, Slevogt H. S100A12 is up-regulated in pulmonary tuberculosis and predicts the extent of alveolar infiltration on chest radiography: an observational study. *Sci Rep*. 2016;6(1):31798.
16. Kirkwood BR, Sterne JAC. *Essential Medical Statistics*. 2nd Editio. Wiley-Blackwell; 2003.
17. Thada S, Horvath GL, Müller MM, Dittrich N, Conrad ML, Sur S, Hussain A, Pelka K, Gaddam SL, Latz E, Slevogt H, Schumann RR, Burkert S. Interaction of TLR4 and TLR8 in the Innate Immune Response against Mycobacterium Tuberculosis. *Int J Mol Sci*. 2021;22(4):1560.
18. Ugolini M, Gerhard J, Burkert S, Jensen KJ, Georg P, Ebner F, Volkers SM, Thada S, Dietert K, Bauer L, Schäfer A, Helbig ET, Opitz B, Kurth F, Sur S, Dittrich N, Gaddam S, Conrad ML, Benn CS, Blohm U, Gruber AD, Hutloff A, Hartmann S, Boekschoten M V., Müller M, Jungersen G, Schumann RR, Suttorp N, Sander LE. Recognition of microbial viability via TLR8 drives TFH cell differentiation and vaccine responses. *Nat Immunol*. 2018;19(4):386-396.
19. Varzari A, Deyneko I V., Vladei I, Grallert H, Schieck M, Tudor E, Illig T. Genetic variation in TLR pathway and the risk of pulmonary tuberculosis in a Moldavian population. *Infect Genet Evol*. 2019;68:84-90.
20. Dalgic N, Tekin D, Kayaalti Z, Cakir E, Soylemezoglu T, Sancar M. Relationship between toll-like receptor 8 gene polymorphisms and pediatric pulmonary tuberculosis. *Dis Markers*. 2011;31(1):33-38.
21. Selvaraj P, Harishankar M, Singh B, Jawahar MS, Banurekha VV. Toll-like receptor and TIRAP gene polymorphisms in pulmonary tuberculosis patients of South India. *Tuberculosis*. 2010;90(5):306-310.
22. Wang C-H, Eng H-L, Lin K-H, Liu H-C, Chang C-H, Lin T-M. Functional polymorphisms of TLR8 are associated with hepatitis C virus infection. *Immunology*. 2014;141:540-548.
23. Booty MG, Barreira-Silva P, Carpenter SM, Nunes-Alves C, Jacques MK, Stowell BL, Jayaraman P, Beamer G, Behar SM. IL-21 signaling is essential for optimal host resistance against Mycobacterium tuberculosis infection. *Sci Rep*. 2016;6(October):1-13.
24. Cheekatla SS, Tripathi D, Venkatasubramanian S, Paidipally P, Welch E, Tvinnereim AR, Nurieva R, Vankayalapati R. IL-21 Receptor Signaling Is Essential for Optimal CD4 + T Cell Function and Control of Mycobacterium tuberculosis Infection in Mice. *J Immunol*. 2017;199(8):2815-2822.
25. Zimmermann N, Thormann V, Hu B, Köhler A, Imai-Matsushima A, Locht C, Arnett E, Schlesinger LS, Zoller T, Schürmann M, Kaufmann SH, Wardemann H. Human isotype-dependent inhibitory antibody responses against Mycobacterium tuberculosis. *EMBO Mol Med*. 2016;8(11):1325-1339.
26. Abubakar I, Pimpin L, Ariti C, Beynon R, Mangtani P, Sterne JAC, Fine PEM, Smith PG, Lipman M, Elliman D, Watson JM, Drumright LN, Whiting PF, Vynnycky E, Rodrigues LC. Systematic review and meta-analysis of the current evidence on the duration of protection by bacillus Calmette-Guérin vaccination against tuberculosis. *Health Technol Assess*. 2013;17(37):1-372, v-vi.
27. Deng Y, Bao L, Yang X. Evaluation of immunogenicity and protective efficacy against Mycobacterium tuberculosis infection elicited by recombinant Mycobacterium bovis BCG expressing human Interleukin-12p70 and Early Secretory Antigen Target-6 fusion protein. *Microbiol Immunol*. 2011;55(11):798-808.
28. McNab FW, Ewbank J, Howes A, Moreira-Teixeira L, Martirosyan A, Ghilardi N, Saraiva M, O'Garra A. Type I IFN Induces IL-10 Production in an IL-27–Independent Manner and Blocks Responsiveness to IFN-γ for Production of IL-12 and Bacterial Killing in Mycobacterium tuberculosis –Infected Macrophages. *J Immunol*. 2014;193(7):3600-3612.
29. Zhang X, Sun Y, He C, Qiu X, Zhou D, Ye Z, Long Y, Tang T, Su X, Ma J. The immune characterization of interferon-β responses in tuberculosis patients. *Microbiol Immunol*. 2018;62(4):281-290.

7. Eidesstattliche Versicherung

„Ich, Sanne Burkert, versichere an Eides statt durch meine eigenhändige Unterschrift, dass ich die vorgelegte Dissertation mit dem Thema: „Die Rolle mykobakterieller Nukleotid-Erkennung im Allgemeinen und des SNPs TLR8 A1G im Besonderen bei der humanen angeborenen Immunantwort auf *M. tuberculosis* und deren Einfluss auf Suszeptibilität und Verlauf einer Tuberkulose“ (The role of nucleotide recognition and the SNP TLR8 A1G in particular on the human innate immune response to *M. tuberculosis* and their impact on susceptibility toward tuberculosis and the course of disease) selbstständig und ohne nicht offengelegte Hilfe Dritter verfasst und keine anderen als die angegebenen Quellen und Hilfsmittel genutzt habe.
Alle Stellen, die wörtlich oder dem Sinne nach auf Publikationen oder Vorträgen anderer Autoren/innen beruhen, sind als solche in korrekter Zitierung kenntlich gemacht. Die Abschnitte zu Methodik (insbesondere praktische Arbeiten, Laborbestimmungen, statistische Aufarbeitung) und Resultaten (insbesondere Abbildungen, Graphiken und Tabellen) werden von mir verantwortet.

Ich versichere ferner, dass ich die in Zusammenarbeit mit anderen Personen generierten Daten, Datenauswertungen und Schlussfolgerungen korrekt gekennzeichnet und meinen eigenen Beitrag sowie die Beiträge anderer Personen korrekt kenntlich gemacht habe (siehe Anteilserklärung). Texte oder Textteile, die gemeinsam mit anderen erstellt oder verwendet wurden, habe ich korrekt kenntlich gemacht.

Meine Anteile an etwaigen Publikationen zu dieser Dissertation entsprechen denen, die in der untenstehenden gemeinsamen Erklärung mit dem Erstbetreuer, angegeben sind. Für sämtliche im Rahmen der Dissertation entstandenen Publikationen wurden die Richtlinien des ICMJE (International Committee of Medical Journal Editors; www.icmje.og) zur Autorenschaft eingehalten. Ich erkläre ferner, dass ich mich zur Einhaltung der Satzung der Charité – Universitätsmedizin Berlin zur Sicherung Guter Wissenschaftlicher Praxis verpflichte.

Weiterhin versichere ich, dass ich diese Dissertation weder in gleicher noch in ähnlicher Form bereits an einer anderen Fakultät eingereicht habe.

Die Bedeutung dieser eidesstattlichen Versicherung und die strafrechtlichen Folgen einer unwahren eidesstattlichen Versicherung (§§156, 161 des Strafgesetzbuches) sind mir bekannt und bewusst.“

Datum Unterschrift

8. Anteilserklärung an den erfolgten Publikationen

Declaration of contributions to publications

Sanne Burkert hatte folgenden Anteil an den folgenden Publikationen:
Sanne Burkert contributed the following parts to the respective publications:

Publikation 1: Ugolini M*, Gerhard J*, **Burkert S***, Jensen KJ, Georg P, Ebner F, Volkers SM, Thada S, Dietert K, Bauer L, Schäfer A, Helbig ET, Opitz B, Kurth F, Sur S, Dittrich N, Gaddam S, Conrad ML, Benn CS, Blohm U, Gruber AD, Hutloff A, Hartmann S, Boekschoten M V., Müller M, Jungersen G, Schumann RR, Suttorp N, Sander LE. Recognition of microbial viability via TLR8 drives TFH cell differentiation and vaccine responses. ***Nat Immunol*. 2018;19(4):386-396**. doi:10.1038/s41590-018-0068-4. *** equal contribution**

Beitrag im Einzelnen: Die Generierung, Genotypisierung und Analyse der indischen TB-Kohorte, sowie die sich anschließenden funktionellen Studien in APCs und HEK293-Zellen, welche zur Figure 8, zur Supplementary Figure 8 und zur Supplementary Table 2-4 geführt haben, sowie zu den entsprechenden Teilen in der Einleitung, Ergebnisse (letzter Absatz) und Diskussion, sind der Anteil von Sanne Burkert an dem oben genannten Paper.

Publikation 2: Thada S, Horvath GL, Müller MM, Dittrich N, Conrad ML, Sur S, Hussain A, Pelka K, Gaddam SL, Latz E, Slevogt H, Schumann RR*, **Burkert S***. Interaction of TLR4 and TLR8 in the Innate Immune Response against Mycobacterium Tuberculosis. ***Int J Mol Sci*. 2021;22(4):1560.** doi:10.3390/ijms22041560. *** equal contribution**

Beitrag im Einzelnen: Der Anteil von Sanne Burkert an oben genanntem Paper liegt in der Konzeptualisierung, der Erstellung der Experimentabläufe, der Kohortengenerierung, der statistischen Auswertung der TB-Kohorte (Tabelle 1-2, S1-S5), im Schreiben der korrespondierenden Teile der Einleitung, Ergebnisse und der Diskussion, sowie in der Supervision, Korrektur und in der Korrespondenz mit dem Journal.

Particular contribution: The contribution of Sanne Burkert to the above-cited paper consisted in the conceptualisation, the creation of experimental plans, the generation of the TB-cohort and its statistical analysis (leading to table 1-2, S1-S5), writing of the corresponding parts in the introduction, results and discussion part, as well as in supervision, corrections and correspondence with the journal.

Publikation 3: Thada S, **Burkert S**, Sivangala R, Hussain A, Sur S, Dittrich N, Conrad ML, Slevogt H, Latha Gaddam S, Schumann RR. A SNP upstream of the cyclic GMP-AMP synthase (cGAS) gene protects from relapse and extra-pulmonary TB and relates to BCG vaccination status in an Indian cohort. ***Genes Immun*. 2020;21(1):13-26**. doi:10.1038/s41435-019-0080-1

Beitrag im Einzelnen: Der Anteil von Sanne Burkert an oben genanntem Paper liegt in der Kohortengenerierung und dessen statistischer Auswertung, welche zur Tabelle 1-9 führte, sowie im Schreiben der entsprechenden Teile der Einleitung, Ergebnisse und Diskussion.

Particular contribution: The contribution of Sanne Burkert to the above-cited paper consisted in the generation of the TB-cohort and its statistical analysis (leading to table 1-9) and in writing of the corresponding parts in the introduction, results and discussion part.

Publikation 4: Dittrich N, Berrocal-Almanza LC, Thada S, Goyal S, Slevogt H, Sumanlatha G, Hussain A, Sur S, **Burkert S**, Oh D-Y, Valluri V, Schumann RR, Conrad ML. Toll-like receptor 1 variations influence susceptibility and immune response to Mycobacterium tuberculosis. ***Tuberculosis (Edinb)*. 2015;95(3):328-335**. doi:10.1016/j.tube.2015.02.045

Beitrag im Einzelnen: Sanne Burkert hat an der Kohortengenerierung in Indien sowie der statistischen Auswertung dieser Kohorte mitgewirkt. Die von Sanne Burkert etablierten HEK-Blue-Null1-Zellen haben zur Änderung des Experimentaufbaus in oben genanntem Paper geführt und finden sich in Abbildung 4 wieder.

Particular contribution: Sanne Burkert participated in the generation of the TB-cohort and the statistical analysis. HEK-Blue-Null1 cells were furthermore established in the respective laboratory by Sanne Burkert and were used to conduct experiments leading to figure 4.

_____

Unterschrift der Doktorandin

9. Publikation 1: Ugolini et al. (2018)

nature immunology

ARTICLES

https://doi.org/10.1038/s41590-018-0068-4

Recognition of microbial viability via TLR8 drives T_{FH} cell differentiation and vaccine responses

Matteo Ugolini[1,16], Jenny Gerhard[1,16], Sanne Burkert[2,16], Kristoffer Jarlov Jensen[3,4], Philipp Georg[1], Friederike Ebner[5], Sarah M. Volkers[1], Shruthi Thada[2,6], Kristina Dietert[7], Laura Bauer[8], Alexander Schäfer[9], Elisa T. Helbig[1], Bastian Opitz[1,10], Florian Kurth[1], Saubashya Sur[2], Nickel Dittrich[2], Sumanlatha Gaddam[6,11], Melanie L. Conrad[12], Christine S. Benn[3,13], Ulrike Blohm[9], Achim D. Gruber[7], Andreas Hutloff[8], Susanne Hartmann[5], Mark V. Boekschoten[14], Michael Müller[14,15], Gregers Jungersen[4], Ralf R. Schumann[2], Norbert Suttorp[1,10] and Leif E. Sander[1,10]*

Live attenuated vaccines are generally highly efficacious and often superior to inactivated vaccines, yet the underlying mechanisms of this remain largely unclear. Here we identify recognition of microbial viability as a potent stimulus for follicular helper T cell (T_{FH} cell) differentiation and vaccine responses. Antigen-presenting cells (APCs) distinguished viable bacteria from dead bacteria through Toll-like receptor 8 (TLR8)-dependent detection of bacterial RNA. In contrast to dead bacteria and other TLR ligands, live bacteria, bacterial RNA and synthetic TLR8 agonists induced a specific cytokine profile in human and porcine APCs, thereby promoting T_{FH} cell differentiation. In domestic pigs, immunization with a live bacterial vaccine induced robust T_{FH} cell and antibody responses, but immunization with its heat-killed counterpart did not. Finally, a hypermorphic *TLR8* polymorphism was associated with protective immunity elicited by vaccination with bacillus Calmette-Guérin (BCG) in a human cohort. We have thus identified TLR8 as an important driver of T_{FH} cell differentiation and a promising target for T_{FH} cell–skewing vaccine adjuvants.

Live attenuated microbes represent the first generation of vaccines and have contributed to the extinction of, or a substantial reduction in, deadly diseases such as smallpox or rabies[1–3]. The unparalleled success of live vaccines is based on empiricism[4], yet their exact mechanisms of action, their frequently observed superiority over inactivated vaccine preparations[5] and their exceptional ability to induce protective, often lifelong, immunity still remain largely unexplained. The innate immune system detects microbial invaders and carefully determines the level of infectious threat in order to elicit appropriate, well-measured immune responses[6]. Mouse innate immune cells possess an inherent ability to discriminate live microorganisms from dead microorganisms[7]. Viable and thus potentially harmful microorganisms contain pathogen-associated molecular patterns (PAMPs) specific for live microbes. Bacterial mRNA has been identified as such a viability-associated PAMP ('vita-PAMP'), the detection of which elicits distinct inflammatory immune responses and promotes humoral immunity in mice[7]. However, the role of vita-PAMPs and their receptors in regulating human immune responses remains unknown.

Given the importance of innate immune signals in shaping adaptive immune responses[8], we sought to determine whether recognition of bacterial viability by the innate immune system affects the ensuing helper T cell responses and, in particular, the differentiation of T_{FH} cells. T_{FH} cells are pivotal regulators of the germinal-center response and humoral immunity[9,10], and intense research has unraveled the complexity of the development of T_{FH} cells and their interactions with B cells[10–14]. However, the early stages of T_{FH} cell differentiation and the role of APC-derived innate immune signals in controlling this process, especially in humans, have remained unclear. Targeted mobilization of T_{FH} cell responses poses a major hurdle for vaccine development. Therefore, the identification of particular innate immune pathways with T_{FH} cell–skewing ability in humans would be highly desirable for the rational design of T_{FH} cell–targeted vaccine adjuvants.

[1]Department of Infectious Diseases and Pulmonary Medicine, Charité–Universitätsmedizin Berlin, corporate member of Freie Universität Berlin, Humboldt-Universität zu Berlin, and Berlin Institute of Health, Berlin, Germany. [2]Institute of Microbiology and Hygiene, Charité–Universitätsmedizin Berlin, corporate member of Freie Universität Berlin, Humboldt-Universität zu Berlin, and Berlin Institute of Health, Berlin, Germany. [3]Research Center for Vitamins and Vaccines, Bandim Health Project, Statens Serum Institut, Copenhagen, Denmark. [4]Department of Biotechnology and Biomedicine, Technical University of Denmark, Kgs Lyngby, Denmark. [5]Department of Veterinary Medicine, Institute of Immunology, Freie Universität Berlin, Berlin, Germany. [6]Bhagwan Mahavir Medical Research Centre, Hyderabad, India. [7]Department of Veterinary Medicine, Institute of Veterinary Pathology, Freie Universität Berlin, Berlin, Germany. [8]Chronic Immune Reactions, German Rheumatism Research Centre, a Leibniz Institute, Berlin, Germany. [9]Institute of Immunology, Friedrich-Loeffler-Institut, Federal Research Institute for Animal Health, Greifswald—Island of Riems, Germany. [10]German Center for Lung Research (DZL), Berlin, Germany. [11]Department of Genetics, Osmania University, Hyderabad, India. [12]Department of Internal Medicine and Dermatology, Division of Psychosomatic Medicine, Charité–Universitätsmedizin Berlin, corporate member of Freie Universität Berlin, Humboldt-Universität zu Berlin, and Berlin Institute of Health, Berlin, Germany. [13]Odense Patient Data Explorative Network (OPEN), Odense University Hospital/Department of Clinical Research, University of Southern Denmark, Odense, Denmark. [14]Nutrition, Metabolism and Genomics Group, Division of Human Nutrition, Wageningen University, Wageningen, The Netherlands. [15]Norwich Medical School, University of East Anglia, Norwich, UK. [16]These authors contributed equally: Matteo Ugolini, Jenny Gerhard and Sanne Burkert. *e-mail: leif-erik.sander@charite.de

In this study, we found that human APCs distinguished viable bacteria from dead bacteria independently of virulence, by virtue of TLR8-dependent detection of bacterial RNA. The recognition of bacterial viability by the innate immune system led to transcriptional remodeling in human APCs and induced T_{FH} cell–promoting signals, most importantly interleukin 12 (IL-12). Activation of TLR8 by live bacteria, bacterial RNA or synthetic agonists promoted the differentiation of fully functional T_{FH} cells, whereas killed bacteria or other TLR agonists and adjuvants failed to do so. In domestic pigs, we observed robust T_{FH} cell and antibody responses following immunization with a commonly used vaccine containing live attenuated *Salmonella* but not following immunization with the same vaccine containing a heat-killed version of the *Salmonella*. Moreover, a case-control study revealed a strong association of a hypermorphic *TLR8* polymorphism with BCG-induced protection from infection with *Mycobacterium tuberculosis*, which linked function to protective immunity in response to a live attenuated vaccine in humans. In summary, we identified recognition of bacterial viability as a conserved innate immune checkpoint that preferentially promoted T_{FH} cell differentiation and humoral immunity.

Results

Detection of live bacteria promotes T_{FH} cell differentiation. In order to assess the contribution of innate immune signals to the differentiation of human T_{FH} cells, we co-cultured human $CD14^+CD16^-$ monocytes (as APCs) with autologous naive $CD4^+$ T cells isolated by negative selection of $CD45RO^+CD4^+$ T cells. APCs were stimulated with either live avirulent thymidine-auxotrophic (*thyA*$^-$; replication-defective) *Escherichia coli* (called 'EC' here)[7] or a heat-killed version of the same *E. coli* (HKEC). We chose avirulent auxotrophic bacteria to selectively analyze the effect of bacterial viability without the confounding effects of virulence factors and bacterial replication[7]. Following 90 min of stimulation of human $CD14^+CD16^-$ monocytes with EC or HKEC, naive $CD4^+$ T cells were added, together with antibiotics, and helper T cell differentiation was assessed 5 d later. Notably, EC-stimulated APCs induced naive $CD4^+$ T cells to produce large amounts of IL-21 and interferon-γ (IFN-γ), which are characteristic cytokines of T_{FH} cells and the T_H1 subset of helper T cells, respectively (Fig. 1a,b). This response was almost completely absent in cultures with APCs stimulated with HKEC or medium alone (Fig. 1a,b). T cell proliferation rates were similar in all conditions, and IL-17 was produced in moderate amounts regardless of bacterial viability (Fig. 1a,b). In line with the increased IL-21 production, stimulation with EC promoted the expression of the T_{FH} cell markers CXCR5, ICOS and PD-1, but stimulation with HKEC did not[15–17] (Fig. 1c,d and Supplementary Fig. 1a).

The transcription factor BCL-6 is required for successful development of T_{FH} cells[11,12]. APCs stimulated with EC induced co-expression of BCL-6 and IL-21 in $CD4^+$ T cells, as assessed by flow cytometry, whereas APCs stimulated with killed bacteria failed to do so (Fig. 1e,f). The expression of mRNA encoding the transcription factors T-bet and GATA-3 was downregulated in T cells incubated with APCs stimulated with EC or HKEC, relative to such expression in T cells activated with unstimulated APCs, whereas expression of mRNA encoding the transcription factors RORγt and Maf was slightly increased by the incubation of T cells with APCs stimulated with either EC or HKEC, as measured by hybridization-based multiplexed gene-expression quantitation (Fig. 1g and Supplementary Fig. 1b). The specific induction of T_{FH} cells upon sensing of live EC by the innate immune system was not specific to $CD14^+CD16^-$ monocytes, as similar results were obtained with primary human $CD1c^+$ myeloid dendritic cells (DCs) as APCs (Fig. 1h,i).

In order to assess the functionality of newly generated T_{FH} cells as true helpers of B cells, we sorted $CD4^+CD45RA^-CXCR5^+$ T_{FH} cells from the APC–T cell co-culture system at day 5 and compared them with naive $CD4^+CD45RA^+CXCR5^-$ T cells sorted from the blood of the same donor, assessing their ability to promote plasma-cell differentiation when co-cultured with heterologous tonsillar memory B cells. $CXCR5^+$ T_{FH} cells induced by EC-stimulated APCs promoted robust differentiation of $CD27^{hi}CD38^+$ plasma cells, while naive $CXCR5^-$ T cells from the same donor failed to do so (Fig. 1j,k). In addition, $CXCR5^+$ T_{FH} cells stimulated robust production of immunoglobulin G (IgG), which was not observed with naive T cells or in B cell–only cultures (Fig. 1l). $CXCR5^-$ T cells sorted from the co-cultures at day 5 provided weaker help than did $CXCR5^+$ T cells (Supplementary Fig. 1c–f). Collectively, these results indicated that the recognition of bacterial viability by human APCs of the innate immune system elicited potent differentiation signals for the generation of fully functional T_{FH} cells.

Recognition of bacterial viability modulates the cytokine profile of human APCs. In order to characterize the innate immune signals that control T_{FH} cell programming after the recognition of bacterial viability, we compared the transcriptome of $CD14^+CD16^-$ monocytes in response to live bacteria with that in response to dead bacteria. Detection of either EC or HKEC led to similar regulation of 1,051 transcripts in human monocytes (Fig. 2a), which indicated substantial similarity between the two stimuli, both of which contain an abundance of PAMPs and thereby engage a multitude of pattern-recognition receptors[7]. We detected a set of 193 genes that were regulated differentially in $CD14^+CD16^-$ monocytes in response to EC relative to their regulation in response to HKEC, including genes encoding the inflammatory cytokines TNF (*TNF*) and IL-12p40 (*IL12B*) (Fig. 2a,b and Supplementary Table 1). Accordingly, we detected release of IL-12 and TNF (assessed by ELISA) nearly exclusively in response to EC, not in response to HKEC, whereas the cytokines IL-6, IL-10, IL-23 and GM-CSF were produced regardless of bacterial viability (Fig. 2c).

Our finding of differential expression of IL-12 and TNF was in contrast to published observations of mouse macrophages and DCs, which produce large amounts of TNF and IL-12 in response to either live bacteria or killed bacteria or purified bacterial cell-wall components[7]. Similar to results obtained for mouse macrophages and DCs[7], release of IL-1β was induced by EC, but not by HKEC, in human monocytes (Fig. 2c), indicative of inflammasome activation. Production of TNF and IL-12 could not be restored by higher doses of HKEC (Fig. 2d). Other bacterial species, including avirulent Gram-positive *Bacillus subtilis*, as well as BCG (an attenuated strain of *Mycobacterium bovis* and widely used live vaccine against tuberculosis (TB)), elicited comparable cytokine patterns (Fig. 2e), which indicated that the response to bacterial viability was conserved and was largely independent of features specific to the bacterial species. Both EC and HKEC induced similar upregulation of the expression of maturation markers such as CD40 (Fig. 2f), which indicated intact innate recognition of both stimuli. Thus, human $CD14^+CD16^-$ monocytes discriminated precisely between live bacteria and dead bacteria independently of virulence or bacterial species, and they responded to bacterial viability with a distinct transcriptional program and cytokine profile.

'Viability-induced' T_{FH} cell responses are mediated by APC-derived IL-12. Next, we investigated whether APC-derived cytokines induced by the detection of live bacteria were driving the T_{FH} cell differentiation. $CD4^+$ T cells (isolated by negative selection from peripheral blood) showed high expression of IL-21 and BCL-6 and of CXCR5, ICOS and PD-1 when activated via CD3 and CD28 in the presence of supernatants of EC-stimulated $CD14^+CD16^-$ monocytes (Fig. 3a,b). Supernatants of HKEC-stimulated APCs did not induce a T_{FH} cell phenotype in $CD4^+$ T cells (Fig. 3a,b), while proliferation rates and IL-17 production were induced similarly by supernatants of EC-conditioned APCs and supernatants of HKEC-conditioned APCs (Supplementary Fig. 2a–c). These results

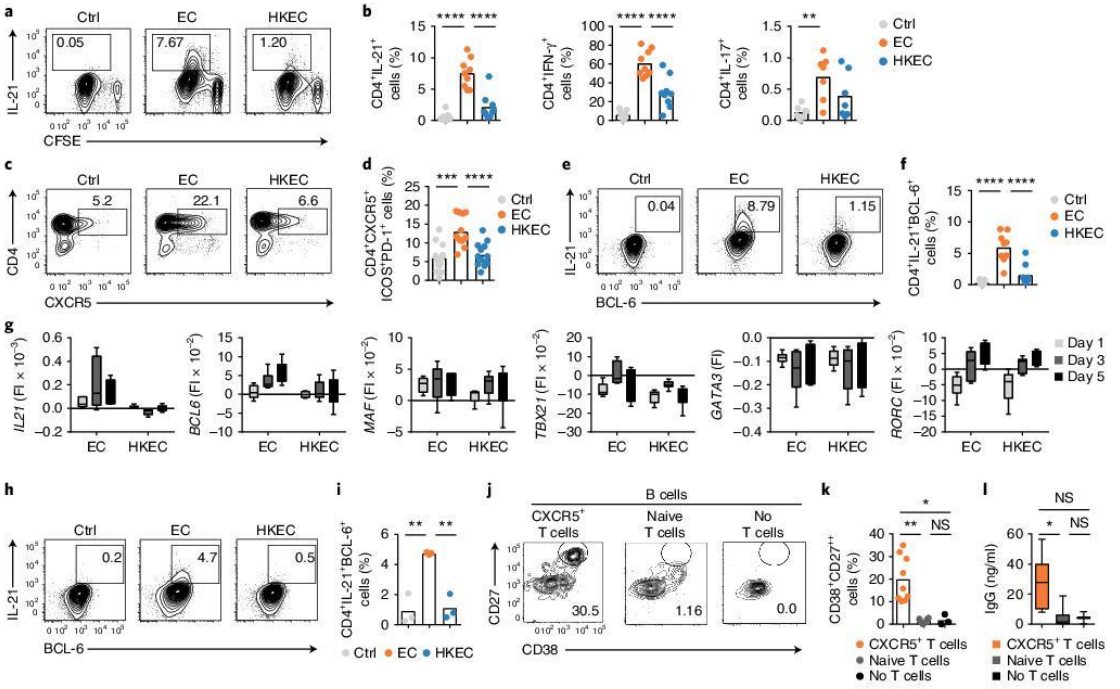

Fig. 1 | The recognition of live bacteria by the innate immune system promotes T_{FH} cell differentiation. a, Flow-cytometry analysis of the IL-21 expression and proliferation of autologous naive CD4+ T cells cultured for 5 d, in the presence of staphylococcal enterotoxin B (T cell antigen receptor stimulus in all T cell conditions), with human monocytes (as APCs) previously stimulated with medium (Ctrl), live EC or HKEC (above plots); proliferation was assessed as dilution of the division-tracking dye CFSE. **b**, Frequency of cytokine-positive CD4+ T cells in co-cultures as in **a** (key). **c**,**d**, Flow-cytometry analysis of the expression of CXCR5 (**c**), ICOS and PD-1 (Supplementary Fig. 1a) by T cells cultured as in **a** (above plots), and frequency of T cells positive for all three in such cultures (key) (**d**). **e**,**f**, Flow-cytometry analysis of the expression of IL-21 and BCL-6 by cells cultured as in a (above plots) (**e**), and frequency of IL-21+BCL-6+ cells in such cultures (key) (**f**). **g**, Fluorescent hybridization-based multiplex assay measuring the expression of genes encoding IL-21 (*IL21*) and the transcription factors BCL-6 (*BCL6*), Maf (*MAF*), T-bet (*TBX21*), GATA-3 (*GATA3*) and RORγt (*RORC*) in CD4+ T cells on day 1, 3 or 5 (key) of culture as in **a** (horizontal axis) ($n = 6$ donors), presented as corrected fluorescence intensity (FI), calculated by subtraction of the fluorescence intensity of the control sample at the same time point. **h**,**i**, Flow-cytometry analysis of the expression of IL-21 and BCL-6 by cells cultured as in **a** (above plots) but with CD1c+ myeloid DCs as APCs (**h**), and frequency of IL-21+BCL-6+ cells in such cultures (key) (**i**). **j**–**l**, Flow-cytometry analysis of the expression of CD27 and CD38 by tonsillar memory B cells cultured for 7 d alone (left) or with $CD4^+CD45RA^-CXCR5^+$ T_{FH} cells from day 5 of culture with EC-stimulated APCs as in **a** (left) or autologous naive $CD4^+CD45RA^+$ T cells from same donor (middle) (**j**), frequency of $CD38^+CD27^{hi}$ plasma cells in cultures as in **j** (key) (**k**) and ELISA of IgG in supernatants of cultures as in **j** (key) (**l**). Numbers adjacent to or in outlined areas (**a**,**c**,**e**,**h**,**j**) indicate percent cells in each throughout. Each symbol (**b**,**d**,**f**,**i**,**k**,**l**) represents an individual donor ($n = 9$ (IL-21), 9 (IFN-γ) or 7 (IL-17) (**b**); $n = 13$ (**d**); $n = 9$ (**f**); $n = 3$ (**i**); or $n = 9$ (CXCR5+ T cells), 9 (Naive T cells) or 3 (No T cells) (**k**,**l**)); error bars indicate maximum and minimum (**g**,**l**). NS, not significant ($P > 0.05$); $^*P < 0.05$, $^{**}P < 0.01$, $^{***}P < 0.001$ and $^{****}P < 0.0001$ (one-way analysis of variance (ANOVA) with post-hoc correction for multiple comparisons). Data are representative of one experiment per donor.

indicated a dominant role for APC-derived soluble factors in the initial stages of T_{FH} cell differentiation in response to live EC.

Various cytokines and cytokine combinations, including IL-21, IL-6, IL-27 and type I interferons, have been reported to promote T_{FH} cell differentiation in mice[9,18,19], whereas the differentiation of human T_{FH} cells is mediated mainly by the cytokines IL-12, IL-23 and TGF-β[10,20]. The cytokine requirements for vita-PAMP–induced human T_{FH} cell differentiation remain unclear. We found a strong correlation between the amount of IL-12 and TNF in supernatants of EC-stimulated APCs and the production of IL-21 by the activated T cells, whereas the amount of IL-6 in supernatants of APCs did not correlate with the production of IL-21 by T cells (Fig. 3c). The addition of a neutralizing antibody against IL-12 to the supernatants of EC-induced APCs almost completely abolished T_{FH} cell differentiation without affecting T cell proliferation rates (Fig. 3d–f and Supplementary Fig. 2a,d–f). Neutralization of IL-6 or IL-27 had no significant effect, whereas blockade of TNF partially inhibited T_{FH} cell differentiation, relative to such differentiation after the addition of isotype-matched control antibodies (Fig. 3d–f). Conversely, supplementing supernatants of unstimulated (control) APCs with recombinant IL-12 restored T_{FH} cell differentiation (Fig. 3d,e,g). Supplementation with recombinant TNF alone did not promote T_{FH} cell differentiation (Fig. 3g), which indicated that TNF might have a minor role or act in concert with IL-12 or other APC-derived factors. Neutralization of IL-1β in the supernatants of EC-induced APCs partially diminished T_{FH} cell differentiation, while supplementation of supernatants of unstimulated (control) APCs with recombinant IL-1β alone was insufficient to support T_{FH} cell differentiation (Supplementary Fig. 2d–f); this indicated that IL-1β might have additive effects in humans, consistent with published observations[20].

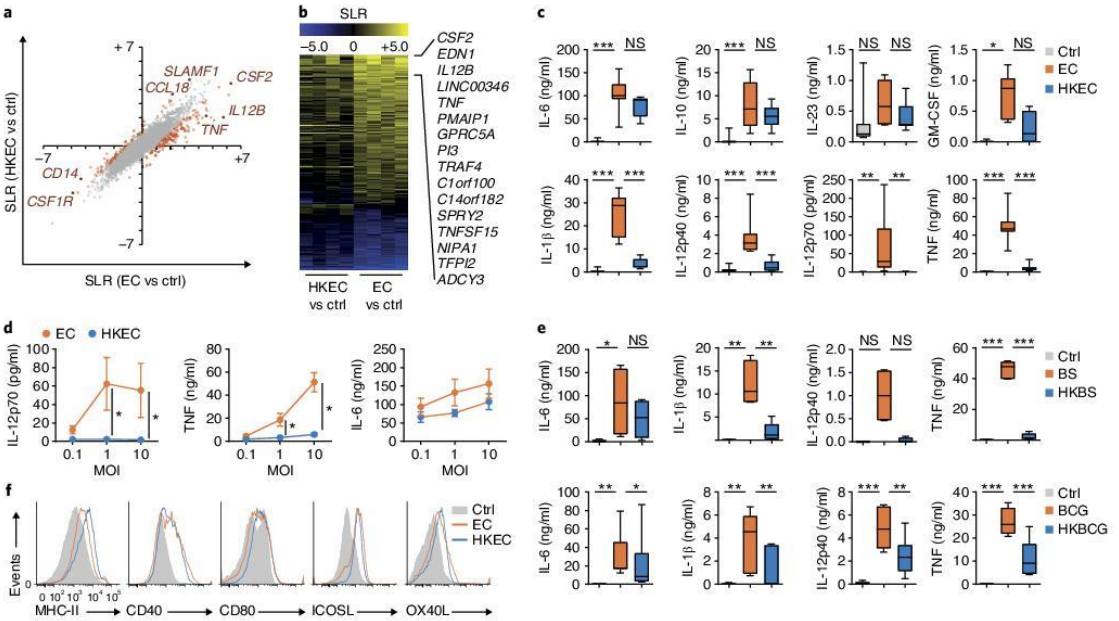

Fig. 2 | Detection of viable bacteria skews the cytokine profile of human monocytes. a, Genome-wide transcriptional analysis of human CD14$^+$CD16$^-$ monocytes ($n = 4$ donors) stimulated for 6 h with medium (control (Ctrl)), EC or HKEC, presented as the mean signal log ratio (SLR) of each gene in EC-treated cells relative to that in control cells (EC vs Ctrl) plotted against that of HKEC-treated cells relative to that of control cells (HKEC vs Ctrl); red symbols indicate genes with a difference in SLR of >2 in EC-treated cells relative to that in HKEC-treated cells. **b**, Heat map of 193 genes with a change in SLR of >2 or ≤2 (key) in EC–versus–Ctrl compared with HKEC–versus–Ctrl as in **a** (below plot). **c**, Concentration of cytokines secreted by APCs ($n = 3$–6 donors) left untreated (Ctrl) or stimulated for 18 h with EC or HKEC (key). **d**, Concentration of cytokines secreted by APCs ($n = 4$ donors) stimulated with EC or HKEC (key) at an increasing multiplicity of infection (MOI) (horizontal axis). **e**, Concentration of cytokines secreted by APCs ($n = 2$–5 donors (top row) or $n = 4$ donors (bottom row)) that were left untreated (Ctrl) or stimulated with live *B. subtilis* (BS) or heat-killed *B. subtilis* (HKBS) (key) (top row) or with live *M. bovis* strain BCG (BCG) or heat-killed *M. bovis* strain BCG (HKBCG) (key) (bottom row). **f**, Flow-cytometry analysis of the surface expression of various markers on APCs ($n = 5$ donors) at 18 h after treatment as in **c** (key). $^*P < 0.05$, $^{**}P < 0.01$ and $^{***}P < 0.001$ (one-way ANOVA (**c**,**e**) or multiple *t*-tests with post-hoc correction for multiple comparisons (**d**)). Data are representative of four independent experiments (one per donor; **a**,**b**), three to six experiments (one per donor: $n = 6$ (IL-1β and IL-12p70), $n = 5$ (IL-6, IL-10, IL-12p40 and TNF), $n = 4$ (IL-23) or $n = 3$ (GM-CSF); (**c**), eight experiments (**d**; error bars, mean ± s.e.m.) or five experiments (top row) or four experiments (bottom row) (**e**) (error bars (**c**,**e**), maximum and minimum).

Blocking IFN-β or supplementation with recombinant IFN-β did not alter the differentiation of human T_{FH} cells (Supplementary Fig. 2d–f). Although membrane-bound mediators such as ICOSL[14] and OX40L[21] contribute to different stages of T_{FH} cell differentiation in vivo, we found no major difference in their surface expression on APCs stimulated with EC relative to that on APCs stimulated with HKEC (Fig. 2f), an observation that does not exclude the possibility of a role at later stages of differentiation. Thus, IL-12 was the critical innate immune signal produced in response to live bacteria to instruct early priming of T_{FH} cells in humans.

TLR8 is a vita-PAMP receptor that mediates IL-12 production and T_{FH} cell differentiation. In order to identify potential targets for T_{FH} cell–skewing adjuvants, we next investigated the nature of the innate immune receptor(s) and the ligands that elicited 'viability-induced' T_{FH} cell differentiation signals. We supplemented HKEC with various PAMPs and compared subsequent cytokine responses in CD14$^+$CD16$^-$ monocytes. Of the five different PAMPs tested here, only ligands of the endosomal single-stranded-RNA receptors TLR7 and TLR8 restored the production of IL-12 and TNF to levels comparable to those induced by EC (Fig. 4a). Inhibition of actin polymerization and phagocytosis via cytochalasin D, as well as blockade of endolysosomal acidification with bafilomycin A, abolished the EC-induced production of IL-12, but not that of IL-6 (Supplementary Fig. 3a), indicative of a role for endosomal receptors in the sensing of viable bacteria.

Since human monocytes expressed TLR8 but had only low expression of TLR7 (Supplementary Fig. 3b), and TLR8 recognizes bacterial RNA[22,23], we investigated whether TLR8 was the primary human vita-PAMP receptor for live bacteria. Endosomal delivery of bacterial RNA fully restored the production of TNF and IL-12 to levels comparable to those induced by EC and synthetic agonists of TLR7 and TLR8 (Fig. 4b) and induced upregulation of the expression of CD40, CD80 and other maturation markers (Supplementary Fig. 3c). Conversely, silencing the expression of the gene encoding TLR8 or the gene encoding its signaling adaptor MyD88 by RNA-mediated interference (with small interfering RNA (siRNA)) in CD14$^+$CD16$^-$ monocytes abolished the release of IL-12p70 and TNF in response to EC (Fig. 4c,d). The production of IL-6 was not affected by the silencing of either of those genes (Fig. 4c,d). In line with the proposed critical role for TLR8 as a vita-PAMP receptor, we found that ligation of TLR8 in APCs by the synthetic agonists CL075 or R848 potently promoted the differentiation of IL-21$^+$BCL-6$^+$ T_{FH} cells (Fig. 5a–c). In contrast, all other TLR ligands tested, including the licensed vaccine adjuvants MPLA (monophosphoryl lipid A; a TLR4 agonist) and CpG DNA (a TLR9 agonist), did not promote

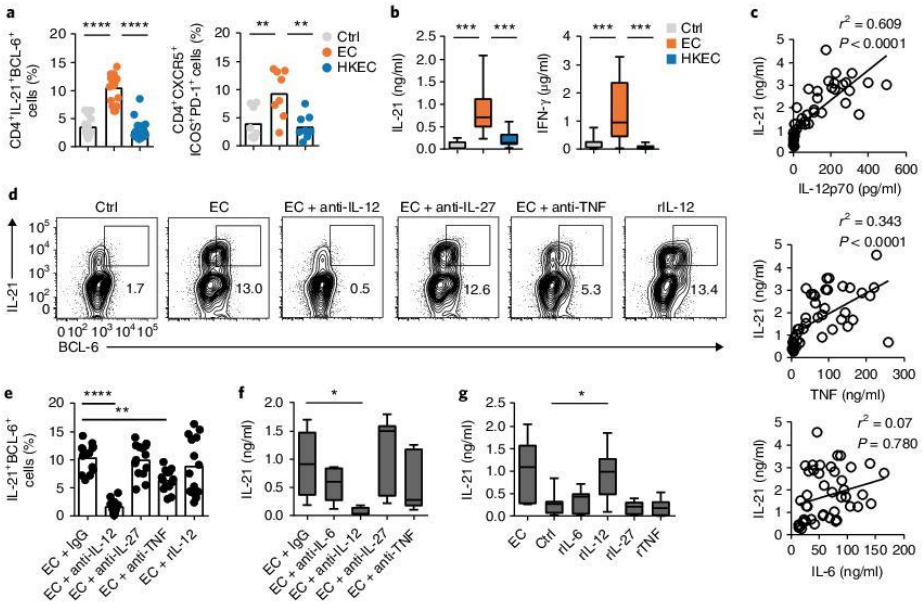

Fig. 3 | IL-12 is a critical signal for 'viability-induced' T_{FH} cell differentiation. a,**b**, Frequency of IL-21$^+$BCL-6$^+$ cells (left) or CXCR5$^+$ICOS$^+$PD-1$^+$ cells (right), assessed by flow cytometry (**a**), and ELISA of IL-21 (left) and IFN-γ (right) in supernatants (**b**) of CD4$^+$ T cells polyclonally activated by plate-bound antibody to CD3 and soluble antibody to CD28 in the presence of supernatants collected from APCs left unstimulated (Ctrl) or stimulated for 18 h with EC or HKEC (key) ($n = 19$ donors (IL-21$^+$BCL-6$^+$) or 8 donors (CXCR5$^+$ICOS$^+$PD-1$^+$) (**a**); or $n = 11$ donors (**b**)). **c**, Linear-regression analysis of the concentration of IL-21 produced by CD4$^+$ T cells versus that of IL-12p70 (top), TNF (middle) or IL-6 (bottom) in supernatants of APCs (samples from nine donors in five independent experiments; $n = 45$ (IL-12p70), 21(TNF) or 21 (IL-6)) in cultures as in **a**. **d**–**g**, Flow-cytometry analysis of the expression of IL-21 and BCL-6 (**d**), frequency of IL-21$^+$BCL-6$^+$ cells, assessed as in **d** (**e**) ($n = 14$), and ELISA of IL-21 in supernatants (**f**,**g**) ($n = 7$) of T cells cultured as in **a**,**b** with supernatants of EC-stimulated APCs in the presence or absence of the irrelevant control antibody IgG or neutralizing antibodies (anti-) or supernatants of control APCs supplemented with recombinant (r) cytokines (above plots (**d**) or horizontal axis (**e**–**g**)). Each symbol (**a**,**e**) represents an individual donor. $^*P < 0.05$, $^{**}P < 0.01$ and $^{***}P < 0.001$ (one-way ANOVA with post-hoc correction for multiple comparisons). Data are representative of 19 experiments (**a**,**b**), 45 experiments (**c**), 14 experiments (**d**,**e**) or 7 experiments (**f**,**g**) (error bars (**b**,**f**,**g**), maximum and minimum).

T_{FH} cell responses, even at high concentrations (Fig. 5a–c). Similar to its activation by live bacteria, the activation of TLR8 by purified bacterial RNA resulted in the robust differentiation of T_{FH} cells and their production of IL-21 (Fig. 5d,e), which demonstrated that the recognition of bacterial RNA by the innate immune system was a potent stimulator of T_{FH} cell–differentiation signals. Silencing *TLR8* expression in CD14$^+$CD16$^-$ monocytes diminished their ability to promote T_{FH} cell differentiation in response to EC, relative to the corresponding ability of EC-stimulated monocytes treated with control siRNA with a scrambled sequence (Fig. 5f,g). Collectively, these results identified TLR8 as the key sensor for bacterial viability in human APCs and a critical driver of IL-12 production and subsequent T_{FH} cell responses.

Recognition of bacterial viability is conserved in porcine APCs. Domestic pigs (*Sus scrofa domestica*) are increasingly used for biomedical and pharmaceutical studies due to the substantial analogies between porcine physiology and human physiology[24,25]. The porcine and human immune systems also share many similarities[25], including the expression and function of TLR8[26]. Thus, we next assessed T_{FH} cell differentiation in response to viable bacteria in pigs. Porcine CD172$^+$CD14$^+$ monocytes and CD172$^+$CD14$^-$ DCs were sorted from spleen samples of domestic pigs and were stimulated with live and dead bacteria. We used the thymidine-auxotrophic *E. coli* (EC) or a live attenuated strain of *Salmonella enterica* serovar Typhimurium (ST) (distributed under the trade name 'Salmoporc-STM') as a live *Salmonella* vaccine for pigs[27]. Salmoporc-STM bacteria are histidine–adenine auxotrophs, leading to severe growth attenuation. Porcine CD172$^+$CD14$^+$ monocytes and CD172$^+$CD14$^-$ DCs secreted large amounts of IL-12 in response to live EC and ST and the TLR8 agonist CL075 but not after stimulation with heat-killed ST (HKST) or HKEC (Fig. 6a,b). Secretion of IL-6 was induced similarly by live and dead EC and ST (Fig. 6a,b). Selective induction of IL-12 by live EC and ST was consistently observed (Fig. 6a–c), yet statistical testing did not reveal significant differences in this, due to limited sample size and high inter-experimental variation in cytokine production. Purified EC RNA also promoted increased secretion of IL-12p40 by porcine CD14$^+$ monocytes, as assessed by ELISA, a result that was not observed for ligands of TLR2 and TLR4 (Supplementary Fig. 4a). To determine whether the mechanisms of 'viability recognition' are conserved between human APCs and porcine APCs, we used RNA-mediated interference to silence the expression of the gene encoding TLR8 in porcine CD14$^+$ monocytes. Knockdown of *TLR8* abolished the expression of IL-12p40 in response to live ST, whereas the production of IL-6, which is induced independently of bacterial viability, was unaffected (Fig. 6c). We next assessed the effect of bacterial viability on porcine T_{FH} cell differentiation. Pig splenocytes (populations that included APCs and CD4$^+$ T cells) were stimulated for 1 h with varying doses of ST or HKST, followed by the addition of antibiotics

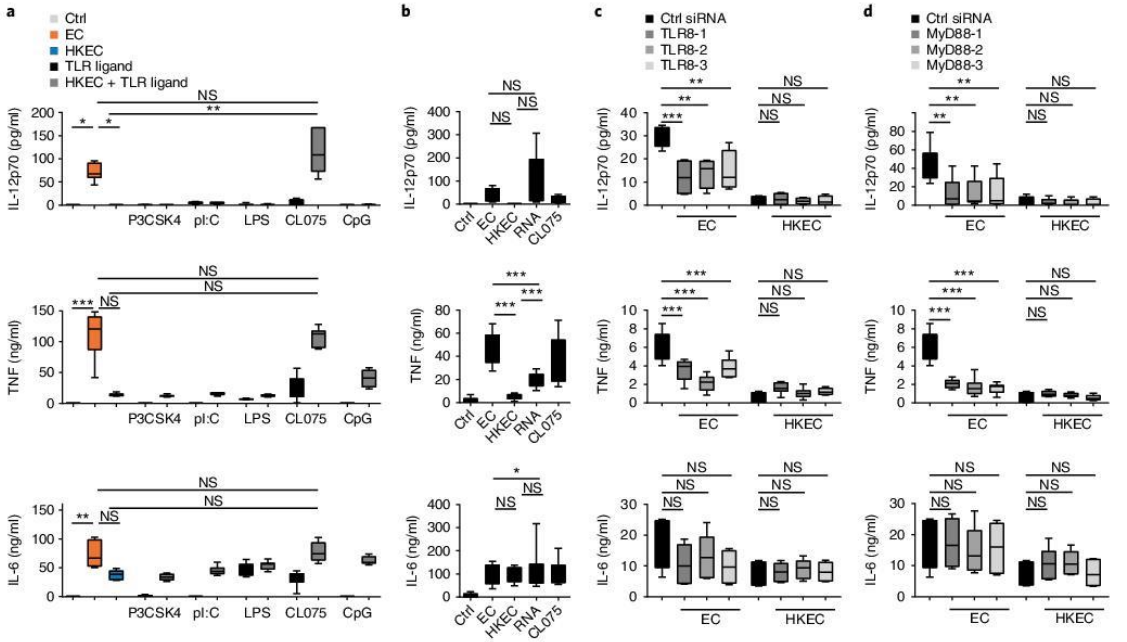

Fig. 4 | APCs sense live bacteria via TLR8. a, ELISA of IL-12p70 (top), TNF (middle) and IL-6 (bottom) in supernatants of monocytes ($n = 3$ donors) left untreated (Ctrl) or exposed to EC or HKEC or the TLR2 ligand Pam_3CSK_4 (P3CSK4), the TLR3 ligand poly(I:C) (pI:C), the TLR7 and TLR8 ligand CL075 or the TLR9 ligand CpG (horizontal axis) alone or exposed to HKEC supplemented with those TLR ligands (key). **b**, ELISA of cytokines as in **a** in supernatants of monocytes ($n = 4$ donors) left unstimulated (Ctrl) or stimulated with EC, HKEC, bacterial RNA (RNA) or CL075 (horizontal axis). **c**,**d**, ELISA of cytokines as in **a** in supernatants of human monocytes ($n = 3$ donors) treated with control siRNA with a scrambled sequence (Ctrl siRNA) or one of three siRNAs (-1, -2, -3; key) directed against TLR8 (**c**) or MyD88 (**d**) and stimulated with EC or HKEC (below plot). $^{**}P < 0.01$ and $^{***}P < 0.001$ (one-way ANOVA (**a**,**b**) or two-way ANOVA (**c**,**d**) with post-hoc correction for multiple comparisons). Data are representative of three experiments (**a**,**c**,**d**) or four experiments (**b**) (error bars, maximum and minimum).

to prevent residual bacterial growth, plus concanavalin A to induce polyclonal T cell proliferation. We observed a dose-dependent increase in the frequency of $CD4^+IL\text{-}21^+BCL\text{-}6^+$ T_{FH} cell–like cells in response to ST, compared with the frequency of such cells in response to stimulation with HKST (Fig. 6d,e). Next we compared the ability of soluble PAMPs to induce a T_{FH} cell phenotype in pig splenocytes in vitro. The TLR8 agonists bacterial RNA and CL075 induced $CD4^+IL21^+BCL\text{-}6^+$ T cells, but the TLR4 agonist LPS did not (Fig. 6f). Thus, recognition of bacterial viability via TLR8 constituted a critical stimulus of porcine T_{FH} cell differentiation.

Bacterial viability promotes T_{FH} cell differentiation in vivo. To directly assess the role of the detection of bacterial viability by the innate immune system in T_{FH} cell responses in vivo, we vaccinated domestic pigs with live attenuated ST (Salmoporc-STM), an equivalent dose of HKST or solvent (saline; as a control). The frequency of $CD4^+IL\text{-}21^+BCL\text{-}6^+$ T_{FH} cell–like cells was greater in the draining lymph nodes (dorsal superficial cervical nodes) and spleen of pigs immunized with Salmoporc-STM than in that of pigs immunized with HKST or saline (Fig. 7a,b) Other markers of effector T cell differentiation, including T-bet and FoxP3, were similarly altered in T cells from the ST-vaccinated or HKST-vaccinated groups (Supplementary Fig. 4b–e). We observed an increased number of $PAX5^+$ B cell follicles in the spleen of ST-vaccinated pigs relative to the number of such follicles in the spleen of saline-treated pigs, a result that was not observed for the HKST-vaccinated group compared with the saline-treated group (Fig. 7c,d), although the difference between the ST-vaccinated group and the HKST-vaccinated group did not reach statistical significance. B cell follicles in the spleen of ST-vaccinated pigs showed considerable enrichment for $Ki67^+PAX5^+$ B cells (Fig. 7e and Supplementary Fig. 5a), indicative of active germinal centers, but B cell follicles were negative for BCL2 (Supplementary Fig. 5b), which ruled out the possibility of malignant transformation. We also found an increased frequency of antibody-forming cells and plasma cells, which can be further separated into $CD3^-CD8^-SLAII^+IgM^+CD2^+CD21^-$ effector and $CD3^-CD8^-SLAII^+IgM^+CD2^-CD21^-$ resting antibody-forming cells and plasma cells[28], in ST-vaccinated pigs relative to the number of such cells in HKST-vaccinated pigs (Fig. 7f). Notably, higher levels of *Salmonella*-binding serum IgG were detected after vaccination with live ST than after vaccination with HKST (Fig. 7g), which demonstrated enhanced humoral immunity in response to the live vaccine. These results indicated that the recognition of bacterial viability was an essential driver of vaccine-induced T_{FH} cell and antibody responses in vivo.

A *TLR8* polymorphism is associated with vaccine protection in humans. Several functional polymorphisms in *TLR8* in humans have been described[29,30]. The *TLR8* single-nucleotide polymorphism (SNP) TLR8-A1G (rs3764880; called 'TLR8-G' here) alters the start codon ATG into a GTG triplet[29], which shifts the signal peptide by three amino acids, with a second in-frame ATG (M4) being used as an alternative start codon. According to in silico modeling predictions based on the published crystal structure of TLR8[31],

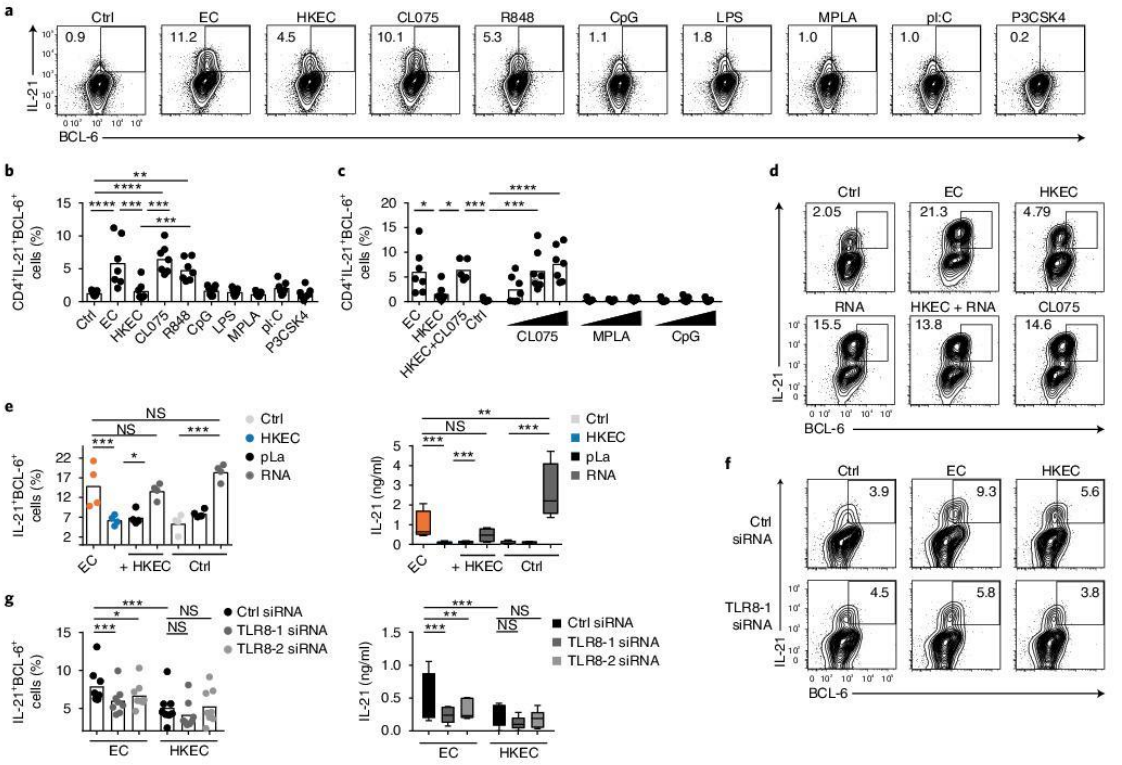

Fig. 5 | TLR8 senses bacterial viability and drives T_{FH} cell differentiation. a, Flow-cytometry analysis of the expression of IL-21 and BCL-6 by CD4+ T cells ($n = 7$ donors) stimulated in the presence of supernatants of APCs previously left unstimulated (Ctrl) or stimulated with EC or HKEC or various TLR ligands (above plots). **b**, Frequency of IL-21+BCL-6+ cells in cultures as in **a** (horizontal axis). **c**, Frequency of IL-21+BCL-6+ T cells (assessed by flow cytometry) following co-culture with APCs (as in Fig. 1) left unstimulated (Ctrl) or stimulated with EC, HKEC or HKEC plus CL075 or with increasing concentrations (wedges) of CL075 (0.1, 0.5 or 1 μg/ml), MPLA (0.1, 0.5 or 1 μg/ml) or CpG (0.1, 1 or 2.5 μM) (horizontal axis) . **d**, Flow-cytometry analysis of the expression of IL-21 and BCL-6 by CD4+ T cells stimulated by supernatants of APCs previous left unstimulated (Ctrl) or stimulated with EC, HKEC, bacterial RNA, HKEC plus bacterial RNA, or CL075 (above plots). **e**, Frequency of IL-21+BCL-6+ cells in cultures of CD4+ T cells stimulated by supernatants of APCs previously left unstimulated (Ctrl) or stimulated with EC or HKEC (horizontal axis) and the polycationic polypeptide poly-L-arginine (pLa) or bacterial RNA (key) (left), and ELISA of IL-21 in supernatants of those cultures (right). **f**,**g**, Flow-cytometry analysis of the expression of IL-21 and BCL-6 by CD4+ T cells stimulated by supernatants of APCs previously left unstimulated (Ctrl) or stimulated with EC or HKEC (above plots) and treated with control or TLR8-specific siRNA (left margin) (**f**), frequency of IL-21+BCL-6+ cells in cultures as in **f** (key) (**g**, left) and ELISA of IL-21 in supernatants of cultures as in **f** (key) (**g**, right). Each symbol (**b**,**c**,**e**,**g**) represents an individual donor ($n = 7$ (**b**), $n = 7$ (**c**), $n = 4$ (**e**) or $n = 8$ (**g**)). *$P < 0.05$, **$P < 0.01$, ***$P < 0.001$ and ****$P < 0.0001$ (one-way ANOVA (**b**,**c**) or two-way ANOVA (**e**,**g**) with post-hoc correction for multiple comparisons). Data are representative of seven experiments (**a**–**c**), four experiments (**d**,**e**) or eight experiments (**f**,**g**) (error bars (**e**,**g**, right), maximum and minimum).

the amino-acid truncation leads to significant structural alterations to the protein (Supplementary Fig. 6 and Supplementary Note 1). The increased disorder, free energy and increased flexibility of the protein encoded by TLR8-G (Supplementary Fig. 6) probably make the receptor better adapted to side-chain rearrangement and dimerization. The larger volume of clefts and cavities on the surface of the protein encoded by TLR8-G than on that encoded by TLR8-A (the protein encoded by *TLR8* without the SNP rs3764880) might increase its potential for ligand binding, whereas functional pockets and nests are slightly decreased (Supplementary Fig. 7). These models suggest altered receptor functionality, which might cause a gain of function for the receptor encoded by the TLR8-G variant. In line with those predictions, APCs from individuals expressing the TLR8-G variant showed a slightly enhanced release of IL-12 in response to stimulation of TLR8, but not in response to the TLR4 agonist LPS, relative to the response of APCs derived from carriers of TLR8-A (Supplementary Fig. 8a,b). We also studied HEK293T human embryonic kidney cells expressing a reporter gene to measure actvity of the transcription factor NF-κB. Such cells stably expressing the TLR8-G variant showed higher NF-κB-reporter activity in response to TLR8 ligands than that of their TLR8-A-expressing counterparts (Supplementary Fig. 8c), in support of the proposed gain-of-function phenotype of the TLR8-G variant.

Carriage of the TLR8-G allele has been associated with slower progression of infection with human immunodeficiency virus[29] and protection against pulmonary TB (PTB)[32]. Here we assessed distribution of the TLR8-G allelein 293 patients with confirmed TB and 165 of their healthy household contacts (control subjects; Supplementary Table 2). Significantly more control subjects (53.9%) than patients with TB (41.3%) were homo- or hemizygous carriers

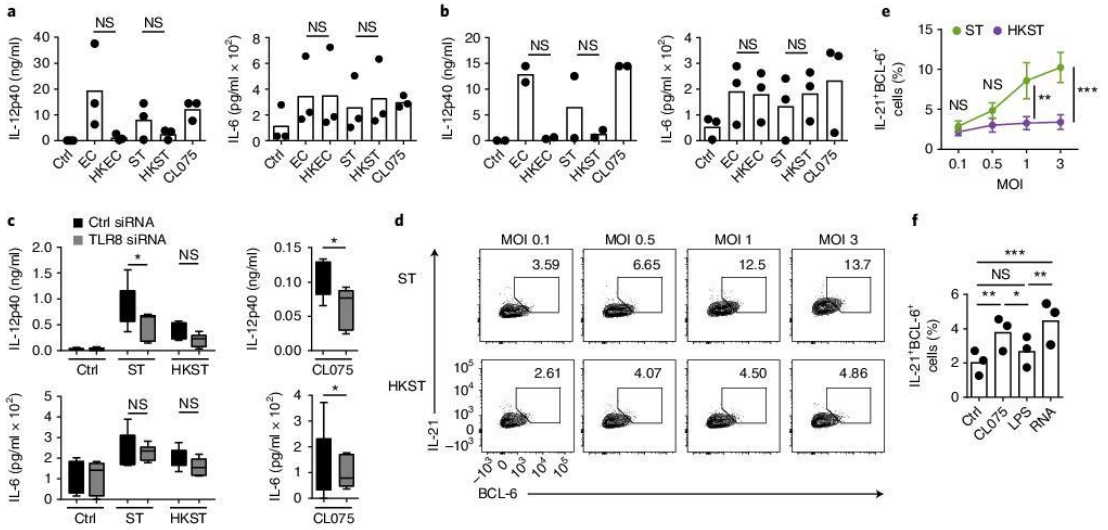

Fig. 6 | Detection of viable bacteria via TLR8 by porcine APCs promotes T_{FH} cell differentiation. a,**b**, Multiplex bead array of IL-12p40 (left) and IL-6 (right) in cultures of porcine CD14⁺CD172⁺ monocytes (**a**) or CD14⁻CD172⁺ DCs (**b**) sorted from spleen samples and stimulated with medium (Ctrl), EC, HKEC, ST, HKST or CL075 (horizontal axis). **c**, ELISA of IL-12p40 (top) and IL-6 (bottom) in supernatants of porcine splenic CD14⁺ monocytes ($n = 3$ pigs) treated with control siRNA or siRNA directed against porcine TLR8 (key) and stimulated with medium (Ctrl), ST, HKST or CL075 (horizontal axis). **d**, Flow-cytometry analysis of the expression of IL-21 and BCL-6 by CD4⁺ T cells among porcine splenocytes stimulated for 4 d with concanavalin A in the presence of increasing doses (above plots) of ST (top) or HKST (bottom) (left margin). **e**, Frequency of IL-21⁺BCL-6⁺ cells in cultures as in **d** ($n = 3$ pigs). **f**, Frequency of IL-21⁺BCL-6⁺ cells among CD4⁺ T cells in cultures of porcine splenocytes stimulated for 4 d with medium (Ctrl), CL075, LPS or bacterial RNA (horizontal axis) in the presence of concanavalin A. Each symbol (**a**,**b**,**f**) represents an individual pig ($n = 3$ (IL-6 (**a**,**b**)) or 2 (IL-12p40 (**b**)) (**a**,**b**), or $n = 3$ (**f**)). $^*P < 0.05$, $^{**}P < 0.01$ and $^{***}P < 0.001$ (one-way ANOVA (**a**,**b**,**f**) or two-way ANOVA (**c**, **e**) with post-hoc correction for multiple comparisons). Data are representative of three experiments (error bars, maximum and minimum (**c**) or mean ± s.e.m. (**e**)).

of TLR8-G (Fig. 8a and Supplementary Table 3). The TLR8-A allele was associated with significantly increased odds for infection with *M. tuberculosis* (odds ratio = 1.94 [95% confidence interval, 1.194–3.156]; $P = 0.007$), and similar results were obtained for the subgroup of patients with PTB (Fig. 8a and Supplementary Table 3), indicative of a protective effect of TLR8-G against PTB, as has been reported[32]. Further subgroup analysis revealed that distribution of the *TLR8* allele was in fact significantly different only for subjects who had previously received the live BCG vaccine against TB ($P = 0.002$), whereas its distribution was not significantly different for unvaccinated subjects ($P = 0.754$) (Fig. 8a and Supplementary Table 4). In this study, vaccination with BCG was associated with significant risk protection in carriers of the TLR8-G allele (odds ratio = 0.280 [95% confidence interval, 0.105–0.742]) but not in carriers of the TLR8-A allele (Fig. 8b and Supplementary Table 4). These epidemiological results indicated that TLR8-G was associated with improved BCG vaccine–mediated protection without affecting susceptibility to PTB itself, and they linked the function of TLR8 to protective immunity in response to a live bacterial vaccine in a large human cohort.

Discussion

Here we have identified the recognition of microbial viability as a hard-wired, conserved immune checkpoint that regulates innate and adaptive immunity. We have described TLR8 as a receptor for vita-PAMPs in humans and pigs. Activation of TLR8 by bacterial RNA served to distinguish live bacteria from dead bacteria and controlled downstream cytokine and T_{FH} cell responses. Accordingly, we found that carriage of a hypermorphic *TLR8* polymorphism was associated with improved vaccine-induced protection. Immunization with live attenuated bacteria induced T_{FH} cell differentiation and antibody responses in pigs, but immunization with the killed version of the same vaccine did not. Hence, we have provided experimental and epidemiological evidence to support the proposal of a critical role for viability recognition and TLR8 signals in the immune response to live attenuated vaccines.

Despite the need for improved vaccine adjuvants, knowledge about the innate signals that control the differentiation of human T_{FH} cells is scarce. Heat-killed bacteria and LPS have been reported to induce T_{FH} cell differentiation mediated by human monocyte-derived DCs[33]. The apparent discrepancy with our findings that LPS and dead bacteria were poor stimulators of T_{FH} cell responses in primary monocytes and DCs can probably be explained by the fact that monocyte-derived DCs readily produce IL-12 due to differentiation in IL-4-containing medium[34], whereas we used primary cells not grown in IL-4-containing medium. Published mouse studies have suggested a T_{FH} cell–promoting effect of TLR agonists such as CpG DNA[35,36]. In human APCs, most TLR ligands are weak inducers of T_{FH} cell differentiation, relative to stimulation with viable bacteria or TLR8 agonists. However, the repertoire and function of innate immune receptors of mouse APCs differ from those of human APCs. For example, mouse TLR8 is unresponsive to single-stranded RNA[37]. The cytokine requirement for the differentiation of human T_{FH} cells is also different from that for mouse T_{FH} cells[9,18,20,38]. Thus, while innate sensing of bacterial RNA is a conserved trigger for T_{FH} cell and antibody responses in both species[7,39], the different signaling pathways have to be taken into account in the translation of findings from mouse vaccine studies to human vaccine studies. Interestingly, TLR8 agonists have been shown to possess unique adjuvant activity in other species, including non-human primates[40,41]. Here we studied

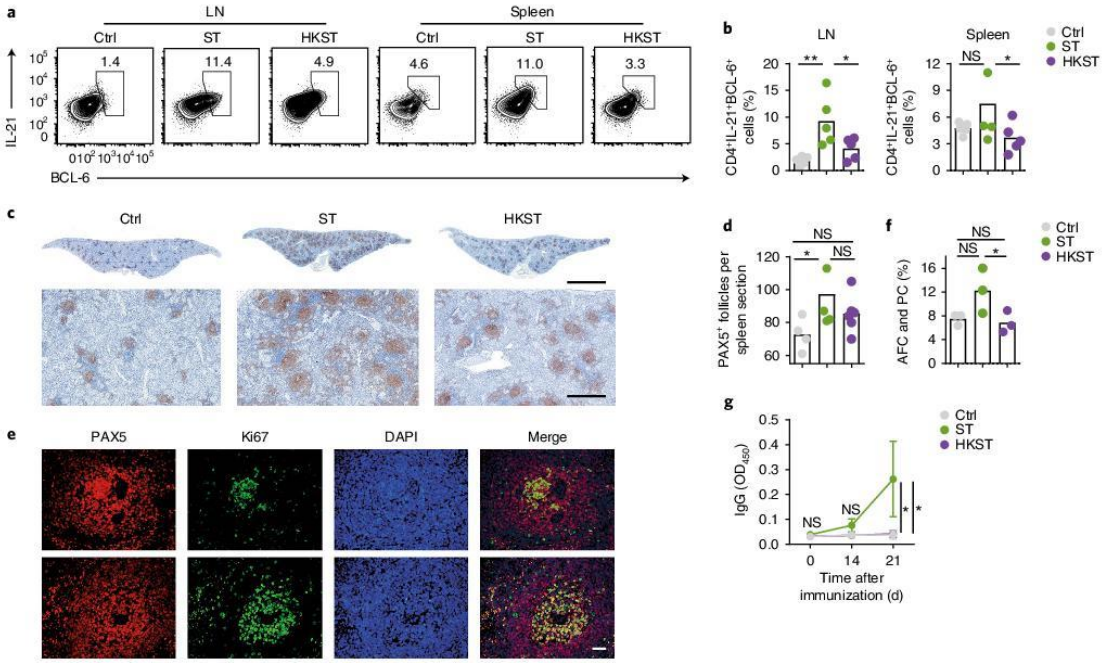

Fig. 7 | A live attenuated vaccine promotes T_{FH} cell differentiation in swine. a, Flow-cytometry analysis of the expression of IL-21 and BCL-6 by CD4+ T cells from the draining lymph nodes (LN) or spleen of 5-week-old domestic piglets on day 30 after subcutaneous immunization with saline (Ctrl), ST or HKST (above plots). **b**, Frequency of IL-21+BCL-6+ cells in lymph nodes or spleen (above plots) of pigs as in **a** (key). **c**, Microscopy of paraffin-embedded sections of spleen tissues from pigs as in **a** (above images), stained for the transcription factor PAX5. Scale bars, 5 mm (top) or 500 µm (bottom). **d**, Morphometric quantification of PAX5+ follicles in spleen sections of pigs as in **c** (key). **e**, Microscopy of co-immunofluorescence staining of PAX5 (red) and Ki67 (green) on sections of spleen from pigs vaccinated with ST; cell nuclei were stained with the DNA-binding dye DAPI (blue). Each row shows a follicle from a separate pig. Scale bar, 50 µm. **f**, Frequency of antibody-forming cells (AFC) and plasma cells (PC) among lymphocytes in spleen samples of pigs as in **c** (key), assessed by flow cytometry. **g**, ELISA of anti-*Salmonella* IgG in serum samples obtained from pigs as in **c** (key) before vaccination (day 0) and on day 14 and 21 after vaccination (horizontal axis), presented as the optical density at 450 nm (OD_{450}). Each symbol (**b**,**d**,**f**) represents an individual pig ($n = 5$ per group (**b**) or ($n = 3$ per group (**f**)). $^*P < 0.05$ and $^{**}P < 0.01$ (one-way ANOVA (**b**,**d**) or two-way ANOVA (**g**) with post-hoc correction for multiple comparisons). Data are representative of one experiment with various numbers of pigs in each panel (as indicated in legend above; error bars (**g**), mean ± s.e.m.).

vaccine responses to live attenuated bacteria in domestic pigs, given the closer resemblance of their physiology to human physiology than that of laboratory mice in terms of size, life span, organ anatomy, diet, circadian rhythm and immunity[24,42]. More importantly, domestic farm animals represent critical vaccine populations. Efficient vaccines would help to lower antibiotic consumption and thereby reduce the development of antibiotic resistance[43]. The emergence of zoonotic infections has added to the need for efficacious veterinary vaccines. Our study has provided the first evidence, to our knowledge, of T_{FH} cell–like cells in pigs and has described the induction of such cells after the recognition of live attenuated bacteria. While additional studies are needed for full characterization of the generation of protective immunity in pigs, our study contributes new insights into the mechanisms of live attenuated vaccines and highlights swine as a valuable species for research into T_{FH} cells and vaccines.

Our epidemiological study linked a hypermorphic *TLR8* polymorphism to enhanced vaccine-induced protection. The epidemiological data support our experimental observations and might also help to explain the variable efficacy of vaccination with BCG[44]. In contrast to several SNPs, primary TLR8 deficiency has not been reported so far. Patients with genetic defects in the TLR adaptors MyD88 or IRAK4 suffer from recurrent bacterial infections[45,46], but the frequency of T_{FH} cells in people with these rare gene defects has not been investigated. Individuals with loss-of-function mutations in the gene encoding the IL-12 receptor (*IL12RB1*) have a lower number of circulating T_{FH} cells and reduced GC formation in lymph nodes[38]. Other studies have reported a less-pronounced reduction in T_{FH} cells; however, these studies included fewer subjects[47,48]. Notably, antibody levels are largely normal in *IL12RB1*-deficient persons; however, the avidity of their serum IgG for some antigens is lower[38]. Better characterization of human immune responses in patients with primary immunodeficiencies might facilitate the identification of non-redundant pathways for efficient T_{FH} cell responses.

Given the broad functionality of high-affinity antibody responses, it has been proposed that microbial stimulation, or PAMPs in general, induce the formation of T_{FH} cells[9]. However, while high-affinity antibodies are indeed a versatile mechanism of defense against most pathogens, uncontrolled activation of T_{FH} cells can cause debilitating diseases and must be tightly controlled[17,49]. Antimicrobial immune responses are therefore tightly scaled to the level of the microbial threat[6]. The recognition of bacterial RNA as a molecular signature of microbial viability and increased microbial threat[7] constitutes a critical trigger for T_{FH} cell differentiation. This provides an efficient checkpoint for T_{FH} cell responses without limiting the versatility of high-affinity antibodies in antimicrobial host defense. Although live vaccines are diverse and activate multiple pathways, we propose

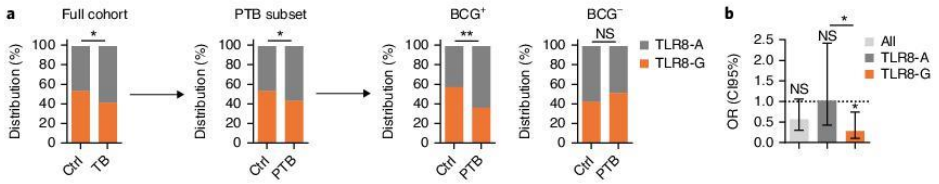

Fig. 8 | Association of a *TLR8* SNP with BCG-induced immunity. a, Distribution of the TLR8-A and TLR8-G alleles (key) in the entire cohort of subjects ($n=458$: $n=293$ subjects with confirmed TB and $n=165$ household contacts (Ctrl); horizontal axis) (far left) and in a subset of subjects ($n=345$: $n=180$ subjects with confirmed PTB and $n=165$ household contacts (Ctrl); horizontal axis) (middle left), and distribution of those alleles in BCG-vaccinated (BCG^+) and unvaccinated (BCG^-) subjects (above plots) with confirmed PTB and their household contacts (horizontal axis) (right; one subject excluded due to unclear vaccination status). **b**, Odds ratio (adjusted for sex, age and body mass index) for PTB in BCG-vaccinated versus unvaccinated subjects, calculated for the whole study population (All) and separately for each *TLR8* genotype (key), presented as odds ratio (OR) (bars) and 95% confidence interval (CI95%) (error bars). $^*P<0.05$ and $^{**}P<0.01$, TLR8-A versus TLR8-G (Wald's test).

the sensing of microbial viability by the innate immune system as a unifying motif of live attenuated vaccines. Thus, the identification of TLR8 as a critical sensor of vita-PAMPs will provide opportunities for the development of T_{FH} cell–targeted vaccine adjuvants, which are sorely needed to improve existing and future inanimate subunit vaccines directed against a broad range of infectious and non-infectious diseases.

Methods

Methods, including statements of data availability and any associated accession codes and references, are available at https://doi.org/10.1038/s41590-018-0068-4.

Received: 19 July 2016; Accepted: 15 February 2018;
Published online: 19 March 2018

References

1. Barquet, N. & Domingo, P. Smallpox: the triumph over the most terrible of the ministers of death. *Ann. Intern. Med.* **127**, 635–642 (1997).
2. Plotkin, S. A. & Plotkin, S. L. The development of vaccines: how the past led to the future. *Nat. Rev. Microbiol.* **9**, 889–893 (2011).
3. Minor, P. D. Live attenuated vaccines: Historical successes and current challenges. *Virology* **479–480**, 379–392 (2015).
4. De Gregorio, E. & Rappuoli, R. From empiricism to rational design: a personal perspective of the evolution of vaccine development. *Nat. Rev. Immunol.* **14**, 505–514 (2014).
5. Rauh, L. W. & Schmidt, R. Measles immunization with killed virus vaccine. Serum antibody titers and experience with exposure to measles epidemic. *Am. J. Dis. Child.* **109**, 232–237 (1965).
6. Blander, J. M. & Sander, L. E. Beyond pattern recognition: five immune checkpoints for scaling the microbial threat. *Nat. Rev. Immunol.* **12**, 215–225 (2012).
7. Sander, L. E. et al. Detection of prokaryotic mRNA signifies microbial viability and promotes immunity. *Nature* **474**, 385–389 (2011).
8. Iwasaki, A. & Medzhitov, R. Control of adaptive immunity by the innate immune system. *Nat. Immunol.* **16**, 343–353 (2015).
9. Crotty, S. T follicular helper cell differentiation, function, and roles in disease. *Immunity* **41**, 529–542 (2014).
10. Vinuesa, C. G., Linterman, M. A., Yu, D. & MacLennan, I. C. Follicular helper T cells. *Annu. Rev. Immunol.* **34**, 335–368 (2016).
11. Johnston, R. J. et al. Bcl6 and Blimp-1 are reciprocal and antagonistic regulators of T follicular helper cell differentiation. *Science* **325**, 1006–1010 (2009).
12. Nurieva, R. I. et al. Bcl6 mediates the development of T follicular helper cells. *Science* **325**, 1001–1005 (2009).
13. Linterman, M. A. et al. IL-21 acts directly on B cells to regulate Bcl-6 expression and germinal center responses. *J. Exp. Med.* **207**, 353–363 (2010).
14. Weber, J. P. et al. ICOS maintains the T follicular helper cell phenotype by down-regulating Kruppel-like factor 2. *J. Exp. Med.* **212**, 217–233 (2015).
15. Breitfeld, D. et al. Follicular B helper T cells express CXC chemokine receptor 5, localize to B cell follicles, and support immunoglobulin production. *J. Exp. Med.* **192**, 1545–1552 (2000).
16. Schaerli, P. et al. CXC chemokine receptor 5 expression defines follicular homing T cells with B cell helper function. *J. Exp. Med.* **192**, 1553–1562 (2000).
17. Ueno, H., Banchereau, J. & Vinuesa, C. G. Pathophysiology of T follicular helper cells in humans and mice. *Nat. Immunol.* **16**, 142–152 (2015).
18. Cucak, H., Yrlid, U., Reizis, B., Kalinke, U. & Johansson-Lindbom, B. Type I interferon signaling in dendritic cells stimulates the development of lymph-node-resident T follicular helper cells. *Immunity* **31**, 491–501 (2009).
19. Batten, M. et al. IL-27 supports germinal center function by enhancing IL-21 production and the function of T follicular helper cells. *J. Exp. Med.* **207**, 2895–2906 (2010).
20. Schmitt, N. et al. The cytokine TGF-β co-opts signaling via STAT3-STAT4 to promote the differentiation of human TFH cells. *Nat. Immunol.* **15**, 856–865 (2014).
21. Jacquemin, C. et al. OX40 ligand contributes to human lupus pathogenesis by promoting T follicular helper response. *Immunity* **42**, 1159–1170 (2015).
22. Eigenbrod, T., Pelka, K., Latz, E., Kreikemeyer, B. & Dalpke, A. H. TLR8 senses bacterial RNA in human monocytes and plays a nonredundant role for recognition of *Streptococcus pyogenes*. *J. Immunol.* **195**, 1092–1099 (2015).
23. Bergstrom, B. et al. TLR8 senses *Staphylococcus aureus* RNA in human primary monocytes and macrophages and induces IFN-β production via a TAK1-IKKβ-IRF5 signaling pathway. *J. Immunol.* **195**, 1100–1111 (2015).
24. Meurens, F., Summerfield, A., Nauwynck, H., Saif, L. & Gerdts, V. The pig: a model for human infectious diseases. *Trends Microbiol.* **20**, 50–57 (2012).
25. Mair, K. H. et al. The porcine innate immune system: an update. *Dev. Comp. Immunol.* **45**, 321–343 (2014).
26. Zhu, J., Lai, K., Brownile, R., Babiuk, L. A. & Mutwiri, G. K. Porcine TLR8 and TLR7 are both activated by a selective TLR7 ligand, imiquimod. *Mol. Immunol.* **45**, 3238–3243 (2008).
27. Springer S., Lindner T., Steinbach G., Selbitz H. J. Investigation of the efficacy of a genetically-stabile live *Salmonella typhimurium* vaccine for use in swine. *Berl. Munch. Tierarztl. Wochenschr.* **114**,342–345 (2001).
28. Sinkora, M., Stepanova, K. & Sinkorova, J. Different anti-CD21 antibodies can be used to discriminate developmentally and functionally different subsets of B lymphocytes in circulation of pigs. *Dev. Comp. Immunol.* **39**, 409–418 (2013).
29. Oh, D. Y. et al. A functional toll-like receptor 8 variant is associated with HIV disease restriction. *J. Infect. Dis.* **198**, 701–709 (2008).
30. Wang, C. H. et al. TLR7 and TLR8 gene variations and susceptibility to hepatitis C virus infection. *PLoS One* **6**, e26235 (2011).
31. Tanji, H., Ohto, U., Shibata, T., Miyake, K. & Shimizu, T. Structural reorganization of the Toll-like receptor 8 dimer induced by agonistic ligands. *Science* **339**, 1426–1429 (2013).
32. Davila, S. et al. Genetic association and expression studies indicate a role of toll-like receptor 8 in pulmonary tuberculosis. *PLoS Genet.* **4**, e1000218 (2008).
33. Schmitt, N. et al. Human dendritic cells induce the differentiation of interleukin-21-producing T follicular helper-like cells through interleukin-12. *Immunity* **31**, 158–169 (2009).
34. Hochrein, H. et al. Interleukin (IL)-4 is a major regulatory cytokine governing bioactive IL-12 production by mouse and human dendritic cells. *J. Exp. Med.* **192**, 823–833 (2000).
35. Jones, S. C., Brahmakshatriya, V., Huston, G., Dibble, J. & Swain, S. L. TLR-activated dendritic cells enhance the response of aged naive CD4 T cells via an IL-6-dependent mechanism. *J. Immunol.* **185**, 6783–6794 (2010).
36. Chakarov, S. & Fazilleau, N. Monocyte-derived dendritic cells promote T follicular helper cell differentiation. *EMBO Mol. Med.* **6**, 590–603 (2014).

37. Heil, F. et al. Species-specific recognition of single-stranded RNA via toll-like receptor 7 and 8. *Science* **303**, 1526–1529 (2004).
38. Schmitt, N. et al. IL-12 receptor beta1 deficiency alters in vivo T follicular helper cell response in humans. *Blood* **121**, 3375–3385 (2013).
39. Barbet, G. et al. Sensing microbial viability through bacterial RNA augments T follicular helper cell and antibody responses. *Immunity* (in the press).
40. Dowling, D. J. et al. TLR7/8 adjuvant overcomes newborn hyporesponsiveness to pneumococcal conjugate vaccine at birth. *JCI Insight* **2**, e91020 (2017).
41. Dowling, D. J. et al. Toll-like receptor 8 agonist nanoparticles mimic immunomodulating effects of the live BCG vaccine and enhance neonatal innate and adaptive immune responses. *J. Allergy Clin. Immunol.* **140**, 1339–1350 (2017).
42. Fairbairn, L., Kapetanovic, R., Sester, D. P. & Hume, D. A. The mononuclear phagocyte system of the pig as a model for understanding human innate immunity and disease. *J. Leukoc. Biol.* **89**, 855–871 (2011).
43. Landers, T. F., Cohen, B., Wittum, T. E. & Larson, E. L. A review of antibiotic use in food animals: perspective, policy, and potential. *Public Health Rep.* **127**, 4–22 (2012).
44. Colditz, G. A. et al. Efficacy of BCG vaccine in the prevention of tuberculosis. Meta-analysis of the published literature. *J. Am. Med. Assoc.* **271**, 698–702 (1994).
45. de Beaucoudrey, L. et al. Revisiting human IL-12Rβ deficiency: a survey of 141 patients from 30 countries. *Medicine (Baltimore)* **89**, 381–402 (2010).
46. Picard, C. et al. Clinical features and outcome of patients with IRAK-4 and MyD88 deficiency. *Medicine (Baltimore)* **89**, 403–425 (2010).
47. Ma, C. S. et al. Functional STAT3 deficiency compromises the generation of human T follicular helper cells. *Blood* **119**, 3997–4008 (2012).
48. Ma, C. S. et al. Monogenic mutations differentially affect the quantity and quality of T follicular helper cells in patients with human primary immunodeficiencies. *J. Allergy Clin. Immunol.* **136**, 993–1006 (2015).
49. Rao, D. A. et al. Pathologically expanded peripheral T helper cell subset drives B cells in rheumatoid arthritis. *Nature* **542**, 110–114 (2017).

Acknowledgements

We thank D. Kunkel, S. Warth and A. Linke for technical advice; the flow cytometry facility of the Berlin Brandenburg Center for Regenerative Therapies (BCRT) of the Charité Berlin; S. Springer and IDT Biologika for assistance in planning the animal studies and for the Salmoporc STM vaccine; and R. Nifosi for critical review of the modelling analysis. Supported by the German Research Council (DFG grant SA1940-2/1 and SFB-TR84 TP C8 to L.E.S.; SFB-TR84 TP B1 to N.S.; SFB-TR-84 TP A1/A5 to B.O.; SFB-TR84 TP Z1b to A.D.G.; DFG-GRK 1673 project to R.R.S.; and DFG-GRK 2046, TP4 to S.H.), the European Research Council and the Federal Ministry of Education and Research (FP-7 ERA-NET / Infect-ERA consortium "HaploINFECT" / BMBF 031A402A to L.E.S., VIP + VALNEMCYS project and InfectControl 2020, consortium Art4Fun to S.H.), the European Society of Clinical Microbiology and Infectious Diseases (ESCMID research grant to L.E.S.), the Jürgen Manchot Foundation (Doctoral Research Fellowship to P.G., E.T.H. and S.M.V.), the Netherlands Nutrigenomics Center, Wageningen University, The Netherlands (to M.M. and M.B.), the Fritz Thyssen Foundation (research grant to A.H.), The Danish National Research Foundation (grant no. DNRF108 to) to Research Centre for Vitamins and Vaccines (CVIVA) supporting K.J.J., and The Novo Nordisk Foundation supporting the pig vaccination experiments at Technical University of Denmark, Federal Ministry of Education and Research.

Author contributions

M.U. and J.G. designed and performed experiments; S.B. analyzed clinical data and performed experiments; K.J.J., C.S.B., G.J. and L.E.S. planned and performed animal studies; P.G., F.E., S.M.V., S.T., K.D., L.B. and E.T.H. performed experiments; M.U., J.G., P.G., F.E., S.M.V., K.D., B.O., F.K., A.D.G., A.H., S.H., M.M., N.S. and L.E.S. analyzed data and wrote the manuscript; S.S. performed structure prediction analysis; N.D., S.G., M.L.C. and R.R.S. designed and performed clinical studies; A.S. and U.B. provided samples and conceptual input; M.V.B. performed transcriptome analysis; and L.E.S. conceived of the study and designed experiments.

Competing interests

The authors declare no competing interests.

Additional information

Supplementary information is available for this paper at https://doi.org/10.1038/s41590-018-0068-4.

Reprints and permissions information is available at www.nature.com/reprints.

Correspondence and requests for materials should be addressed to L.E.S.

Publisher's note: Springer Nature remains neutral with regard to jurisdictional claims in published maps and institutional affiliations.

Methods

Cell isolation and culture. Human monocytes, T cells and B cells used in this study were either freshly isolated from peripheral venous blood of healthy volunteers or from buffy coats obtained from the German Red Cross Blood Transfusion Service, Berlin, Germany. Permission for experiments with human primary cells was obtained from Charité ethic committee (Charité – Universitätsmedizin Berlin, Germany). Peripheral blood mononuclear cells (PBMCs) were isolated by density gradient centrifugation over Histopaque-1077 (Sigma-Aldrich). $CD14^+CD16^-$ monocytes were purified by negative selection via immunomagnetic separation using EasySep monocyte isolation kits with CD16 depletion (StemCell Technologies) according to the manufacturer's instructions. Isolated monocytes were cultured at a density of 1×10^6 cells per ml in RPMI1640 supplemented with 10% FCS, 1% glutamine, 1% HEPES buffer and 1% non-essential amino acids (all from Sigma-Aldrich). T cells were cultured in RPMI1640 supplemented with 10% human serum (from the same T cell donor), 1% glutamine, 1% HEPES buffer and 1% non-essential amino acids; some T cell conditions were supplemented with 2.5 ng/ml of TGF-β (eBioscience). All cells were grown at 37 °C, 5% CO_2 in a humidified incubator.

Untreated human $CD1^+$ mDCs were purified by negative selection via immunomagnetic bead separation (Miltenyi Biotec) following the manufacturer's instructions.

Naive $CD4^+$ T cells were purified by immunomagnetic separation using negative selection (MagniSort Human CD4 Naive T cell Enrichment Kit, eBioscience). Total $CD4^+$ T cells (used in Figs. 3a,b,d and 4f,g and Supplementary Fig. 3) were isolated by magnetic separation using negative selection (MagniSort Human CD4 T cell Enrichment Kit, eBioscience).

Untreated naive human B cells were isolated by immunomagnetic bead separation (Miltenyi Biotec) following the manufacturer's instructions.

Cell purity was routinely checked by flow cytometry and only cells with a purity of > 85% (monocytes) or > 95% (T cells and B cells) were used for subsequent experiments.

Bacteria and infection. *Escherichia coli* K12, strain DH5α, thymidine auxotrophs (*thyA*$^-$) were selected as previously described[4]. Auxotrophy was confirmed by inoculation and overnight culture of single colonies in LB medium. *ThyA*$^-$ *E. coli* (EC) grew only in the presence of thymidine and were resistant to trimethoprim. For phagocytosis experiments, EC were grown to mid-log phase and were washed twice in phosphate-buffered saline (PBS) to remove thymidine and LB salts before addition to cells. For heat killing, EC were grown to log phase, were washed and re-suspended in PBS at an optical density at 600 nm (OD_{600}) of 0.6, and were subsequently incubated at 60 °C for 90 min. Heat-killed *thyA*$^-$ *E. coli* (HKEC) were used immediately after killing or were stored at –80 °C for up to 3 months. Efficient killing was confirmed by overnight plating on thymidine-trimethoprim–supplemented LB-agar plates. Alternatively, *Bacillus subtilis* strain 168 was used for analogous infection experiments. For heat killing, *B. subtilis* were grown to mid-log phase, were washed and re-suspended in PBS at an optical density at 600 nm (OD_{600}) of 0.6, and were subsequently incubated at 95 °C for 30 min. Efficient killing was confirmed by overnight plating on LB-agar plates. For heat killing, *S. enterica* serovar Typhimurium were grown to mid-log phase, were washed and re-suspended in PBS at an optical density at 600 nm (OD_{600}) of 0.6, and were subsequently incubated at 95 °C for 30 min. Efficient killing was confirmed by overnight plating on LB-agar plates. Infection of human monocyte was performed at the multiplicity of infection (MOI) indicated in the figure or text.

BCG were grown in Middlebrook 7H9 medium supplemented with 0.05% Tween 80. For phagocytosis experiments, BCG were grown to mid-log phase, were washed once in phosphate buffered saline (PBS) and were resuspended in complete cell culture media via repeated tuberculin type needle passages (10×). For heat killing, BCG were grown to log phase and were incubated at 60 °C for 90 min. Heat-killed BCG (HKBCG) were used immediately after killing. Efficient killing was confirmed by 96 h of inoculation in competent media.

Co-culture assay. For monocyte–T cell co-cultures, monocytes were cultured as described above and were stimulated as indicated (for example, EC, HKEC MOI 1–25) in antibiotics-free medium. After 1.5 h, penicillin-streptomycin (1%) was added, together with autologous naive $CD4^+$ T cells at a monocyte/T cell ratio of 2:1, plus staphylococcal enterotoxin B (SEB, Sigma) at a concentration of 1.0 µg/ml. After 5 d of co-culture T cells were harvested and washed, then were restimulated with phorbol-12-myristat-13-acetat (PMA, 50ng/ml) and ionomycin (1 µg/ml, both obtained from Sigma), stained and analyzed by flow cytometry.

For T cell–B cell co-cultures, T cells were differentiated by co-culture with autologous monocytes for 6 d as described in the previous subsection. $CXCR5^+ICOS^+PD\text{-}1^{hi}$ T cells were sorted by flow cytometry (BD FACSAria II) and were added to naive autologous B cells at a T cell/B cell ratio of 1:2 in the presence of SEB (1µg/ml). After 12 d of co-culture, B cells and T cells were harvested and analyzed by flow cytometry. For analysis of plasmablast differentiation, sorted T_{FH} cells ($CD19^-CD4^+CD45RA^-CXCR5^+$) or naive T cells ($CD19^-CD4^+CD45RA^+$) were co-cultured with memory B cells at a ratio of 1:1 in the presence of 4 ng/ml SEB for 7 d.

Antibodies and reagents. Antibodies to the following antigens were used for flow cytometry: CD3 (UCHT1, cat.: 300415), CD4 (OKT4, cat.: 317424), IFN-γ (4S.B3, cat.: 502528), IL-17 (BL168, cat.: 512306), CXCR5 (J252D4, cat.: 356904), PD-1 (EH12.2H7, cat.: 329922), ICOS (C398.4A, cat.: 313510), CD19 (HIB19, cat.: 302228 or SJ25C1, cat.: 363022), CD20 (2H7, cat.: 302324), CD27 (O323, cat.: 302810), CD38 (HIT2, cat.: 303516 or or M-T271, cat.: 356418), IgM (MHM-88, cat.: 314520), IgD (IA6-2, cat.: 348216), MHC2 (L243, cat.: 307610), IL-1β (H1B-27, cat.: 511604), mouse-IgG (Poly4053, cat.: 405317) or Zombie violet (cat.: 423113) (all from BioLegend); IFNAR (polyclonal, cat.: ab10739, Abcam); BCL-6 (K112-91, cat.: 561522/ 561525, BD); IL-21 (ebio3A3-N2, cat.: 50-7219, eBioscience); CD14 (TÜK4, cat.: 130-096-875, Miltenyi Biotec); CD38 (OKT 10, CRL-8022, ATCC); porcine monocyte-granulocyte (74-22-15A, cat.: 561499), porcine CD3 (BB23-8E6-8C8, cat.: 561478), porcine CD4 (74-12-4-RUO, cat.: 561472), porcine CD8b (295/33-25, cat.: 561484) and porcine CD8a (76-2-11, cat.: 561475) (all from BD); IL-21 (polyclonal, cat.: orb9043, Biorbyt); porcine CD2 (MSA4, cat.: WS0590S-100) and porcine TCR1 δ (PGBL22A, cat.: WS0621S-100 (both from Kingfischer Biotech); porcine SLA class II DR (2E9/13, cat.: MCA2314F, AbD Serotec); porcine CD21 (BB6-11C9.6, cat.: SBA-4530-09, Southern Biotech); porcine IgM (polyclonal, cat.: AAI48B, Bio-Rad); and streptavidin (cat.: 25-4317-82), Foxp3 (FJK-16s, cat.: 48-5773-82) and T-bet (eBio4B10, cat.: 12-5825-82) (all from eBioscience). Fixable Viability Dyes (cat.: 65-0865-14 and 65-0866-14) were from eBioscience).

Neutralizing antibodies were as follows: anti-IL-6 (6708, cat.: MAB206-SP, R&D Systems), anti-IL-12 (B-T21, cat.: BMS152, eBioscience) and anti-TNF (MAb11, cat.: 502901, Biolegend), used at 10 µg/ml; and anti-IL-27 (307426, cat.: MAB25261 F, R&D Systems), used at 5µg/ml.

Recombinant cytokines were as follows: rIL-12 (eBioscience), used at 100 pg/ml; and rTNF, rIL-6 (eBioscience) and rIL-27 (R&D Systems), used at 10 ng/ml.

The following TLR ligands were purchased from Invivogen and were used at the following concentrations: CL075 (3M002; 1 µg/ml), LPS-EK Ultrapure (2 µg/ml), Pam_3CSK_4 (200 ng/ml), poly(I:C) LMW (2 µg/ml) and ODN 2395 (5 µM). Bacterial RNA was isolated from mid-log phase cultures of DH5alpha *E. coli* using Trizol (Life Technologies, Karlsruhe, Germany). Transfection of bacterial RNA into human monocytes was performed using polycationic polypeptide poly-L-arginine (pLa) (Sigma-Aldrich).

Enzyme-linked immunosorbent assay (ELISA). The concentration of TNF, IL-1β, IL-6, IL-10, IL-12p40, IL-23, GM-CSF and IL-27 in culture supernatants was measured by ELISA (all purchased from eBioscience) according to standard manufacturer's recommendations. Concentrations of IL-12p70 were measured using a human IL-12p70 High Sensitivity ELISA kit (eBioscience). The samples were analyzed for absorbance at 450 nm using FilterMax F5 Multi-Mode Microplate Reader (Molecular Devices). The concentration of porcine IL-12p40 and IL-6 in culture supernatants were measured by ProcartaPlex Pig Kit (eBioscience) or by Quantikine ELISA kit (R&D Systems), and results were collected using a Luminex MAGPIX instrument (Merck Millipore). Human IgG was determined by ELISA using polyclonal goat anti-human IgG (polyclonal, cat.: AHI0301, TAGO Immunologicals) and purified human IgG (purified from serum, cat.: I2511, Sigma) as standard. Results were collected on a Spark multimode reader (Tecan, Männedorf, Switzerland).

Anti–*S. enterica* IgG ELISA. 96-well microtiter plates were coated overnight with lysates of *S. enterica* serovar Typhimurium (Salmoporc-STM) (3µg/ml) that we generated from log-phase cultures of *Hys*$^-$ *Ade*$^-$ *S. enterica*. Serum samples from immunized pigs were serially diluted (12 dilutions) and were incubated in the pre-coated plates for 12 h at 4 °C, followed by washing and incubation with affinity-purified polyclonal goat antibody to swine IgG labeled with HRP (goat anti-pig IgG (gamma)-HRP, SeraCare Life Sciences, cat.:5220-0363 14-14-06, polyclonal) for 1 h. Bound goat anti-pig IgG (gamma)-HRP was visualized by the addition of TMB substrate (Thermo Fisher), and the titer of antibodies to *S. enterica* for each animal was visualized as absorbance readings at 450 nm at a set serum dilution of 1 to 51,200.

RNA isolation. $CD14^+CD16^-$ human monocytes were sorted by flow cytometry and were infected with EC at MOI = 10 or stimulated with HKEC at 10:1 ratio of bacteria to cells. After 6 h, cells were harvested, washed once in PBS and lysed in Trizol (Life Technologies). Total RNA was prepared according to the manufacturer's suggested protocol.

Gene array. Total RNA was prepared from four independent experiments (four separate donors) according to the Trizol manufacturer's protocol. Samples were further purified on columns (RNeasy Micro Kit, Qiagen).

RNA integrity was checked on an Agilent 2100 Bioanalyser (Agilent Technologies) with 6000 Nano Chips. RNA was judged as suitable only if samples showed intact bands of 18 S and 28 S ribosomal RNA subunits, displayed no chromosomal peaks or RNA degradation products, and had a RNA integrity number (RIN) above 8.0.

100 ng RNA was used for whole-transcript cDNA synthesis with the Ambion WT expression kit (Life Technologies). Hybridization, washing and scanning

of an Affymetrix GeneChip Human Gene 1.1 ST 24-array plate was carried out according to standard Affymetrix protocols on a GeneTitan instrument (Affymetrix).

Quality control, normalization and statistical analysis were performed using MADMAX, a pipeline consisting of integrated Bioconductor packages[50]. Probe sets were redefined according a published article using current genome information[51]. Normalized gene-expression estimates were obtained from the raw intensity values by using the robust multiarray analysis preprocessing algorithm available in the library AffyPLM using default settings[52]. Only genes that were targeted by at least seven probes, reached $\log_2$ expression of > 4.32 on at least three microarrays and had a $\log_2$ interquartile range value of > 0.25 across all samples were considered for further analysis. Intensity-based moderated *t*-statistics were applied for pairwise comparisons to identify differentially regulated genes[53]. To correct for multiple testing, a false-discovery rate method was used to calculate *q* values[54]. A *q* value of < 0.01 was considered significant.

RNA-mediated interference. Silencer Select siRNA duplexes targeting TLR8 (sequence ID: s27920, s27921 and s27922), MyD88 (sequence ID: s9136, s9137 and s9138) and negative controls were obtained from Life Technologies. Monocytes cultured in 96-well plates were transfected with 25 nM of each siRNA using Viromer Blue transfection reagent (Lipocalyx) following manufacturer recommendations for sensitive cells and reverse transfection. Cells were plated at a density of 5×10^5 cells per ml in a final volume of 100 µl in 96-well plates. At 48 h after transfection, cells were infected or treated as described in the text or figure legends. Knockdown of TLR8 and Myd88 was confirmed 48 h after transfection of siRNA by RT-PCR using specific primers (TLR8: forward primer 5′-AGTTTCTCTTCTCGGCCACC-3′ and reverse primer, 5′-ACATGTTTTCCATGTTTCTGTTGT -3′, MyD88: forward primer 5′-TCTCCAGGTGCCCATCAGAA-3′ and reverse primer 5′-GGTTGGTGTAGTCGCAGACA-3′).

Four custom-designed Silencer Select siRNA duplexes targeting porcine TLR8 (combination of four siRNA duplexes) were purchased from Life Technologies, with the following sequences:

TLR8-1 sense: 5′-GCAAAUUGAUUUACCAUUTT-3′;
antisense: 5′-AAUGGUAAAAUCAAUUUGCTT-3′;
TLR8-2 sense: 5′-GAUUUAAGCUUGAACAGUATT-3′;
antisense: 5′-UACUGUUCAAGCUUAAAUCTA-3′;
TLR8-3 sense: 5′-GCAUCUUUACUUUAACAGATT-3′;
antisense: 5′-UCUGUUAAAGUAAAGAUGCTG-3′;
TLR8-4 sense: 5′-CAAUAUUCGUUUUAACCAATT-3′;
antisense: 5′-UUGGUUAAAACGAAUAUUGTC-3′;

Porcine $CD14^+$ monocytes cultured in 96-well plates were transfected with 25 nM of each siRNA following the protocol described above for human cells. At 48 h after transfection, cells were infected or treated as described in the text or figure legends.

Flow cytometry and cell sorting. Flow cytometry regularly was performed on a BD FACSCanto II cytometer Data was analyzed using FlowJo software Version: 7.6.5 (Treestar).

$CD14^+CD16^-$ monocytes were sorted from PBMCs on a BD FACSAria II SORP cell sorter (BD Biosciences) $CD4^+CXCR5^+$ and $CD4^+CXCR5^-$ T cells were sorted from monocyte–T cell co-cultures on a BD FACSAria II SORP cell sorter. In vitro–generated T_{FH} cells were sorted on a FACSARIA II sorter as $CD19^-CD4^+CD45RA^-CXCR5^+$ cells, and naive T cells were sorted as $CD19^-CD4^+CD45RA^+$ cells. Memory B cells were sorted from human tonsils as $CD4^-CD19^+IgD^-CD38^-$ cells. Cell-purity checks were performed, and a purity of > 97% was confirmed.

QuantiGene Plex transcript analysis. Quantigene multiplex-plex assay (Affymetrix) was performed to quantify the expression of *GATA3*, *MAF*, *IL21*, *TBX21*, *RORC*, *FOXO1* and *BCL6* and two housekeeper genes (*ACTB* and *HPRT1*) according to the manufacturer's protocol. In brief, $CD4^+$ T cells were lysed at a concentration of 500 cells per microliter of lysis mixture supplemented with proteinase K and were incubated at 50 °C for 30 min before their addition to a hybridization plate. The hybridization plate was sealed with heat-sealing foil and was placed in a shaking incubator (VorTemp 56) at 54 ± 1 °C and 600 r.p.m. to allow the samples to hybridize for 18–22 h. Fluorescent bead signal detection was obtained using Bio-Plex Suspension Array System (Bio-Rad Laboratories). The mean fluorescence intensity for each probe was recorded.

Animal experiments. The animal experiments were performed in accordance with the Danish Animal Welfare Act under approval and authorization issued by the Danish Animal Experiment Inspectorate.

In total, 18 5-week-old pigs (Danish Landrace/Danish Yorkshire crossbreeds, paternal lineage Duroc) of both sexes, raised on a commercial farm (Bøgekærgård, Faxe, Denmark), were stratified by size (6.3–10.4 kg; average, 8.0 kg) and sex and were distributed into three groups. Animals in each group received 1 ml subcutaneous vaccination in the right side of the neck as follows: 1, live *Salmonella enterica* serovar Typhimurium vaccine (Salmoporc STM Ch.-B. 022 07 15, IDT Biologika) containing 3.32×10^8 CFU per dose, according to the product insert); 2, heat-inactivated (65° for 90 min) Salmoporc STM vaccine (HKST) using the same dose as in condition 1); or 3, saline alone. The live vaccine was administered within 2 h of reconstitution. The same immunization regimen was repeated as booster injections on day 14. Heat killing of the vaccine was confirmed by absence of bacterial growth on LB plates incubated at 37 °C for 24 h. Throughout the experiment, the pigs were housed in two adjoining boxes, each box housing equal numbers of animals from each of the three treatment groups. One pig in the live vaccine group was euthanized on day 19 of the experiment due to severe umbilical hernia unrelated to the vaccine. One pig in the control group developed fever, dyspnea and generalized fatigue on day 0 of the experiment and was suspected of having pneumonia; this pig was therefore treated successfully with 160 mg benzylpenicillin and 200 mg dihydrostreptomycin (0.8 ml Streptocillin Vet) over 3 consecutive days and was excluded from the analysis. Five animals per group were included in the final analyses.

Animals were killed according to regulations. Transverse sections of spleen and prescapular lymph node (LN, cervicalis superficialis dorsalis) draining from the injection site were fixated in 10% neutral-buffered formalin (4% formaldehyde, Pioneer Research Chemicals Ltd) for immunohistochemistry. The remaining LN and spleen tissues samples were homogenized using disposable scalpels, and single-cell suspensions were isolated by forcing homogenized tissue samples through a cell strainer (70 µm, Greiner Bio-One), followed by two washes with RPMI1640 and subsequent culture in RPMI1640 supplemented with 10% FCS (FCS), 1% glutamine, 1% HEPES buffer and 1% non-essential amino acids (all from Sigma-Aldrich).

For in vitro experiments reported in Fig. 6 and Supplementary Fig. 4, spleen samples were collected from German Landrace pigs of both sexes between 8 weeks and 1 year of age. Single-cell suspensions were prepared as described above.

Splenocytes were cultured in IMDM (Pan-Biotech) supplemented with 10% FCS and were stimulated with ST, HKST (MOI: 0.1, 0.5, 1, 3), LPS (2 µg/ml), CL075 (1 µg/ml) or pLa (280 ng) plus RNA (237 ng) in the presence of concavalin A (2 µg/ml) (Fisherscientific). After 1 h, penicillin-streptomycin (1%) was added. After 4 d, cells were restimulated with phorbol-12-myristat-13-acetat (PMA, 50 ng/ml) and ionomycin (1 µg/ml) (both obtained from Sigma) and then were harvested, washed and analyzed by flow cytometry. Live and dead cells were discriminated using Zombie Violet Fixable Viability Kit (Biolegend); dead cells were excluded from the analysis.

Immunohistochemistry. Spleen samples were immersion-fixed in formalin and embedded in paraffin and were cut into 2-µm sections for immunohistochemical analyses after dewaxing in xylene and rehydration in decreasing ethanol concentrations. For detection of PAX5, Ki67 and BCL22, heat-mediated antigen retrieval was performed in 10 mM citric acid (pH 6.0), microwaved at 600 W for 12 min. Spleen sections were incubated with a purified mouse monoclonal antibody to PAX5 (1:400, clone 24/Pax5, BD Biosciences) or BCL2 (1:100, LS-B2352, LSBio) or with a purified rabbit antibody monoclonal to Ki67 (1:150, clone SP6, Cell Marque) at 4 °C overnight. Incubation with an irrelevant immunopurified mouse antibody (Anti-MUC5b, ab77995, clone 19.4E, Abcam) or rabbit antibody (Anti-Villin, ab130751, clone SP145, Abcam) at the same dilution served as negative controls. Slides were incubated with the biotinylated secondary antibodies goat anti-mouse IgG (1:200, BA 9200, Vector) or goat anti-rabbit IgG (1:200, BA 1000, Vector) and HRP-coupled streptavidin. Diaminobenzidine (DAB) was used as substrate for color development. All slides were counterstained with hematoxylin, dehydrated through graded ethanol, were cleared in xylene and were coverslipped. Whole slide images of spleen tissues were generated by Aperio CS2 digital pathology scanner (Leica Biosystems Imaging).

Immunofluorescence. For immunofluorescent co-staining of PAX5 and Ki67, slides were incubated with the purified mouse monoclonal antibody to PAX5 (clone 24/Pax5, 610863, BD Biosciences,1:50) overnight at 4 °C as described above and with the Alexa Fluor 568–conjugated secondary antibody goat anti-mouse IgG (1:200, polyclonal, A-21124, Thermo Fisher Scientific) for 45 min at room temperature. Slides were then incubated with a purified rat antibody monoclonal to Ki67 (1:100, clone SolA15, eBioscience) at 4 °C overnight, then were incubated with the Alexa Fluor 488–conjugated secondary antibody goat anti-rat IgG (1:200, Thermo Fisher Scientific) for 45 min at room temperature and were mounted with Roti-Mount Fluor-Care DAPI (4,6-diaminidino-2-phenylindole, Carl Roth). Adequate negative controls, including incubation of slides with only one primary but both secondary antibodies, were conducted. Slides were analyzed by immunofluorescence microscopy with an Olympus BX41 microscope equipped with a DP80 camera (Olympus).

Case-control study. Samples of patients with TB and healthy volunteers were collected at Mahavir Hospital, Hyderabad (India); the generated cohort has been described before[55]. Informed consent was obtained from all subjects, and all investigations were conducted according to the principles of the Helsinki Declaration. Written approval was obtained from the research ethics board of the Central University of Hyderabad and Mahavir Hospital. Patients were enrolled in the Revised National Tuberculosis Control Program (RNTCP) of India, and recruited into the study on the day of treatment initiation (according to DOTS

strategy). Subjects positive for human immunodeficiency virus and those who had relapsed with TB were excluded from the cohort. The diagnosis of TB was based on clinical examination, chest X-ray, positive sputum test or histopathology. Healthy household contacts of the patients with TB were recruited as controls to ensure comparable exposure rates and environmental conditions. BCG-vaccination status was determined by the presence of a BCG-related skin scar. The cohort consisted of 293 patients and 165 control subjects. 61,4% of the patients with TB had pulmonary TB (PTB) and 38.6% had extra-pulmonary TB (ETB). The control subjects were significantly older (34.2 ± 9.3 years of age (mean ± s.e.m. throughout)) than the patients (25.4 ± 10.4 years of age; $t(456) = 8.787$; $P < 0.0001$) and had a significantly higher mean BMI (23.8 ± 4.9 (control) versus 18.0 ± 4.1 (patient); $t(292.8) = 12.995$; $P < 0.0001$). Sex distribution did not differ significantly between control subjects (59.4% females) and patients (61.8% females). The differences in age and BMI were corrected for through the use of a binary logistic regression model.

SNP analysis. DNA was extracted from buccal swabs of all study subjects using a FlexiGene DNA extraction Kit (Qiagen). *TLR8* SNPs were analyzed by real-time PCR on a Light Cycler instrument (Roche) using the following PCR primer sets:
forward 5′-TCAGGAAGTTAGCCAGTTTCTC-3′,
reverse 5′-CCTGCATTTACAGTTGTTTCGAT-3′,
sensor 5′-AAATAGAAGTGGCTTACCACGTTTCTG-3′T-FITC,
anchor Cy5-5′-TTCTAATTTTTCATTCCGTAACTTGCAGCAGCGCA-3′.
On the basis of previous observations that the presence of an A nucleotide defines the functionality, we defined the A/AA/AG as the allele encoding TLR8-A, and G/GG as the status of the allele encoding TLR8-G for our analysis.

Statistical analysis. Statistical analyses of in vitro experiments were performed using one-way ANOVA and Holm-Sidak's multiple comparisons test, or two-way ANOVA, or Wilcoxon's matched-pairs signed-rank test, or linear-regression analysis where appropriate. Calculations were performed using GraphPad Prism 6 Software (GraphPad Software).

For all statistical analysis, a P value of < 0.05 was considered statistically significant. 95% confidence intervals are provided in squared brackets in Supplementary Tables 3 and 4 (as '[CI 95%]'). Baseline characteristics of the study population were analyzed using Atudent's t-test or Pearson's chi-squared (χ^2) test. *TLR8* allele frequencies were compared using binary logistic regression, summarizing recessive genotypes and adjusting for age, BMI and sex. The interaction between BCG stats and TLR8-A or TLR8-G was assessed using Wald's statistics. Statistical tests were performed using IBM SPSS Statistics 21 software and figures were generated using GraphPad Prism 6 Software.

Life Sciences Reporting Summary. Further information on experimental design is available in the Life Sciences Reporting Summary.

Data availability. The datasets generated during and/or analyzed during the current study are available from the corresponding author on reasonable request. The gene array data are publicly available in the Gene Expression Omnibus database (accession code GSE68255).

References

50. Lin, K. et al. MADMAX - Management and analysis database for multiple ~omics experiments. *J. Integr. Bioinform.* **8**, 160 (2011).
51. Dai, M. et al. Evolving gene/transcript definitions significantly alter the interpretation of GeneChip data. *Nucleic Acids Res.* **33**, e175 (2005).
52. Irizarry, R. A. et al. Exploration, normalization, and summaries of high density ol array probe level data. *Biostatistics* **4**, 249–264 (2003).
53. Sartor, M. A. et al. Intensity-based hierarchical Bayes method improves testing for differentially expressed genes in microarray experiments. *BMC Bioinformatics* **7**, 538 (2006).
54. Storey, J. D. & Tibshirani, R. Statistical significance for genomewide studies. *Proc. Natl. Acad. Sci. USA* **100**, 9440–9445 (2003).
55. Dittrich, N. et al. Toll-like receptor 1 variations influence susceptibility and immune response to Mycobacterium tuberculosis. *Tuberculosis (Edinb.)* **95**, 328–335 (2015).

Supplementary Table 2

Categories	Number n (%)	Gender[a] male	female	Age[b] mean±SD	BMI[c] mean±SD
Controls (household contacts)	165 (36.0%)	67 (40.6%)	98 (59.4%)	34.2±9.3	23.8±4.9
all TB patients	293 (64.0%)	112 (38.2%)	181 (61.8%)	25.4±10.4	18.0±4.1
pulmonary TB (PTB)	180 (61.4%)	75 (41.7%)	105 (58.3%)	25.9±11.0	16.6±3.0
extrapulmonary TB (ETB)	113 (38.6%)	37 (32.7%)	76 (67.3%)	24.7±9.4	20.1±4.7

Baseline characteristics.
Baseline characteristics of the study cohort. A total of 458 individuals (293 cases with tuberculosis infection confirmed by radiology and/or positive culture, and 165 of their household contacts as controls) were recruited and genotyped for TLR8-SNP. [a]Gender did not significantly differ between Controls and Patients ($\chi 2(1)=0.251$; p=.616). [b]mean age significantly differed between controls and patients (t(456)=8.787; p<.0001). [c]mean BMI significantly differed between controls and patients (t(292.8)=12.995; p<.0001).

Supplementary Table 3

TLR8 M1V	controls	patients	χ^{2a}	p-Value	OR [CI]	*adjusted χ^{2b}*	*adjusted p-Value*	*adjusted OR [CI]*
whole cohort								
A	76 (46.1%)	172 (58.7%)	6.795	.009	1.66 [1.134-2.445]	*7.157[c]*	*.007*	*1.941 [1.194-3.156]*
G	89 (53.9%)	121(41.3%)	-	-	-	-		-
PTB								
A	76 (46.1%)	101(56.1%)	3.481	.062	1.50 [0.979-2.289]	*4.869[d]*	*.027*	*2.020 [1.082-3.773]*
G	89 (53.9%)	79 (43.9%)	-	-	-	-		-
ETB:								
A	76 (46.1%)	71 (62.8%)	7.571	.006	1.98 [1.214-3.226]	*3.643[e]*	*0.56*	*1.756 [0.985-3.131]*
G	89 (53.9%)	42 (37.2%)	-	-	-	-	-	-
PTB: BCG-neg.								
A	24(57.1%)	42(48.3%)	0.891	.345	0.7 [0.333-1.471]	*0.098[f]*	*.754*	*0.858 [0.327-2.246]*
G	18(42.9%)	45(51.7%)						
PTB: BCG-pos.								
A	52(42.6%)	59(63.4%)	9.158	.002	2.34 [1.342-4.065]	*9.577[g]*	*.002*	*4.032 [1.667-9.752]*
G	70(57.4%)	34(36.6%)	-	-	-	-		-

TLR8 distribution and odd ratios in controls and patients.
Distribution of TLR8-SNP alleles (TLR8-A and TLR8-G) in the controls and TB patients (whole cohort) and separately in controls, PTB, and ETB patients. χ^2 , p-values and odd ratios (ORs) were calculated based on distribution (black). The values were further adjusted and corrected for age, gender, and BMI differences in the case and control groups (red, italic) using a binary logistic regression model.
[a]based on Pearson's χ^2 test.
[b]based on Wald's statistic, computed with a binary logistic regression, adjusted for age, gender, BMI
[c]model: $\chi^2(4)=168.767$; p<.0001; r^2(Nagelkerke)=0.423
[d]model: $\chi^2(4)=207.485$; p<.0001; r^2(Nagelkerke)=0.604
[e]model: $\chi^2(4)=76.904$; p<.0001; r^2(Nagelkerke)=0.326
[f]model: $\chi^2(4)=55.619$; p<0.0001; r^2(Nagelkerke)=0.489
[g]model: $\chi^2(4)=142.955$; p<0.0001; r^2(Nagelkerke)=0.654

Supplementary Table 4

TLR8 allele	BCG-status	controls	PTB	χ^{2a}	p-Value	OR [CI]	*adjusted χ^{2b}*	*adjusted p-Value*	*adjusted OR [CI]*
whole cohort	not-vaccinated	42 (25.6%)	87 (48.3%)						
	vaccinated	122 (74.4%)	93 (51.7%)	18.906	<.0001	0.368 [0.233-0.581]	*3.187[c]*	*.074*	*0.563 [0.300-1.058]*
A	not-vaccinated	24 (31.6%)	42 (41.6%)						
	vaccinated	52 (68.4%)	59 (58.4%)	1.856	.173	0.648 [0.347-1.211]	*0.002[d]*	*.965*	*1.019 [0.428-2.429]*
G	not-vaccinated	18 (20.5%)	45 (57.0%)						
	vaccinated	70 (79.5%)	34 (43.0%)	23.617	<.0001	0.194 [0.098-0.385]	*6.543[e]*	*.011*	*0.279 [0.105-0.742]*

Distribution of BCG-vaccination status and odd ratios for its effect on PTB for the whole cohort and each genotype.
Distribution of BCG-vaccination Status (vaccinated and not-vaccinated) in the different groups. Odd ratios (ORs) were calculated based on distribution (black). The values were further adjusted and corrected for age, gender, and BMI differences in the case and control groups using a binary logistic regression model. Adjusted ORs for BCG-vaccination in PTB were calculated for the whole cohort and each TLR8 genotype separately, right columns (in red, italic) show age, sex and BMI -adjusted values (displayed as bar graph in Fig. 4J). ORs differ significantly between TLR8-A and TLR8-G as calculated by Wald's test.
[a]based on Pearson's χ^2 test.
[b]based on Wald's statistic, computed with a binary logistic regression, adjusted for age, gender, BMI
[c]model: $\chi^2(4)=205.951$; p<.0001; r^2(Nagelkerke)=0.602
[d]model: $\chi^2(4)=101.571$; p<.0001; r^2(Nagelkerke)=0.586
[e]model: $\chi^2(4)=111.175$; p<.0001; r^2(Nagelkerke)=0.652

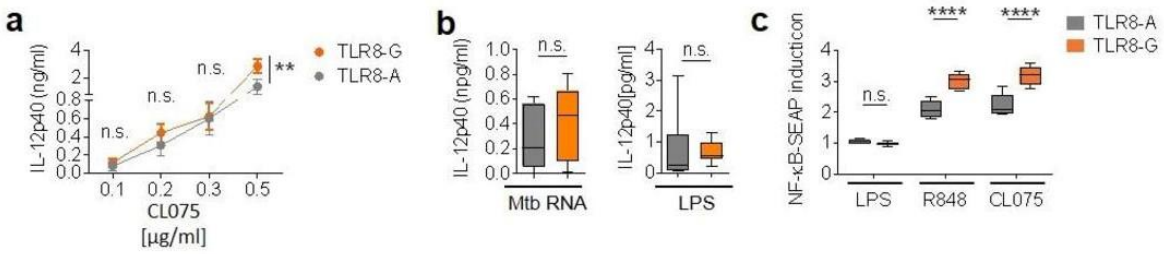

Supplementary Figure 8

TLR8-G displays a slight gain-of-function phenotype

PBMC from healthy donors, screened for either TLR8-A or TLR8-G, variant stimulated with **(a)** the TLR8 agonist CL075 (at the indicated concentrations), **(b)** *Mycobacterium tuberculosis* RNA or LPS as a negative control for 18h. Cytokine release was analyzed by ELISA (n=16, TLR8-A n=7, TLR8-G n=9). **(c)** HEK-Blue Null-I reporter cells were stably transfected with either TLR8-A or TLR8-G variants and stimulated with TLR8 agonist (CL075, R848) or LPS as a negative control for 18h. NF-kB-activation was determined in the SEAP Reporter Gene Assay. Induction values were normalized to stimulation with saline. (n=6). Two-way ANOVA with post hoc correction for multiple comparisons. Error bars are mean ± SEM. (**; p<0.01, ****; p<0.0001)

10. Publikation 2: Thada et al. (2021)

International Journal of *Molecular Sciences*

MDPI

Article

Interaction of TLR4 and TLR8 in the Innate Immune Response against Mycobacterium Tuberculosis

Shruthi Thada [1,2], Gabor L. Horvath [3], Mario M. Müller [4], Nickel Dittrich [1], Melanie L. Conrad [1], Saubashya Sur [5], Abid Hussain [6], Karin Pelka [7,8], Suman Latha Gaddam [2,9], Eicke Latz [3], Hortense Slevogt [4], Ralf R. Schumann [1,†] and Sanne Burkert [10,*,†]

1 Institute of Microbiology, Infectious Diseases and Immunology, Charité Universitätsmedizin Berlin, Corporate Member of Freie Universität Berlin, Humboldt-Universität zu Berlin and Berlin Institute of Health, 12203 Berlin, Germany; shruthi.thada@gmail.com (S.T.); nickel.dittrich@gmail.com (N.D.); melanie.conrad@charite.de (M.L.C.); ralf.schumann@charite.de (R.R.S.)
2 Bhagwan Mahavir Medical Research Centre, Hyderabad 500004, India; sumanlathag@yahoo.com
3 Institute of Innate Immunity, University Hospitals Bonn, University of Bonn, 53127 Bonn, Germany; horvathg@uni-bonn.de (G.L.H.); eicke.latz@uni-bonn.de (E.L.)
4 Host Septomics, ZIK Septomics, Jena University Hospital, 07745 Jena, Germany; mario.mueller1@med.uni-jena.de (M.M.M.); hortense.slevogt@med.uni-jena.de (H.S.)
5 Postgraduate Department of Botany, Life Science Block, Ramananda College, Bishnupur 722122, India; saubashya@gmail.com
6 Department of Biotechnology and Bioinformatics, University of Hyderabad, Hyderabad 500046, India; mdabid19@gmail.com
7 Broad Institute of MIT and Harvard, Cambridge, MA 02139, USA; kpelka@broadinstitute.org
8 Center for Cancer Research, Massachusetts General Hospital, Boston, MA 02129, USA
9 Department of Genetics, Osmania University, Hyderabad 500007, India
10 Department of Internal Medicine III, Division of Infectious Diseases, University Hospital of Ulm, 89081 Ulm, Germany
* Correspondence: sanne.burkert@uniklinik-ulm.de; Tel.: +49-731-5000
† These authors contributed equally (shared senior authorship).

check for updates

Citation: Thada, S.; Horvath, G.L.; Müller, M.M.; Dittrich, N.; Conrad, M.L.; Sur, S.; Hussain, A.; Pelka, K.; Gaddam, S.L.; Latz, E.; et al. Interaction of TLR4 and TLR8 in the Innate Immune Response against Mycobacterium Tuberculosis. *Int. J. Mol. Sci.* **2021**, 22, 1560. https://doi.org/10.3390/ijms22041560

Academic Editor: Alexander S. Apt
Received: 26 December 2020
Accepted: 29 January 2021
Published: 4 February 2021

Publisher's Note: MDPI stays neutral with regard to jurisdictional claims in published maps and institutional affiliations.

Abstract: The interaction and crosstalk of Toll-like receptors (TLRs) is an established pathway in which the innate immune system recognises and fights pathogens. In a single nucleotide polymorphisms (SNP) analysis of an Indian cohort, we found evidence for both TLR4-399T and TRL8-1A conveying increased susceptibility towards tuberculosis (TB) in an interdependent manner, even though there is no established TLR4 ligand present in *Mycobacterium tuberculosis* (Mtb), which is the causative pathogen of TB. Docking studies revealed that TLR4 and TLR8 can build a heterodimer, allowing interaction with TLR8 ligands. The conformational change of TLR4-399T might impair this interaction. With immunoprecipitation and mass spectrometry, we precipitated TLR4 with TLR8-targeted antibodies, indicating heterodimerisation. Confocal microscopy confirmed a high co-localisation frequency of TLR4 and TLR8 that further increased upon TLR8 stimulation. The heterodimerisation of TLR4 and TLR8 led to an induction of IL12p40, NF-κB, and IRF3. TLR4-399T in interaction with TLR8 induced an increased NF-κB response as compared to TLR4-399C, which was potentially caused by an alteration of subsequent immunological pathways involving type I IFNs. In summary, we present evidence that the heterodimerisation of TLR4 and TLR8 at the endosome is involved in Mtb recognition via TLR8 ligands, such as microbial RNA, which induces a Th1 response. These findings may lead to novel targets for therapeutic interventions and vaccine development regarding TB.

Keywords: TLR4; TLR8; tuberculosis; SNP analysis; heterodimerisation

1. Introduction

The recognition of potentially pathogenic microorganisms followed by an inflammatory response of the host is regulated by the immediate reaction of the innate immune

system [1]. Activation of this evolutionary older system is also crucial for an efficient function of the second arm of the immune response present only in vertebrates, the acquired immune system. Antigen-presenting cells (APCs) are activated and migrate to the lymph nodes, where they bridge the innate and adaptive immune systems by presenting antigens, leading to the generation of an efficient antibody response [2]. Pattern Recognition Receptors (PRRs), which have been identified and structurally characterised over the last 20 years, play a major role in mounting an effective innate immune response by recognising the presence of pathogens via Pathogen-Associated Molecular Patterns (PAMPs) [3]. Toll-like receptors (TLRs) are one important subgroup of PRRs mainly present on APCs such as alveolar macrophages and dendritic cells (DCs) [4]. Several TLRs located in the cell surface membrane have the main function of recognising bacterial cell wall compounds, internalising the microbe, and activating a nuclear factor kappa-light-chain-enhancer of activated B cells (NF-κB)-mediated inflammatory response. Others are expressed within the endosomal membrane and act to recognise microbial nucleic acids, inducing type I interferons (IFNs) [5]. TLRs act as dimers, and while most receptors organise as homodimers, some have been structurally analysed as functional heterodimers [6]. For example, the plasma membrane located TLR2 can form a heterodimer either with TLR1 or -6, resulting in a change in its ligand-binding capacity and a more specific response to Gram-positive bacteria [7].

Tuberculosis (TB) is caused by *Mycobacterium tuberculosis* (Mtb), and both the cell wall composition and the immune response elicited by Mtb within the host are unique. Certain cell wall compounds of Mtb have been described to interact with PRRs located mainly on the outer cell membrane, particularly TLR2/1 [8,9]. Furthermore, TLR4 has been suggested to recognise mycobacterial lipoarabinomannan (LAM) and lipomannan (LM), although it has remained unclear how a ligand so distinct from the typical TLR4-ligand lipopolysaccharide (LPS) can interact with TLR4 [10]. TLR4 can be localised either on the cell surface or the endosomal membrane. For the interaction of TLR4 with LPS, MD-2 and CD14 are required [11,12]; however, for other ligands, this might not be the case. Furthermore, MD-2 and CD14 promote the LPS-induced endocytosis of TLR4 [13].

Interestingly, the endosomal localisation of TLR4 changes the utilisation of adapter molecules, leading to a differentiated inflammatory response. TLR4 activated within the endosome does not recruit its standard adaptor protein myeloid differentiation primary response 88 (MyD88) but instead, it recruits TIR-domain-containing adapter-inducing interferon-β (TRIF), which activates the transcription factor IFN regulatory factor (IRF)-3 and thereby changes the immune response from NF-κB-dependent cytokines to type I IFNs [14,15]. Generally, TLR4 activation promotes a T helper (Th)1 response by activating APCs and promoting DC maturation, inducing interleukin (IL)-12, tumour necrosis factor (TNF)α, IFNγ, major histocompatibility complex class (MHC)-II, CD80, and 86, and NO, as well as enhancing phagocytosis and inhibiting IL-10 production [16–20]. Mtb is known to strongly inhibit the expression of TLR4 and both its adaptor proteins TRIF and MyD88 [21,22]. Furthermore, mycobacteria evade PRR recognition of the cell wall by persisting intracellularly in macrophageal phagosomes. Therefore, once Mtb is internalised, intracellular PRRs must assume immunosurveillance. Recently, evidence has accumulated that mycobacterial nucleoside recognition both in the endosome (e.g., by TLR8) and within the cytoplasm is important for an effective immune response [23–25]. TLR8 is an endosomal receptor recognising uridine-rich and short ssRNA mainly expressed in macrophages and myeloid DCs [26,27]. Activation leads to an induction of NF-κB via MyD88, resulting in the production of IL-12, TNFα, and IFNγ, as well as the induction of type I IFNs through IRF5 and IRF7 [28]. Thus, a Th1 response is promoted. Similarly to TLR4, mycobacteria have developed mechanisms to impair the function of endosomal PRRs by inhibiting endosomal acidification [29,30].

Evidence for both TLR4 and TLR8 being involved in TB pathogenesis comes from clinical trials assessing the frequency of single nucleotide polymorphisms (SNPs) in the TLR4 and TLR8 genes in TB patients compared to healthy controls. Increased suscepti-

bility toward TB in individuals carrying TLR4 SNPs has been described for the variants Asp299Gly (rs4986790) and Thr399Ile (rs4986791) [31]. For TLR8, susceptibility has been associated with the less functional variant of TLR8 Met1Val (rs3764880) [23,32]. In this study, we confirm the evidence for TLR4 playing a role in TB immunity and hypothesise that the endosomal cooperation of TLR4 and TLR8 by forming a heterodimer modulates the immune response to Mtb.

2. Results

2.1. Cohort Characteristics and Genotyping

We analysed a TB cohort from an unmatched case-control study that was previously described for genetic susceptibility (Table S1, [23,24,33,34]). The cohort consisted of 346 TB patients and 301 controls. TB patients were either diagnosed with pulmonary (224 patients, PTB) or extrapulmonary TB (121 patients, EPTB). Additionally, there were 95 relapse cases. There were significantly more females among the patients (58.9%) than controls (50.9%) and TB patients, on average, were younger (25.5 years) than controls (32.9 years). Among the relapses, 49.5% were female, and the mean age was 30.6 years. More controls than patients had received Bacillus Calmette–Guérin (BCG) vaccine in their childhood (82.9% and 48.8% respectively). Relapse cases had the lowest mean body mass index (BMI, 16.49), followed by pulmonary (16.6) and extrapulmonary cases (19.9), and controls (24.3). Relapse cases also had the lowest portion of BCG positives (36.92%) in comparison to primary TB cases (48.8%) and controls (82.9%).

Regarding SNP distribution, TLR4-Thr399Ile (cytosine (C)>thymine (T)) and TLR4-Asp299Gly (adenine (A)>guanine (G)) were not fully linked (cosegregation in only 73%), unlike among Caucasians (Table S2). TLR4-399T was more frequent among TB patients than controls, and there was evidence that it conveyed susceptibility towards TB (OR = 1.97 [1.15–3.37]; $p = 0.013$; Table 1, for full model Table S3). There was no evidence for effect modulation by BCG vaccination ($p = 0.392$). There was also no evidence for a different distribution of TLR4-A299G alleles between TB patients and controls (OR = 0.72 [0.49–1.07], $p = 0.101$), nor for an impact of allele distribution on the site of manifestation (PTB or EPTB) for TLR4-C399T (OR = 0.85 (0.51–1.41), $p = 0.523$) or TLR4-A299G (OR = 1.24 (0.74–2.05), $p = 0.413$). As we previously reported [23], TLR8-1A was associated with a susceptibility towards being a TB case (OR = 1.68 (1.08–3.63); $p = 0.022$; Table 1), with weak evidence for an interaction between BCG and TLR8-Met1Val (A > G) ($p = 0.071$, Table S4). Interestingly, the susceptibility conveyed by TLR8-1A was only seen in individuals carrying the TLR4-399T allele (OR= 1.97 (1.15–3.37), $p = 0.013$); among homozygote TLR4-399C individuals, no impact of TLR8-1A on TB disease was observed (OR = 1.19 (0.52–2.72); $p = 0.681$, Table 1). Notably, there was no evidence for the statistical interaction of the two SNPs in primary TB ($p = 0.363$) or relapse ($p = 0.750$) cases.

Table 1. Allele distributions of single nucleotide polymorphisms (SNPs) in the Indian cohort among controls and primary TB cases.

TLR SNPs (Nucleotide Change)	Alleles	N	Allele Frequency [N(%)] Controls	Primary TB	OR [95% CI] *	*p*-Value
TLR4-Asp299Gly (A > G)	G	533	72 (27.48)	100 (33.22)	0.72 [0.49–1.07]	0.101
TLR4-Thr399Ile (C > T)	T	552	68 (23.37)	105 (31.44)	1.57 [1.04–2.36]	0.027
TLR8-Met1Val (A > G)	A	556	139 (47.60)	199 (58.70)	1.68 [1.08–2.63]	0.022
TLR8-1, when TLR4-399CT/T	A	395	34 (50.00)	59 (56.19)	1.97 [1.15–3.37]	0.013
TLR8-1, when TLR4-399CC	A	155	105 (47.09)	137 (59.83)	1.19 [0.52–2.72]	0.681

* Odds Ratios (ORs) based on Likelihood Ratio Tests (LRTs) adjusted for gender and age, as well as BCG status in case of TLR8.

Regarding relapses, we did not observe a significantly different distribution between primary TB patients and relapse cases regarding TLR4-A299G (OR = 0.80 (0.49–1.32), $p = 0.381$) or TLR4-C399T (OR = 1.36 (0.81–2.28), $p = 0.245$, Table 2). However, there was also strong evidence for an increased risk for being a relapse case associated with TLR8-1A (OR = 1.99 (1.03–3.82); $p = 0.006$, Table S5). Regarding a potential interaction of TLR4 and TLR8,

the same pattern as above was observed, namely that TLR8-1A conveyed susceptibility to TB depending on TLR4-399T although with only weak evidence (OR = 2.90 (0.87–9.59), $p = 0.069$; Table 2). Again, there was no evidence for formal statistical interaction ($p = 0.750$). Nevertheless, this observation led us to suspect that there might be an interaction on the molecular level between TLR4 and TLR8, and we further investigated this in different in silico and in vitro systems.

Table 2. Allele distributions of SNPs in the Indian cohort among primary TB and relapse cases.

TLR SNPs	Alleles	N	Allele Frequency [N(%)] Primary TB	Allele Frequency [N(%)] Relapses	OR [95% CI] *	*p*-Value
TLR4-Asp299Gly	G	383	100 (33.22)	36 (39.13)	0.80 [0.49–1.32]	0.381
TLR4-Thr399Ile	T	376	105 (31.44)	33 (38.82)	1.36 [0.81–2.28]	0.242
TLR8-Met1Val	A	355	140 (58.70)	68 (72.34)	1.99 [1.03–3.82]	0.035
TLR8-1, when TLR4-399CT/T	A	111	59 (56.19)	25 (75.76)	2.90 [0.87–9.59]	0.069
TLR8-1, when TLR4-399CC	A	231	137 (59.82)	37 (71.15)	1.62 [0.69–3.81]	0.265

* ORs based on LRTs adjusted for gender and age, as well as BCG status in case of TLR8.

2.2. Docking Outcome

To evaluate the possible structural implications of an amino acid residue change in TLR4 at position 399, we performed in silico analysis. Furthermore, we performed molecular docking studies to investigate the idea of interaction between TLR4 and TLR8. The docking outcome revealed that the TLR4-399C molecule (threonine at position 399) could undergo heterodimerisation with TLR8 in presence of the agonistic ligand R848 (Figure 1). Threonine-399 and serine-400 residues of TLR4 could link to the TLR8 molecule by hydrogen bonds of 2.12 and 2.24 angstroms, respectively. The major non-ligand residues from TLR8 involved in the hydrophobic contacts were Tyr353, Gly351, Val378, Ser352, Ile349, and Tyr348. However, the structure of the TLR4-399T molecule (with isoleucine at position 399) did not show this phenomenon. This demonstrated that the ability of TLR4 to form a heterodimer with TLR8 was lost by changing the residue TLR4 residue threonine-399 to isoleucine-399. This change might lead to conformational rearrangements in the protein structure that could alter the ligand-binding capacity and thereby prevent the R848-facilitated formation of a heterodimer with TLR8.

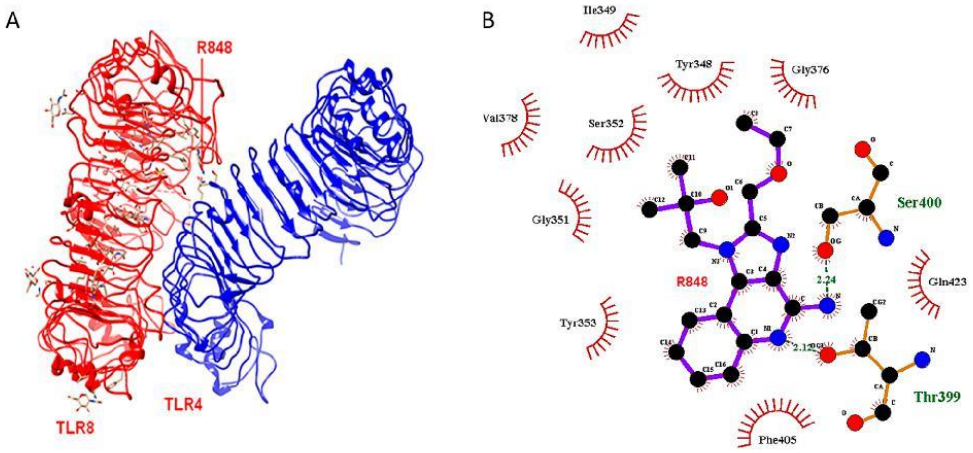

Figure 1. Molecular Docking: (**A**) Toll-like receptor (TLR)4-TLR8 heterodimer mediated by agonistic ligand R848 of TLR8. Both are wild types. (**B**) Ligand plot showing TLR4 variant (Threonin-399, i.e., 399C) interacting with agonistic ligand R848 and assisting in heterodimerisation.

2.3. Mass Spectrometry

To further explore the potential interaction of TLR4 and TLR8, we conducted mass spectrometry analysis on co-immunoprecipitation (IP) to find evidence for heterodimer formation. With IP, we pulled down with anti-human influenza hemagglutinin (HA)-TLR8 in human embryonic kidney (HEK)293 cells that were either transfected with TLR4- and with or without TLR8-HA and analysed the samples for the presence of TLR4, TLR8 and other proteins. As expected, we saw a significant difference in TLR8 intensity between samples transfected with or without TLR8-HA. Furthermore, we identified protein unc-93 homolog B1 (UNC93B1) in the proteomic analysis as statistically significantly enriched when co-immunoprecipitating with TLR8-HA in HEK cells (Figure 2), as expected and reported by others [35]. The TLR4 receptor was identified in five out of six TLR8-HA+TLR4 co-transfected cell lysate immunoprecipitations, with two to five unique peptides, but not in any control sample. However, due to fluctuating LFQ intensities for TLR4, co-IP with TLR8-HA, and high variance in the whole dataset of the experiments, the enrichment of TLR4 in TLR8-HA co-transfected cells immunoprecipitated with anti-HA did not reach statistical significance after Benjamini–Hochberg correction (TLR4 log2 fold change = 4.27 and $p > 0.05$ after B.H. adjustment; before $p = 0.001$). The successful identification of a TLR4 peptide in TLR4/8 co-IP samples by higher-energy collisional dissociation spectrum is shown in Figure S1. Altogether, the data indicate that TLR8 can interact with TLR4 in HEK cells overexpressing both receptors.

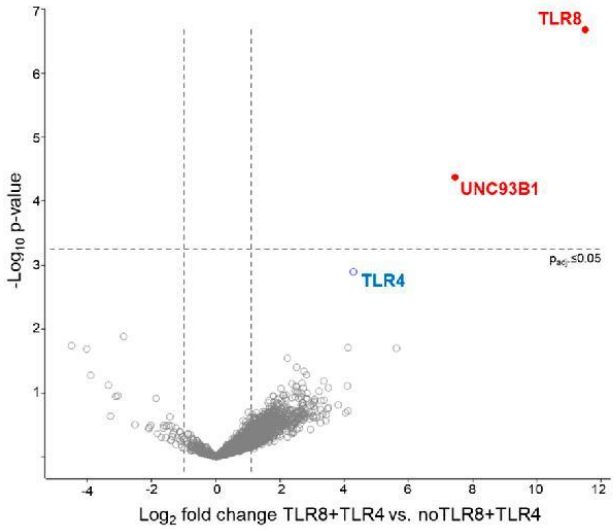

Figure 2. Interaction of TLR8 with TLR4 in HEK cells. Volcano plot of the label-free quantitative MS data plotting the logarithmic difference in protein levels in the HA-immunoprecipitated fraction of TLR8-HA and TLR4 expressing HEK cells and cells expressing TLR4 alone versus the negative logarithmic p values of the t-test performed of six experiments per group. The dotted lines indicate significance thresholds (fold change ≥ 2 and p-value $_{\text{(Benjamini-Hochberg adj.)}} \leq 0.05$). In red (filled circles), statistically significant differentially abundant proteins, in blue (open circle) TLR4, in grey (open circles), proteins with no statistically significant abundance.

2.4. Co-Immunoprecipitation

For further investigation of the potential interaction of TLR4 and TLR8, we performed co-IP experiments with TLR4 variants. HEK293XL/hTLR8-HA+UNC93B1 cells were transiently transfected with TLR4–mCherry–myc 399C or 399T followed by stimulation with LPS, R848, LPS+R848, and Mtb RNA, or left untreated for 2 h. First, the lysates were

immunoprecipitated with anti-HA antibody to pull down TLR8 and then immunoblotted with either anti-TLR4 or anti-HA (for indirect blotting of TLR8) antibody (Figure 3). As expected, without transfection for TLR8, neither TLR4 nor TLR8 were identified in the precipitates. Interestingly, TLR4 was identified in all cells transfected with both TLR4 and TLR8, even in unstimulated cells. The successful blot of TLR4 after precipitation for TLR8 indicated an interaction of the two TLRs. Of note, adding MD2/CD14 to the transfection abolished this effect (Figure S2). In hTLR8HA+UNC93B1 cells co-transfected with TLR4-399C (the variant that we have identified to be able to interact with TLR8), R848 stimulation resulted in higher TLR4 band intensities as compared to other stimulants (Figure 3B). Adding LPS to R848 decreased TLR4-399C band intensity. Comparing the genotypes of TLR4 T399C by the quantification of band intensities, 399T-transfected cells exhibited less TLR4 band intensities upon stimulation with R848 and Mtb RNA, although both input and unstimulated cells showed higher band intensities for 399T than 399C (Figure 4).

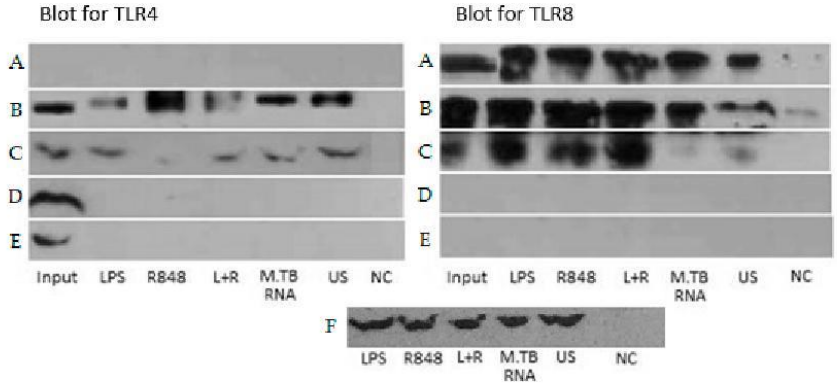

Figure 3. Co-immunoprecipitation. HEK 293 cells transfected as indicated per line, followed by stimulation as indicated per column (2 h for lipopolysaccharide (LPS) (10 ng/mL), R848 (2 μg/mL), LPS and R848 (L+R), 16 h for MTB RNA (1 μg/mL), unstimulated (US) and negative control (NC)). After 2 h, immunoprecipitation procedure was started. The left panel shows immunoprecipitation and -blot with anti-HA antibody (≈110 kDa), indirectly precipitating for TLR8. The right panel shows immunoprecipitation with anti-HA-antibody, followed by immunoblot with anti-TLR4 antibody (100 kDa). (**A**) hTLR8HA+UNC93B1, (**B**) hTLR8HA+UNC93B1+TLR4 399C-mCherry-myc, (**C**) hTLR8HA+UNC93B1+TLR4 399T-mCherry-myc, (**D**) TLR4 399C-mCherry-myc, (**E**) TLR4 399T-mCherry-myc, (**F**) hTLR8HA+UNC93B1 native cells blot with loading control—anti-GAPDH antibody (≈37 kDa). TLR8 was pulled down by anti-HA antibodies and identified in the immunoblot. When HEK cells were co-transfected with both TLR4 and TLR8, TLR4 could be identified in lysates precipitated for HA/TLR8, indicating heterodimerisation.

As a control, we performed the same experiment with hTLR7FLAG instead of hTLR8HA, and no TLR4 was found after IP for FLAG (Figure S3). In order to check different species, we repeated the experiment with Rhesus and C. atys TLR4 FLAG-tagged along with HEK293XL/hTLR8-HA+UNC93B1 with the result of successful identification of TLR4 in the co-IP, which is similar to hTLR4 (Figure S4). Altogether, data from co-IP supported the data from modelling, indicating that TLR4 and TLR8 interact at the endosomal level, particularly in cells co-transfected with TLR4-399C and stimulated with R848.

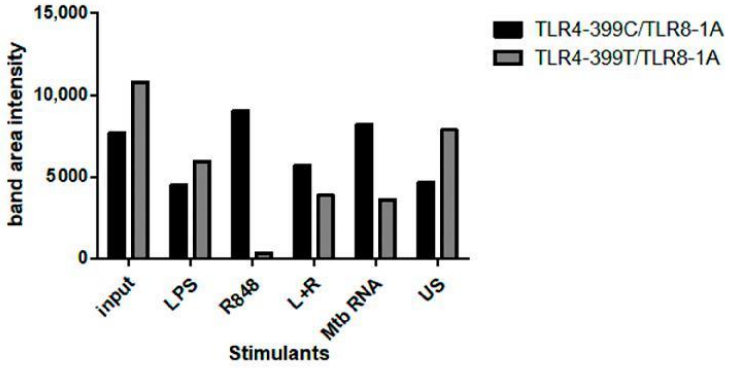

Figure 4. Co-immunoprecipitation quantification. HEK 293 cells transfected with hTLR8HA+UNC93B1+TLR4 399C-mCherry-myc compared with hTLR8HA+UNC93B1+TLR4 399T-mCherry-myc were stimulated with LPS, R848, LPS and R848 (L+R), *Mycobacterium tuberculosis* (Mtb) RNA and unstimulated (US), followed by immunoprecipitation with anti-HA-antibody and immunoblot with anti-TLR4 antibody: In cells stimulated with R8484 and Mtb RNA, the band intensity is higher in hTLR8HA+UNC93B1+TLR4 399C-mCherry-myc transfected cells compared with hTLR8HA+UNC93B1+TLR4 399T-mCherry-myc.

2.5. Co-Localisation

HEK293/hTLR8-HA+UNC93B1 cells were transiently transfected with TLR4-mCherry-myc 399C, as well as the accessory proteins gp96, PRAT4A, CD14, and MD2, and stimulated with LPS, R848, LPS+R848, or left untreated for 2 h. Furthermore, ssRNA40 was used for stimulation, as it produced less cell stress due to easier transfection (already complexed with transfection agent) and higher stability, resulting in clearer results comparted to MTB-RNA/LyoVec. As expected, TLR4 was identified both at the outer cell membrane and the endosome, whereas TLR8 was only seen at the latter. Microscopy showed that within the endosome, TLR4 and TLR8 co-localised in all cells transfected with hTLR8HA+UNC93B1+TLR4-mCherry-myc 399C, irrespective of the stimulant (Figure 5A–E). The number of co-localising endosomes increased in cells stimulated with LPS ($p < 0.003$) or R848 ($p < 0.001$) (Figure 6). For the combination of LPS and R848, an additive effect for co-localisation could be observed ($p < 0.001$). Additionally, cells were treated with dynasore to block the trafficking of TLR4 to the endosome, upon which no co-localisation signal was seen (Figure 5F). Of note, no difference in the results reported was observed for transfection without MD2 and CD14 (data not shown).

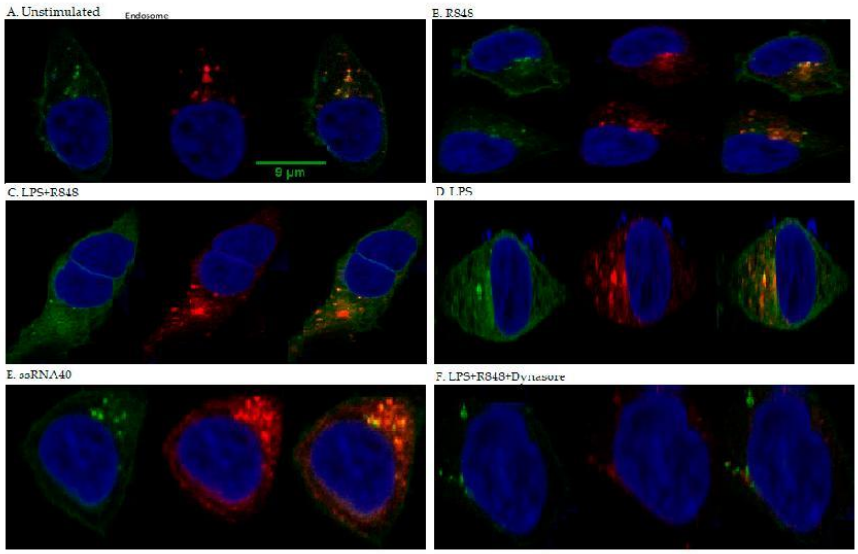

Figure 5. Confocal microscopy. Fluorescence microscopy of HEK293 cells stably transfected with TLR8-HA and transiently transfected with fluorescently tagged TLR4-mcherry along with accessory proteins gp96, PRAT4A, CD14, and MD2. Cells were (**A**) unstimulated or treated with (**B**) R848, (**C**) LPS+R848, (**D**) LPS, (**E**) ssRNA40, and (**F**) LPS+R848+Dynasore for 2 h and stained with an anti-HA Alexa 647-conjugated antibody for TLR8 and Dapi for nuclei. In the false-coloured merged image, double co-localisation of TLR4 (green) and TLR8 (red) in endosomes appears as areas of yellow (arrowhead). Scale bar 9 µm. (**F**) Inhibition of dynamin-dependent endocytosis blocked TLR4-TLR8-triggered downstream pathways by Dynasore.

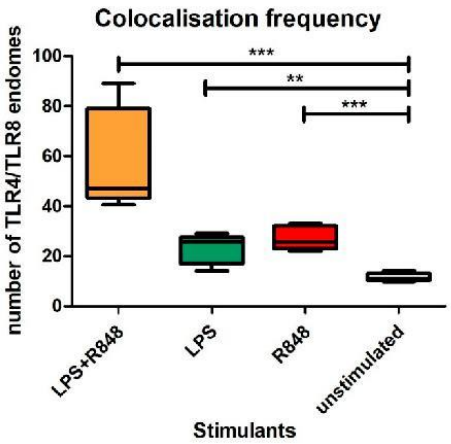

Figure 6. Co-localisation frequency. HEK293 cells stably transfected with TLR8-HA and transiently transfected with fluorescently tagged TLR4-mcherry along with accessory proteins gp96, PRAT4A, CD14 and MD2. Cells were unstimulated or treated with R848 (2 µg/mL), LPS (10 ng/mL), and LPS+R848 for 2 h. Co-localisation was observed under Leica SP5 SMD confocal microscope. The co-localisation frequency increased in cells stimulated with LPS+R848 as compared to LPS, R848, and unstimulated ($p < 0.009$, $p < 0.01$, and $p < 0.006$ respectively). ** $p \leq 0.01$, *** $p \leq 0.001$.

2.6. Functional Studies

We further explored the functional impact of the interaction of TLR4 and TLR8 using experiments with TLR-transfected HEK293-cells, including the different SNPs of interest. First, the different variants of TLR4 were transiently transfected along with MD2 and assessed for LPS responsiveness (Figure 7A). The 'wild-type' variant of TLR4-299A-399C showed the highest NF-κB induction as compared to other variants with a significant difference in comparison to 399-T ($p < 0.01$) but not 299-G ($p < 0.218$). Next, we co-transfected TLR4-variants with TLR8-1A (Figure 7B). NF-κB induction upon LPS stimulation was not detected due to a lack of MD2. Upon stimulation with R848, TLR8-1A co-transfected with TLR4-399C showed a significantly reduced NF-κB induction compared to TLR4-399T ($p < 0.007$). Adding TLR4-399C to TLR8-1A did significantly reduce NF-κB responsiveness ($p < 0.012$), while TLR4-399T failed to do so ($p < 0.148$). Adding MD2 and CD14 to the transfection of TLR4-399C and TLR8 increased LPS and decreased R848 responsiveness (Figure S5). Stimulation with LPS+R848 and mycobacterial RNA showed similar patterns (Figure S6). Of note, as a control, we transfected HEK blue cells with TLR7 and the TLR4 variants of interest and did not observe any differences upon adding TLR4 to TLR7.

To further support the interaction of TLR4 and TLR8 at the endosome, we used CLI-095, which specifically inhibits TLR4 signalling [36]. CLI-095-treated human monocyte-derived macrophages (THP cell line) showed a decreased NF-κB-response upon LPS stimulation ($p < 0.0001$) and increased NF-κB response in the presence of TLR8 ligands R848 ($p < 0.001$) and Mtb RNA ($p < 0.01$; Figure 7C). Furthermore, we blocked endosomal signalling pathways in THP cells with siRNA for MyD88, TRIF-related adaptor molecule (TRAM), or directly TLR4 (Figure 7D). Upon stimulation with TLR8-specific ligands, the NF-κB response was diminished when MyD88, TRAM, and TLR4 were silenced, which was not the case for TLR2-specific stimulation with PAM_3CSK_4. Blocking TLR8 signalling by either completely blocking the endosome through treatment with bafilomycin or siTLR8 abolished NF-κB induction, while LPS-stimulated cells did not show any difference (Figure S7). Altogether, experiments with HEK cells and THP cells indicated that the interaction of TLR4 with TLR8 diminishes NF-κB responsiveness upon TLR8 stimulation, which could be partly reversed by blocking TLR4 signalling and completely inhibited by TLR8-specific or total endosomal blockage.

Next, we analysed peripheral blood mononuclear cells (PBMCs) from healthy controls with TLR8-1A, which differed in TLR4-C399T (Figure 7E). Regarding TNFα, individuals with TLR4-399T exhibited higher levels of TNF release upon stimulation with LPS ($p < 0.001$), R848 ($p < 0.014$), or the combination of LPS and R848 ($p < 0.013$). This effect was even more pronounced when looking at IL12p40, with a remarkable difference in induction upon stimulation with both LPS and R848 ($p < 0.002$) (Figure 7F).

Finally, in order to assess different signalling pathways altered by an interaction of TLR4 and TLR8, we performed Western blotting of IRF3 from supernatants of HEK293 cells transiently transfected with different combinations of TLR4 and TLR8 variants and stimulated with TLR4- and TLR8-specific ligands (Figure 8). Transfection with TLR4, even unstimulated, led to high IRF3 expression, which was strongly increased with TLR8 co-transfection, implying that TLR4 together with TLR8 strongly activates type I IFNs, potentially even by spontaneous heterodimerisation in HEK cells. Cells double transfected with TLR4-399C and TLR8 showed higher band intensities than mono-transfected cells (Figure 9A) or cells transfected with 399T and TLR8 (Figure 9C). With TLR4-399T and TLR8, the differences were less pronounced and only in unstimulated and LPS-stimulated cells IRF3 band intensity was higher in double transfected cells (Figure 9B). Altogether, this would support our hypothesis that with TLR4-399C, the heterodimerisation is more likely than with TLR4-399T.

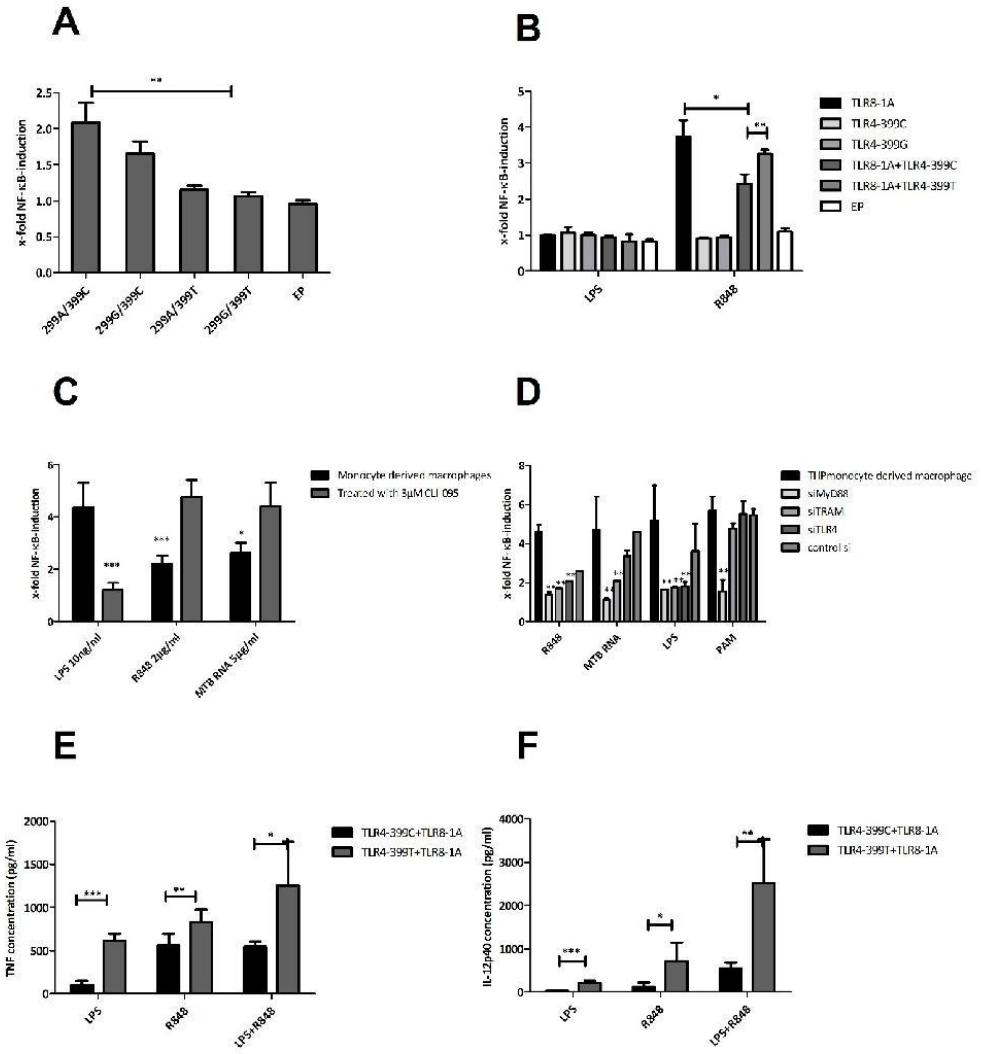

Figure 7. Functional studies within different cell lines to analyse the impact of the SNP TLR4-C399T on the interaction with TLR8. Used cells: (**A**,**B**): HEK293 blue null 1 cells, transiently transfected with TLRs or empty plasmid (EP) as indicated. (**C**,**D**): THP monocyte-derived macrophages. (**E**,**F**): Peripheral blood mononuclear cells (PBMCs) isolated from healthy homozygous volunteers that differed in their status of TLR4-399. Stimulation took place with LPS (100 ng/mL if not otherwise specified), R848 (2 µg/mL if not otherwise specified), Mtb-RNA (5 µg/mL) complexed with Lyovec or PAM_3CSK_4 as indicated for 16 h. NF-κB activation was measured by secreted embryonic alkaline phosphatase (SEAP) reporter gene assay, TNFα and IL12-p40 were measured by enzyme-linked immunosorbent assay (ELISA). (**A**) LPS responsiveness of different TLR4 SNPs: Transfection with variants human TLR4 along with human MD2. NF-κB fold induction was significantly raised in cells transfected with TLR4-299A-399C/MD2 compared to TLR4-299G-399C/MD2 ($p < 0.01$) and TLR4-299G-399T/MD2 ($p < 0.007$). (**B**) Co-transfection of TLR8 with TLR4-variants. Without accessory proteins, LPS

stimulation was insignificant. TLR8 was stimulated successfully with R848. When adding TLR4-399C, NF-κB levels were significantly lower ($p < 0.012$). The difference between TLR8-1A+TLR3-399C and TLR8-1A-399T was also significant ($p < 0.007$). TLR8-1A and TLR8-1A+TLR4-399T did not show a significantly different response ($p < 0.147$). (**C**) Inhibition of TLR4 signalling with CLI-095. THP monocyte-derived macrophages were stimulated with or without 3 μM CLI-095 (LPS at 10 ng/mL). NF-κB response in the presence of TLR8 ligand R848 ($p < 0.001$), Mtb RNA ($p < 0.01$), and LPS ($p < 0.001$) decreased (**D**) TLR signalling adaptor protein inhibition with siRNA. THP monocyte-derived macrophages were with or without silencing MyD88, TRAM, or TLR4 (LPS at 10 ng/mL, R848 at 5 mg/mL). TLR8 ligand stimulation significantly decreased in presence of siMyD88 and siTRAM ($p < 0.05$). (**E**) TNFα and (**F**) IL-12p40-levels of PBMCs. Individuals with TLR4-399T showed more tumour necrosis factor (TNF)α upon stimulation with LPS ($p < 0.001$), R848 ($p < 0.014$), and LPS+R848 ($p < 0.032$) in comparison to individuals with TLR4-399C. Regarding IL-12p40, there were significantly higher concentrations in individuals with TLR4-399T with LPS ($p < 0.001$), R848 ($p = 0.016$), and LPS+R848 ($p < 0.002$) than 399C. * $p \leq 0.05$, ** $p \leq 0.01$, *** $p \leq 0.001$.

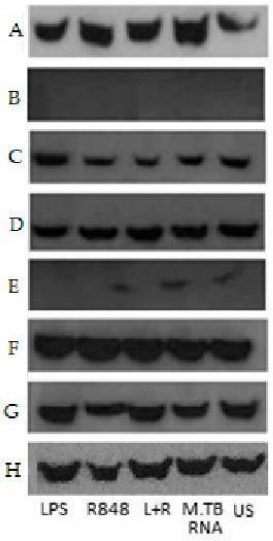

Figure 8. IRF3 Western blotting. (**A**) native HEK293 cells (**B**) HEK293 cells transfected with TLR4-399C/MD2 (**C**) HEK293 cells transfected with TLR4-399C (**D**) HEK293 cells transfected with TLR4-399T (**E**) HEK293 cells transfected with TLR8-1A (**F**) HEK293 cells transfected with TLR4-399C+TLR8-1A (**G**) HEK293 cells transfected with TLR4-399T +TLR8-1A were stimulated with LPS, R8484, LPS+R848 for 2 h and Mtb RNA (16h) or left untreated (US). (**H**) Native HEK293 cells blot with loading control–anti GAPDH antibody (≈37 kDa). IRF3 (≈55 kDa) could be identified in all double-transfected cell lysates.

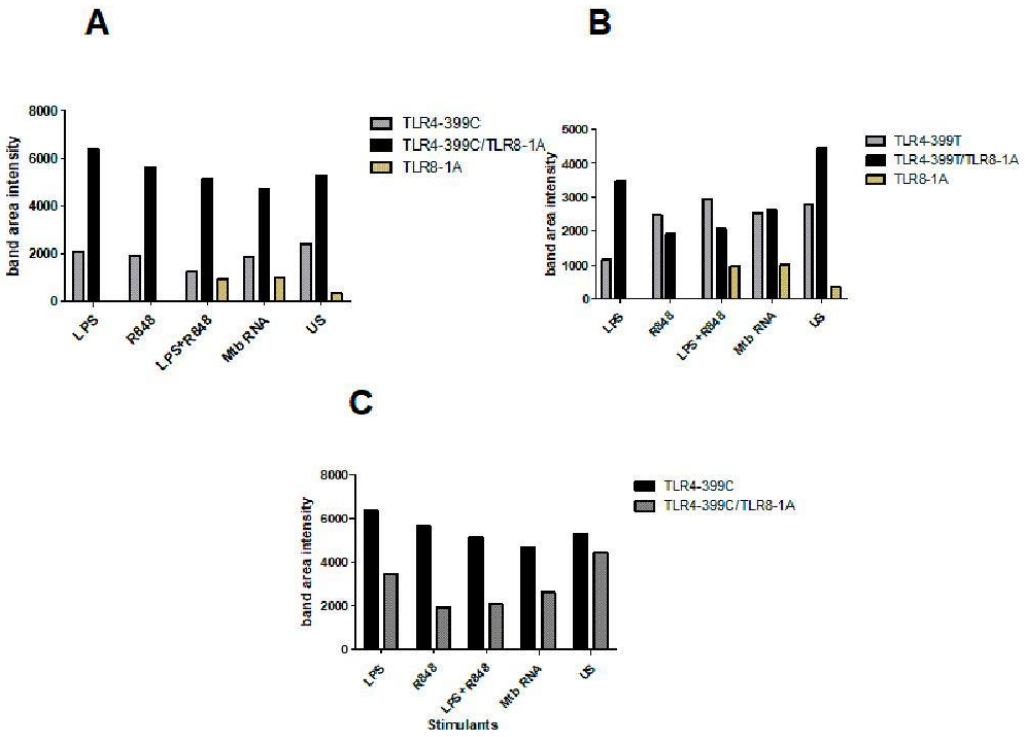

Figure 9. IRF3 Western blot quantification in HEK293 cells: (**A**) cells transfected with TLR4-399C compared with TLR4-399C+TLR8-1A cells. IRF3 band intensity is higher in TLR4-399C+TLR8-1A double transfected cells under LPS, R8484, LPS+R848, Mtb RNA stimulation and unstimulated (US) cells than in cells transfected with TLR4-399C (**B**) in cells transfected with TLR4-399T compared with TLR4-399T+TLR8-1A cells, upon LPS or in unstimulated cells, band intensity is higher in double-transfected cells, whereas with R848 with or without LPS, it was slightly less (**C**) cells transfected with TLR4-399C+TLR8-1A compared with TLR4-399T+TLR8-1A cells. IRF3 band intensity is higher in TLR4-399C+TLR8-1A cells, irrespective of stimulation.

3. Discussion

In this paper, we argue for an interaction of TLR4 and TLR8 as a heterodimer, which has functional importance for TB immunity. We came to this conclusion on the basis of (1) finding TLR4 in co-immunoprecipitated lysates of transfected HEK-cells for TLR8, particularly after R848 stimulation, (2) confirming this result with mass spectrometry, (3) seeing co-localisation with confocal microscopy, which increased upon stimulation, (4) finding a significantly enhanced susceptibility towards TB among individuals with TLR4-399T and TLR8-1A, the latter depending on the first, (5) finding evidence in modelling that TLR4-399C can form a heterodimer with TLR8 in the presence of a TLR8-ligand R848, while TLR4-399T might not, and finally (6) seeing in co-IP that with TLR4-399C, R848 stimulation induced a higher TLR4 band intensity than with TLR4-399T. Regarding the functional impact of this interaction, we found that (1) TLR4-399C showed higher NF-κB levels after LPS stimulation compared to TLR4-399T in HEK-cells, (2) in combination with TLR4, TLR8 transfected HEK cells secreted less NF-κB with TLR4-399C, but not with TLR4-399T, (3) blockage of TLR4 in monocyte-derived macrophages led to higher levels of TLR8-induced NF-κB, (4) in PBMCs, TRL4-399T led to more TNFα and IL12p40, and (5) IRF3 seems to be

with MD2 and CD14 along the transfection for TLR4 and TLR8, no TLR4 could not be identified after the precipitation of TLR8 in co-IP-studies, and R848-induced levels of NF-κB in co-transfected HEK-cells decreased with the addition of MD2 and CD14, arguing for an inhibitory effect on the heterodimerisation of TLR4 and TLR8 by the accessory proteins, which is potentially due to the promotion of the homodimerisation of TLR4. In line with this, adding LPS to R848 in co-transfected cells decreased the intensity of the TLR4 band, which is possibly due to the formation of a homodimer of TLR4, thereby decreasing the chances of interaction with TLR8. Inhibiting the interaction of TLR4 and TLR8 with CLI-095 in THPs reversely led to an increase of TLR8-induced NF-κB-levels. In contrast to that, with siRNA, a slight decrease of the NF-κB-signal upon stimulation could be observed, which is possibly due to more cell stress due to the necessary double transfection, as well as, potentially, a less complete inhibition by siRNA compared to CLI-095.

Furthermore, in HEK cells, we could see that mere co-transfection of TLR4 and TLR8 led to an expression of IRF3, which activated the type I IFN axis. This might explain how TLR4 could negatively regulate NF-κB induction by TLR8 activation, namely by shifting the balance from the NF-κB towards the type I IFN pathway. This might also explain why the blockage of TLR4 enhanced NF-κB induction by TLR8 activation.

The most pronounced difference between the TLR4 variants in co-IP was that TLR4-399C, the variant identified as more prone towards heterodimer formation, when undergoing co-transfection with TLR8, showed increased TLR4 band intensity after TLR8 stimulation with R848 compared to both LPS and unstimulated cells. In contrast to that, with TLR4-399T, R848-stimulated precipitation of TLR4 was decreased as compared to after LPS-stimulated and in unstimulated cells, further supporting the notion that the interaction of TLR4 and TLR8 is impaired with the nucleotide change from C to T. For Mtb RNA, the same trend was observed, although to a lesser extent. This might be because stimulation with RNA requires another transfection medium, thereby increasing cell stress, potentially resulting in reduced reactivity. Another reason might be that modelling actually identified R848 as the ligand promoting heterodimerisation, resulting in higher band intensities in our experiments.

In functional studies, we could show that the combination of TLR4-399T and TLR8-1A led to increased NF-κB, TNFα, and IL12p40 levels in PBMCs and THPs upon stimulation with TLR8 ligands in comparison to TLR4-399C, although both TLR4-399T and TLR8-1A individually are each the less functional variants of the SNP. Based on modelling data, with TLR4-399C, heterodimerisation is more likely to occur, possibly leading to more activation of IRF3, thus potentially leading to more type I IFNs but less direct activation of the NF-κB axis. With TLR4-399T, this effect is hindered, thereby producing more NF-κB. Keeping this rationale in mind, we propose that both loss-of-function alleles of TLR8 and -4 convey susceptibility towards TB by altering the balance of the NF-κB and type I IFN axes, possibly more pronouncedly reducing the latter, and that this interaction plays a crucial role in a successful host response against Mtb.

Eliminating TB is a set goal by the WHO by 2030 [47]. In order to achieve this goal, novel intervention strategies are needed, which will be based on a complete understanding of the pathophysiology. Furthermore, individual risk stratification will be important to improve prevention strategies. Therefore, the interaction of TLR4 and TLR8, by offering new treatment targets and understanding individual progression risk, might contribute to eliminating TB in the future. This is particularly needed in the face of increasing incidence of multi-drug resistant TB.

Implications for the importance of TLR4 and TLR8 interaction might be found beyond TB. Endosomal TLRs recognising RNA such as TLR8 play an important role in viral diseases. Regarding the current SARS-CoV-2 outbreak, i.e., it has been suggested that SARS-Cov-2 contains more RNA sequences recognisable by TLR7/8 than SARS-CoV-1, and by that potentially causing more frequently a hyperinflammatory syndrome [48]. Similarly, there have been studies claiming an important role of TLR4 in SARS-CoV-2, as in silico studies identified TLR4 as very likely to respond to spike proteins of SARS-

enhanced spontaneously upon co-transfection of TLR4 and TLR8, possibly more so with TLR4-399C.

TLR4 has been suggested to be a main receptor involved in TB immunity by recognising mycobacterial antigens upon which a MyD88- and TRIF-dependent Th1 answer is fostered, although no clear explanation for this has been provided [10]. TLR4 involvement has been supported by mechanisms that Mtb has evolved to avoid the host immune system involving TLR4: mycobacterial anti-inflammatory proteins such as phosphatidylinositol mannosides, LM, and LAM that specifically inhibit TLR4-induced pathways or lead to TLR4-triggered immunosuppression [21,37,38]. Furthermore, Mtb is known to block the acidification and maturation of phagosomes, thereby generally inhibiting host immune receptors that require a low pH to function properly.

TLR4 polymorphisms are differently distributed around the world, and they are attributed to evolutionary pressure from infectious diseases and the migration of mankind over time. TLR4-299G without linkage with TLR4-399T can be found among African populations and is reported to be protective against malaria [39]. However, in Europe, this allele is linked with TLR4-399T [40]. We found that among the Indian population, TLR4-399T can occur as a single non-linked mutation, next to the TLR4-299G/-399T haplotype. TLR4-399T has already been associated with increased TB susceptibility [41,42]. Reduced LPS responsiveness is a known functional implication of this SNP, as we saw in HEKs. However, in THPs and PBMCs, we also surprisingly found hyperresponsiveness. These conflicting data have been reported in the literature, and recently, a mouse model with the human SNPs TLR4-299 and TLR4-399 confirmed that both SNPs contribute to cell hyporesponsiveness [43].

TLR8-1A, by being less functional than TLR-1G, is also associated with TB susceptibility [32]. What we report here, and to our knowledge for the first time, is the direct interaction at the endosomal level of TLR4 and TLR8. Our experiments show that synergy through the simultaneous stimulation of both receptors leads to higher levels of IL-12, and others have shown increased IL-12 in monocyte-derived DCs [29] and a higher expression of antigen-presenting, co-stimulatory molecules on matured DCs [30]. Crosstalk between TLRs to modulate the immune response is an established concept; for instance, studies show that the co-activation of both TLR3 and TLR8 is necessary to achieve a strong IL12p70 answer [27]. It is also known that the co-stimulation of TLR8 and -2 induces a shift towards a Th17-immunity [44]. Another example is the endosomal heterodimerisation of TLR4 and -6 in the presence of the co-receptor CD36 in responses to oxidised LDL during atherogenesis, independent of MD-2 and CD14 [45]. This signalling induced both MyD88- and TRIF-dependent genes. Similarly, in our study, we could show that the heterodimerisation of TLR4 and TLR8 activated both NF-κB- and IRF3-linked pathways.

Co-IP showed that the co-transfection of TLR4 and TLR8 lead even in unstimulated cells to the ability to precipitate TLR4 through TLR8, potentially indicating spontaneous heterodimerisation even without stimulation. Mass spectrometry of the lysed precipitates revealed that UNC93B1, a chaperone required for TLR8 endosomal trafficking, was identified alongside TLR8 [35]. For TLR4, UNC93B1 is not required. From our data, we cannot conclude whether UNC93B1 was merely pulled down alongside TLR8 homodimers or promoted heterodimerisation with TLR4, but this might be a focus of further research.

In confocal studies, we saw co-localisation upon co-transfection with an increase of co-localisation frequency even if only one receptor was stimulated. However, in contrast to co-IP, co-localisation frequency even further increased with double simulation, which was possibly due to the different read-outs and the close proximity of the receptors, not being able to distinguish between co-localisation, homo- and heterodimerisation upon stimulation.

The formation of a heterodimer in co-IP studies and confocal microscopy was observed without MD2 and CD14, although it is the established concept that TLR4/MD2/CD14/LPS is necessary for TLR4 internalisation [46]. This might be due to the experimental set-up, as, in HEK-cells, we delivered TLR4 by transfection directly to the endosome. Interestingly,

CoV-2 [49]. Interestingly, TLR4 is also associated with cardiometabolic comorbidities such as obesity and hypertension, which are known risk factors for severe COVID with hyperinflammation [50]. Furthermore, TLR4-deficient mice were less susceptible to acute respiratory distress syndrome (ARDS) upon inhalation trauma [51].

Taken together, our data suggest that TLR4 and TLR8 form a heterodimer changing the immune response towards a Th1 balance. Mutations leading to a loss of function of this specific pathway seem to convey susceptibility towards TB. Thus, the interaction of TLR4 and TLR8 might open up new targets for vaccines or therapeutic drugs. Finally, genetic risk stratification may lead to better prevention strategies of individuals at increased risk.

4. Materials and Methods

4.1. Study Subjects

The cohort of TB patients and controls in Hyderabad has been described before [34]. In brief, the cohort consisted of 346 TB patients with either PTB, EPTB or a relapse, and 301 Controls (HC) including healthy household contacts (HHC). Patients, who attended Free Chest TB Clinic with directly observed treatment surveillance (DOTS) at Mahavir Hospital and Research Centre, Hyderabad, were confirmed with the sputum microscopy for acid-fast bacilli, culture, and chest X-ray or histopathology as per the guidelines of the Revised National Tuberculosis Control Program (RNTCP). Patients with diabetes, hypertension, HIV, and other comorbidities were excluded from the study. Informed consent was obtained from all subjects. The study was approved by the institutional ethics committee of Bhagwan Mahavir Medical Research Centre (BMMRC), Hyderabad, and Charité Medical University Berlin. The German cohort consisted of 853 volunteers, as described earlier [52]. All studies followed the ethical principles of the declaration of Helsinki.

4.2. SNP Analysis

Genomic DNA was extracted from whole blood of TB patients and healthy volunteers using a DNA Blood mini kit (Qiagen GmbH, Hilden, Germany) or from buccal swabs using a DNA kit (Qiagen) according to the manufacturer's protocol. Quantity of DNA was confirmed by NanoDrop and DNA was stored at −20 °C. Functionally relevant SNPs were analysed using Light Cycler Assays (Roche) based on the differentiation of fluorescence signals due to nucleic acid differences and the respective melting curves. Primers used are found in Table S6.

4.3. Modelling and Molecular Docking

Homology model of the human TLR4 with threonine at 399 was determined, using the crystal structure of TLR4 (PDB ID: 4G8A) as a template with MODELLER [53]. The structure 4G8A had isoleucine (I) in position 399. Refinement and quality estimation of the model was carried out using Swiss PDB viewer [54] and SAVES server (https://servicesn.mbi.ucla.edu/SAVES/). The structure of TLR8 (PDB ID: 3W3M) with resiquimod (R848) ligand was obtained from the PDB database (www.rcsb.org). Molecular docking was implemented using PatchDock [55] and FireDock [56]. In this process, transformations of docking elements obtained from PatchDock were given as an input to FireDock. Firedock initially performs coarse refinement followed by refinements and energy-based rankings. Next, it implements chain optimisation to reduce steric clashes [56]. The generated model of TLR4 having threonine (position 399) and the structure TLR8 was used as inputs during docking. Similarly, in another study, the structure of TLR4 (I399) was considered to find out if it formed a dimer with TLR8 in the presence of the ligand R848. The interacting residues were visualised with LigPlot v2.

4.4. In Vitro Experiments

4.4.1. Stimulants and Reagents

The stimulants LPS, R848, ssRNA40, and PAM_3CSK_4 and the antagonists bafilomycin, polymyxin B (PMB), dynasore, and CLI-095 were purchased from Invivogen (Toulouse, France). The concentration of above stimulants and antagonists were standardised as LPS (10 ng/mL), R848 (2 μg/mL), ssRNA40 (5 μg/mL), PAM_3CSK_4 (2 μg/mL), bafilomycin (1 μM), PMB (10 μg/mL), Dynasore (50 μM), and CLI-095 (3 μM). Mycobacterial RNA was extracted from gamma-irradiated Mycobacterium tuberculosis H37Rv (BEI Resources, NR-14819) with InnuPrep RNA Mini Kit (Analytik Jena, Germany). Purity was confirmed by Scandrop analysis (Analytik Jena). A 260 nm/280 nm extinction quotient of 1.9-2.0 was considered pure. For transfection, if not otherwise specified, LyoVec (Invivogen) was used in a 3 μg/100 μL dilution according to protocol.

4.4.2. Mutagenesis

hTLR8-pUno3 and hTLR4-pUno3 plasmid were purchased from Invivogen and hTLR4 mcherry-myc. All these plasmids were mutated with QuikChange II XL Site-Directed Mutagenesis Kit (Agilent Genes, Frankfurt am Main, Germany) according to user's manual using the primers designed with primerX software (Table S7). Maxi Prep of mutated and original plasmid was performed with Plasmid Maxi Kit (Qiagen, Hilden, Germany). Successful mutation was confirmed by Value Read sequencing (Eurofins, Ebersberg, Germany), using the primer 5′CTGTAGTCGACGATTGCTGC3′ for TLR8 and 5′AGGTAAATGAGGTTTCTGAGTGA3′ for TLR4 designed with Primer3 software.

4.4.3. Cell Line Experiments

THP NF-κB (Invivogen) cells were harvested in RPMI 1640 + 10% FCS + 100 μg/mL blasticidin. Cells were counted and plated on 96-well plates with 1×10^5 cells/well in 150 μL of RPMI 1640 + 10% FCS Medium. The cells were differentiated to macrophages by using PMA (50 ng/mL) 3 h prior to transient transfection. Cells were treated with or without bafilomycin, PMB, dynasore, CL-095 1 h prior to stimulation of R848, LPS, or Mtb RNA/Lyovec for 18–24 h. Then, 20 μL of supernatant were transferred to QUANTI-Blue detection medium (Invivogen) for SEAP estimation at 620 nm absorbance, corresponding with NF-κB-activity.

Hek Blue Null 1 (Invivogen) cells were harvested in Dulbecco's Modified Eagle's Medium (DMEM) + 10% fetal calf serum (FCS) + 100 μg/mL zeocin. 1.5×10^5 cells were distributed in T25-flasks and cultured overnight before transient transfection. After 48 h, cells were counted and plated on 96-well plates with 5×10^4 cells/well in 160 μL of Hek Blue Detection Medium (Invivogen). For stimulation, LPS, R848, a combination of LPS/R848 or mycobacterial RNA/LyoVec was added, making up to 200 μL well volume. After 16 h (unless specified) of stimulation, SEAP levels were measured at 620 nm absorbance each value was normalised to the respective negative control (PBS). HEK 293XL hTLR8 HA cells overexpressing UNC93B1-mCitrine cells were cultured in 24-well plates prior to transient transfection [35].

Note: We have confirmed that there was no LPS contamination in the TLR8 ligands by treating THP monocyte-derived macrophages with PMB specifically blocking LPS stimulation by binding to lipid A of LPS (Figure S8).

4.4.4. Transient Transfection

For Co-IP and confocal microscopy, HEK 293XL hTLR8 HA cells were used. HEK 293XL hTLR8 HA transiently transfected using Extreme Gene 9 (Roche) in a 1:3 ratio according to protocol for 24 h. The following plasmids were used for transient transfection: hTLR4 mCherry-myc and its variant forms, with and without the accessory proteins gp96, PRAT4A, CD14, and MD2 as indicated, and empty plasmid (pUno3). All the plasmid combinations were attained to a final concentration of 3 μg. Regarding the additional set of experiments with monkey TLR4 plasmids, pEF1a_rhesus TLR4 N-FLAG IRES DsRed

Express2 and pEF1a_sooty mangabey TLR4 N-FLAG IRES DsRed Express2 (provided by Prof. Dr. Sauter, Ulm) were performed as described above. For functional studies with HEK Blue Null 1 cells, transient transfection as described above was performed with and without MD2 and CD14 as indicated.

THP NF-κB: The cells were transfected using the Amaxa Nucleofector (Amaxa, Cologne, Germany) according to the manufacturer's protocol (Cell Line Nucleofector Kit V, Program T-08) with 2 μg DNA/10^6 cells, psiRNA TLR8, psiRNA TLR4, psiRNA MyD88 or psiRNA Ticam2 (plasmid-based siRNA designed by Invivogen).

4.4.5. Immunofluorescence Staining of TLR8HA/Confocal Microscopy

First, 1×10^5 HEK 293XL hTLR8-HA UNC93B1-mCitrine cells/well were seeded in imaging dishes (Ibidi), which was followed by transfection including accessory proteins gp96, PRAT4A, CD14, and MD2 for 48 h and stimulation with various ligands for 2 h. TLR8-HA was stained with anti-HA antibody (Sigma Aldrich, Munich, Germany) at a dilution of 1:200 in PBS containing 1% (*w/v*) bovine serum albumin (BSA) for 1 h at room temperature. Specimens were washed three times with PBS and incubated with anti-rabbit Alexa647 antibody diluted 1:2000 in PBS containing 1% (*w/v*) BSA for 30 min at room temperature. TLR4 plasmid has mCherry fluroprobe. Then, cells were imaged on a Leica SP5 AOBS with SMD confocal microscope, with a 63×, NA 1.20 water-immersion objective, at a lateral resolution of 120 nm. Cell Profiler and Fiji software were used to analyse the co-alocalisation, which was defined as a spatial overlap of fluorescent TLR4- and TLR8-labels indicated by yellow dots [57].

4.4.6. Co-Immunoprecipitation

Per condition, 5 million cells were lysed in 250 μL NP40 lysis buffer for 30–60 min on ice. Lysates were collected by centrifuging at 4000× *g* for 5 min at 4 °C. Then, 30 μL of lysate was saved as a control, and the rest of the lysate was used for IP. IP was performed with HA agarose beads/anti-FLAG-M2 affinity gel (Sigma Aldrich, Munich, Germany) according to the manual. Per IP, 50 μL of the 1:1 suspension of the anti-HA agarose was used, and IP was performed for 2 h at 4 °C shaking. After the last wash, 30 μL 2× Lämmli was added. The lysate collected before IP (Input) served as a positive control, for negative control (NC) lysis buffer without antibody was used.

4.4.7. Western Blot Procedure

Cell lysates were separated by SDS-PAGE and blotted. Membranes were first exposed to Abs specific for anti-TLR4, anti-HA, anti-FLAG, anti-IRF3, and anti-GAPDH (Santa Cruz Biotechnology, Heidelberg, Germany) and subsequently incubated with secondary Abs. Proteins were detected using electrochemiluminescence (ECL) (32106 Pierce™ ECL Western Blotting Substrate). The band intensities were quantified using image J.

4.5. Mass Spectrometry (MS)

4.5.1. Sample Preparation

Eluted proteins from IPs (1% SDS in PBS) were reduced with 50 mM of Dithiothreitol (5 min, 95 °C) and diluted with 8 M Urea in 100 mM Tris/HCl pH = 8.0. Buffer exchange and protein digestion was done according to the filter-aided sample preparation protocol [58]. In brief, the reduced proteins were transferred to a 30 kDa Microcon filter unit (YM-30 filter units, Millipore) and centrifuged at 14.000× *g* for 20 min in all consecutive steps, and the flow-through discarded. For washing, 200 μL urea buffer (8 M Urea, 100 mM Tris HCL, pH 8.0) was added, and the centrifugation was repeated. Then, 100 μL of alkylation solution (0.1 M iodoacetamide in urea buffer) was added, and samples were incubated for 20 min in the dark. The alkylation solution was removed by centrifugation followed by two additional centrifugation steps with 200 μL 8 M urea buffer. Afterwards, samples were washed and centrifuged twice with 200 μL 50 mM ammonium bicarbonate buffer. Proteins were digested by the addition of 0.5 μg trypsin in 50 μL digestion buffer (50 mM

ammonium bicarbonate). Proteolytic cleavage was allowed for 16 h at 37 °C, and peptides eluted by centrifugation. To collect residual peptides, the centrifugation was repeated twice after the addition of 50 µL ammonium bicarbonate buffer (50 mM). Eluted peptides were dried in a SpeedVac (Thermo Fisher) and reconstituted by adding 20 µL of 0.3% formic acid in water.

4.5.2. Mass Spectrometric and Statistical Analysis

Tryptic peptides were analysed with a Dionex UHPLC (Thermo Scientific) coupled to an Orbitrap Fusion LC-MS/MS system (Thermo Scientific). Full mass spectrometry scans were acquired in the Orbitrap (m/z range 370–1570, quadrupole isolation) at a resolution of 120,000 (full width at half maximum) during a 60 min, non-linear gradient from 2 to 90% acetonitrile/0.1% formic acid. Peptides were fragmented by higher-energy collisional dissociation (HCD, 30% collision energy) and maximum 10 fragment ion spectra were acquired per cycle in the Orbitrap analyser at a resolution of 15,000 using quadrupole isolation (m/z window 1.6). The following conditions were used: spray voltage of 2.1 kV, heated capillary temperature of 275 °C, S-lens RF level of 60%, a maximum automatic gain control (AGC) value of 4×10^5 counts for MS1 with a maximum ion injection time of 50 ms and a maximum AGC value of 5×10^4 for MS2, with a maximum ion accumulation time of 45 ms. A dynamic mass exclusion time window of 5 s was set with a 10 ppm maximum mass window.

All raw files were searched against the human UniProt database (version 05.2016, reviewed sequences) with MaxQuant version 1.5.5.1 (Max Planck Institute of Biochemistry, Germany) [59]. The default parameters were used or set as follows: first search peptide tolerance: 20 ppm, main search peptide tolerance: 4.5 ppm (for MaxQuant); enzyme: trypsin, max. 2 missed cleavages; static modification: carbamidomethylation of cysteine residues; variable modifications: methionine oxidation; min. peptide length: 6, max. peptide mass: 7600 Da. Normalisation was omitted and Label-Free Quantification (LFQ) min. ratio count was set to 1 (unique and razor peptides). Peptide specific match (PSM) and protein false discovery rate was set to 0.01. Label-Free Quantification (LFQ) values of all samples were loaded into Perseus (version 1.5.5.0) [60]. Groups were created, with 6 samples per group: (a) TLR4 with and without stimulation, (b) TLR8+TLR4 with and without stimulation, (c) TLR8 with and without stimulation. The resulting matrix was reduced as proteins were identified as "possible contamination" or "only identified per site", while "reverse identified proteins" and "identified in less than 2 samples per group" were discarded. LFQ values were log2-transformed, and missing values imputed by default parameters. The negative logarithmic difference of the means of protein intensities of MS was plotted against the *p*-values from respective *t*-tests.

4.6. PBMC Experiments

PBMCs from individuals of the Indian cohort differing in their genotype of TLR8-M1V and TLR4-T399I were isolated with lymphocyte separation medium (LSM 1077 GE Healthcare) according to the user's manual, seeded at 3×10^5 cells per well on 96-well plates in RPMI 1640 + 10% FCS and left overnight at 370 in a humidified incubator with 5% CO2. Then, PBMCs were stimulated with LPS, R848, a combination of LPS and R848 or mycobacterial RNA/LyoVec. Cytokines were analysed in the supernatants by enzyme-linked immunoassays according to the respective standard manufacturer's recommendations. TNFα levels were determined after 4 h (BD Pharmingen: 551220, 554511), and IL-12p40 (BD Biosciences) levels were measured after 24 h post-stimulation.

4.7. Statistical Analysis

Statistical analysis was performed using STATA 16. Descriptive characteristics were obtained, and for the assessment of differences of basic characteristics, *t*-tests for continuous variables and chi-square for categorical data tests were used. For assessing the odds associated with a specific allele, genotypes were dichotomised, summarising minor alleles,

and a logistic regression model was used; 95% confidence intervals are given in square brackets. The main outcome was being a TB patient or a relapse, depending on the context. Gender and age were included a priori, as was BCG status whenever a TLR8-SNP was assessed, based on previous reports. Other variables were included according to the evidence for confounding based on comparison of crude and adjusted OR, using Wald's test. Final significance testing and tests for effect modification were based on likelihood ratio tests (LRTs). For analysis of functional, Prism (Version 5.01) was used, performing either Mann–Whitney U or T-tests, as appropriate. For analysis of mass spectrometry, Persus software was used.

Supplementary Materials: The following are available online at https://www.mdpi.com/1422-0067/22/4/1560/s1.

Author Contributions: S.T.—Conducting all in vitro experiments, writing, review of manuscript; G.L.H.—Confocal Microscopy; M.M.M.—MS/MS analysis; N.D., M.L.C. and A.H.—Patient cohort generation; S.S.—Docking studies; K.P.—Stable cell generation (HEK293 XL-hTLR8HA/Unc93B1); S.L.G.—Cohort establishment; E.L.—Supervision of confocal microscopy; H.S.—Facilitation of MS/MS analysis and cohort generation; R.R.S.—Design and supervision of all parts of the study, establishment of collaborations, writing and review of the manuscript. S.B.—General supervision, writing and review of manuscript. All authors have read and agreed to the published version of the manuscript.

Funding: This research was funded by the German Research Foundation (Deutsche Forschungsgemeinschaft, DFG) International Research Training Group (IRTG), GRK 1673 "Functional molecular infection epidemiology" project A5 (to RRS) and project A4 (to HS) and the Sonnenfeld Stiftung, Berlin, Germany (to ST).

Institutional Review Board Statement: The study was approved by the institutional ethics committee of Bhagwan Mahavir Med-ical Research Centre (BMMRC), Hyderabad, and Charité Medical University Berlin.

Informed Consent Statement: Informed consent was obtained from all individual participants included in the study.

Data Availability Statement: Data available within the article or its supplementary materials and on request from the authors.

Acknowledgments: We thank the staff of the free chest clinic Mahavir PPM DOTS, Tuberculosis Unit (T.U), Bhagwan Mahavir Trust and all patients and volunteers participated in this study. We thank Daniel Sauter, Institute of Molecular Virology, Ulm University, Germany for providing the Monkey plasmids. We furthermore thank Lutz Hamann of the Institute for Microbiology, Charité, Berlin for his help in SNP selection and genotyping. We thank Surabhi Goyal, Institute for Microbiology, Charité, Berlin, and ZIK Septomics, Jena, Germany for her co-operation during cohort collection in India. We finally thank Inga Wyroslak and Frauke Schreiber of the Institute for Microbiology, Charité, Berlin for their excellent technical assistance.

Conflicts of Interest: The authors declare no conflict of interest.

Abbreviations

A	Adenine
APC	Antigen-presenting cell
ARDS	acute respiratory distress syndrome
BCG	Bacillus Calmette–Guérin
BMI	Body mass index
BSA	Bovine serum albumin
C	Cytosine
DC	Dendritic cell
DMEM	Dulbecco's Modified Eagle's Medium
ELISA	Enzyme-linked immunosorbent assay

EPTB	Extrapulmonary TB
FCS	Fetal calf serum
G	Guanine
HA	Human influenza hemagglutinin
HC	Healthy control
HEK	Human embryonic kidney
HHC	Healthy household contact
IFN	Interferon
IL	Interleukin
IP	Immunoprecipitation
IRF	Interferon response factor
LAM	Lipoarabinomannan
LM	Lipomannan
LPS	Lipopolysaccharide
LRT	Likelihood ratio test
MHC	Major histocompatibility complex
Mtb	Mycobacerium tuberculosis
MyD88	Myeloid differentiation primary response 88
NF-κB	Nuclear factor kappa-light-chain-enhancer of activated B cells
PAMP	Pathogen-associated molecular pattern
PMB	Polymyxin B
PRR	Pattern recognition receptor
PTB	Pulmonary TB
SEAP	Secreted embryonic alkaline phosphatase
T	Thymine
TB	Tuberculosis
Th	T helper
TLR	Toll-like receptor
TNF	Tumour necrosis factor
TRAM	TRIF-related adaptor molecule
TRIF	TIR-domain-containing adapter-inducing interferon-β
WB	Western blotting

References

1. Medzhitov, R.; Janeway, C., Jr. Advances in immunology: Innate immunity. *N. Engl. J. Med.* **2000**, *343*, 338–344. [CrossRef] [PubMed]
2. Reis e Sousa, C. Activation of dendritic cells: Translating innate into adaptive immunity. *Curr. Opin. Immunol.* **2004**, *16*, 21–25. [CrossRef] [PubMed]
3. Kumar, H.; Kawai, T.; Akira, S. Pathogen Recognition by the Innate Immune System. *Int. Rev. Immunol.* **2011**, *30*, 16–34. [CrossRef]
4. Fitzgerald, K.A.; Kagan, J.C. Toll-like Receptors and the Control of Immunity. *Cell* **2020**, *180*, 1044–1066. [CrossRef]
5. O'Neill, L.A.J.; Golenbock, D.; Bowie, A.G. The history of Toll-like receptors—redefining innate immunity. *Nat. Rev. Immunol.* **2013**, *13*, 453–460. [CrossRef] [PubMed]
6. Gay, N.J.; Symmons, M.F.; Gangloff, M.; Bryant, C.E. Assembly and localization of Toll-like receptor signalling complexes. *Nat. Rev. Immunol.* **2014**, *14*, 546–558. [CrossRef]
7. Kirschning, C.J.; Schumann, R.R. TLR2: Cellular sensor for microbial and endogenous molecular patterns. *Curr. Top. Microbiol. Immunol.* **2002**, *270*, 121–144.
8. Faridgohar, M.; Nikoueinejad, H. New findings of Toll-like receptors involved in Mycobacterium tuberculosis infection. *Pathog. Glob. Health* **2017**, *111*, 256–264. [CrossRef]
9. Chang, J.-S.; Huggett, J.F.; Dheda, K.; Kim, L.U.; Zumla, A.; Rook, G.A.W. Myobacterium tuberculosis Induces Selective Up-Regulation of TLRs in the Mononuclear Leukocytes of Patients with Active Pulmonary Tuberculosis. *J. Immunol.* **2006**, *176*, 3010–3018. [CrossRef]
10. Sepehri, Z.; Kiani, Z.; Kohan, F.; Ghavami, S. Toll-Like Receptor 4 as an Immune Receptor against Mycobacterium tuberculosis: A Systematic Review. *Lab. Med.* **2019**, *50*, 117–129. [CrossRef]
11. Shimazu, R.; Akashi, S.; Ogata, H.; Nagai, Y.; Fukudome, K.; Miyake, K.; Kimoto, M. MD-2, a molecule that confers lipopolysaccharide responsiveness on toll- like receptor 4. *J. Exp. Med.* **1999**, *189*, 1777–1782. [CrossRef]
12. Da Silva Correia, J.; Soldau, K.; Christen, U.; Tobias, P.S.; Ulevitch, R.J. Lipopolysaccharide is in close proximity to each of the proteins in its membrane receptor complex. Transfer from CD14 to TLR4 and MD-2. *J. Biol. Chem.* **2001**, *276*, 21129–21135. [CrossRef]

13. Tan, Y.; Zanoni, I.; Cullen, T.W.; Goodman, A.L.; Kagan, J.C. Mechanisms of Toll-like Receptor 4 Endocytosis Reveal a Common Immune-Evasion Strategy Used by Pathogenic and Commensal Bacteria. *Immunity* **2015**, *43*, 909–922. [CrossRef] [PubMed]
14. Liu, S.; Cai, X.; Wu, J.; Cong, Q.; Chen, X.; Li, T.; Du, F.; Ren, J.; Wu, Y.-T.; Grishin, N.V.; et al. Phosphorylation of innate immune adaptor proteins MAVS, STING, and TRIF induces IRF3 activation. *Science* **2015**, *347*, aaa2630. [CrossRef]
15. Tanimura, N.; Saitoh, S.; Matsumoto, F.; Akashi-Takamura, S.; Miyake, K. Roles for LPS-dependent interaction and relocation of TLR4 and TRAM in TRIF-signaling. *Biochem. Biophys. Res. Commun.* **2008**, *368*, 94–99. [CrossRef] [PubMed]
16. Lv, J.; He, X.; Wang, H.; Wang, Z.; Kelly, G.T.; Wang, X.; Chen, Y.; Wang, T.; Qian, Z. TLR4-NOX2 axis regulates the phagocytosis and killing of Mycobacterium tuberculosis by macrophages. *BMC Pulm. Med.* **2017**, *17*, 194. [CrossRef]
17. Rocha-Ramírez, L.M.; Estrada-García, I.; López-Marín, L.M.; Segura-Salinas, E.; Méndez-Aragón, P.; Van Soolingen, D.; Torres-González, R.; Chacón-Salinas, R.; Estrada-Parra, S.; Maldonado-Bernal, C.; et al. Mycobacterium tuberculosis lipids regulate cytokines, TLR-2/4 and MHC class II expression in human macrophages. *Tuberculosis* **2008**, *88*, 212–220. [CrossRef]
18. Jang, A.-R.; Kim, G.; Hong, J.J.; Kang, S.M.; Shin, S.J.; Park, J.-H. Mycobacterium tuberculosis ESAT6 Drives the Activation and Maturation of Bone Marrow-Derived Dendritic Cells via TLR4-Mediated Signaling. *Immune Netw.* **2019**, *19*, e13. [CrossRef]
19. Kim, W.S.; Jung, I.D.; Kim, J.-S.; Kim, H.M.; Kwon, K.W.; Park, Y.-M.; Shin, S.J. Mycobacterium tuberculosis GrpE, A Heat-Shock Stress Responsive Chaperone, Promotes Th1-Biased T Cell Immune Response via TLR4-Mediated Activation of Dendritic Cells. *Front. Cell. Infect. Microbiol.* **2018**, *8*, 95. [CrossRef] [PubMed]
20. Parveen, N.; Varman, R.; Nair, S.; Das, G.; Ghosh, S.; Mukhopadhyay, S. Endocytosis of Mycobacterium tuberculosis Heat Shock Protein 60 Is Required to Induce Interleukin-10 Production in Macrophages. *J. Biol. Chem.* **2013**, *288*, 24956–24971. [CrossRef] [PubMed]
21. Doz, E.; Rose, S.; Court, N.; Front, S.; Vasseur, V.; Charron, S.; Gilleron, M.; Puzo, G.; Fremaux, I.; Delneste, Y.; et al. Mycobacterial Phosphatidylinositol Mannosides Negatively Regulate Host Toll-like Receptor 4, MyD88-dependent Proinflammatory Cytokines, and TRIF-dependent Co-stimulatory Molecule Expression. *J. Biol. Chem.* **2009**, *284*, 23187–23196. [CrossRef]
22. Mazurek, J.; Ignatowicz, L.; Kallenius, G.; Svenson, S.B.; Pawlowski, A.; Hamasur, B. Divergent Effects of Mycobacterial Cell Wall Glycolipids on Maturation and Function of Human Monocyte-Derived Dendritic Cells. *PLoS ONE* **2012**, *7*, e42515. [CrossRef]
23. Ugolini, M.; Gerhard, J.; Burkert, S.; Jensen, K.J.; Georg, P.; Ebner, F.; Volkers, S.M.; Thada, S.; Dietert, K.; Bauer, L.; et al. Recognition of microbial viability via TLR8 drives TFHcell differentiation and vaccine responses. *Nat. Immunol.* **2018**, *19*, 386–396. [CrossRef] [PubMed]
24. Thada, S.; Burkert, S.; Sivangala, R.; Hussain, A.; Sur, S.; Dittrich, N.; Conrad, M.L.; Slevogt, H.; Latha Gaddam, S.; Schumann, R.R. A SNP upstream of the cyclic GMP-AMP synthase (cGAS) gene protects from relapse and extra-pulmonary TB and relates to vaccination status in an Indian cohort. *Genes Immun.* **2020**, *21*, 13–26. [CrossRef]
25. Burkert, S.; Schumann, R.R. RNA Sensing of Mycobacterium tuberculosis and Its Impact on TB Vaccination Strategies. *Vaccines* **2020**, *8*, 67. [CrossRef]
26. Hornung, V.; Rothenfusser, S.; Britsch, S.; Krug, A.; Jahrsdörfer, B.; Giese, T.; Endres, S.; Hartmann, G. Quantitative expression of toll-like receptor 1-10 mRNA in cellular subsets of human peripheral blood mononuclear cells and sensitivity to CpG oligodeoxynucleotides. *J. Immunol.* **2002**, *168*, 4531–4537. [CrossRef] [PubMed]
27. Ishii, N.; Funami, K.; Tatematsu, M.; Seya, T.; Matsumoto, M. Endosomal Localization of TLR8 Confers Distinctive Proteolytic Processing on Human Myeloid Cells. *J. Immunol.* **2014**, *193*, 5118–5128. [CrossRef]
28. Keegan, C.; Krutzik, S.; Schenk, M.; Scumpia, P.O.; Lu, J.; Pang, Y.L.J.; Russell, B.S.; Lim, K.S.; Shell, S.; Prestwich, E.; et al. Mycobacterium tuberculosis Transfer RNA Induces IL-12p70 via Synergistic Activation of Pattern Recognition Receptors within a Cell Network. *J. Immunol.* **2018**, *200*, 3244–3258. [CrossRef] [PubMed]
29. Vergne, I.; Fratti, R.A.; Hill, P.J.; Chua, J.; Belisle, J.; Deretic, V. Mycobacterium tuberculosis Phagosome Maturation Arrest: Mycobacterial Phosphatidylinositol Analog Phosphatidylinositol Mannoside Stimulates Early Endosomal Fusion. *Mol. Biol. Cell* **2004**, *15*, 751–760. [CrossRef]
30. Stewart, G.R.; Patel, J.; Robertson, B.D.; Rae, A.; Young, D.B. Mycobacterial Mutants with Defective Control of Phagosomal Acidification. *PLoS Pathog.* **2005**, *1*, e33. [CrossRef] [PubMed]
31. Jafari, M.; Nasiri, M.R.; Sanaei, R.; Anoosheh, S.; Farnia, P.; Sepanjnia, A.; Tajik, N. The NRAMP1, VDR, TNF-α, ICAM1, TLR2 and TLR4 gene polymorphisms in Iranian patients with pulmonary tuberculosis: A case–control study. *Infect. Genet. Evol.* **2016**, *39*, 92–98. [CrossRef]
32. Davila, S.; Hibberd, M.L.; Hari Dass, R.; Wong, H.E.E.; Sahiratmadja, E.; Bonnard, C.; Alisjahbana, B.; Szeszko, J.S.; Balabanova, Y.; Drobniewski, F.; et al. Genetic Association and Expression Studies Indicate a Role of Toll-Like Receptor 8 in Pulmonary Tuberculosis. *PLoS Genet.* **2008**, *4*, e1000218. [CrossRef]
33. Berrocal-Almanza, L.C.; Goyal, S.; Hussain, A.; Klassert, T.E.; Driesch, D.; Grozdanovic, Z.; Sumanlatha, G.; Ahmed, N.; Valluri, V.; Conrad, M.L.; et al. S100A12 is up-regulated in pulmonary tuberculosis and predicts the extent of alveolar infiltration on chest radiography: An observational study. *Sci. Rep.* **2016**, *6*, 31798. [CrossRef]
34. Dittrich, N.; Berrocal-Almanza, L.C.; Thada, S.; Goyal, S.; Slevogt, H.; Sumanlatha, G.; Hussain, A.; Sur, S.; Burkert, S.; Oh, D.-Y.; et al. Toll-like receptor 1 variations influence susceptibility and immune response to Mycobacterium tuberculosis. *Tuberculosis* **2015**, *95*, 328–335. [CrossRef]

35. Pelka, K.; Bertheloot, D.; Reimer, E.; Phulphagar, K.; Schmidt, S.V.; Christ, A.; Stahl, R.; Watson, N.; Miyake, K.; Hacohen, N.; et al. The Chaperone UNC93B1 Regulates Toll-like Receptor Stability Independently of Endosomal TLR Transport. *Immunity* **2018**, *48*, 911–922.e7. [CrossRef] [PubMed]
36. Ii, M.; Matsunaga, N.; Hazeki, K.; Nakamura, K.; Takashima, K.; Seya, T.; Hazeki, O.; Kitazaki, T.; Iizawa, Y. A novel cyclohexene derivative, ethyl (6R)-6-[N-(2-chloro-4-fluorophenyl) sulfamoyl]cyclohex-1-ene-1-carboxylate (TAK-242), selectively inhibits toll-like receptor 4-mediated cytokine production through suppression of intracellular signaling. *Mol. Pharmacol.* **2006**. [CrossRef]
37. Huang, Z.; Zhao, G.W.; Gao, C.H.; Chi, X.W.; Zeng, T.; Hu, Y.W.; Zheng, L.; Wang, Q. Mannose-capped Lipoarabinomannan from Mycobacterium tuberculosis induces IL-37 production via upregulating ERK1/2 and p38 in human type II alveolar epithelial cells. *Int. J. Clin. Exp. Med.* **2015**, *8*, 7279–7287. [PubMed]
38. Mpofu, C.M.; Campbell, B.J.; Subramanian, S.; Marshall–Clarke, S.; Hart, C.A.; Cross, A.; Roberts, C.L.; McGoldrick, A.; Edwards, S.W.; Rhodes, J.M. Microbial Mannan Inhibits Bacterial Killing by Macrophages: A Possible Pathogenic Mechanism for Crohn's Disease. *Gastroenterology* **2007**, *133*, 1487–1498. [CrossRef] [PubMed]
39. Mockenhaupt, F.P.; Hamann, L.; von Gaertner, C.; Bedu-Addo, G.; von Kleinsorgen, C.; Schumann, R.R.; Bienzle, U. Common Polymorphisms of Toll-Like Receptors 4 and 9 Are Associated with the Clinical Manifestation of Malaria during Pregnancy. *J. Infect. Dis.* **2006**, *194*, 184–188. [CrossRef]
40. Plantinga, T.S.; Ioana, M.; Alonso, S.; Izagirre, N.; Hervella, M.; Joosten, L.A.B.; van der Meer, J.W.M.; de la Rúa, C.; Netea, M.G. The Evolutionary History of TLR4 Polymorphisms in Europe. *J. Innate Immun.* **2012**, *4*, 168–175. [CrossRef]
41. Schurz, H.; Daya, M.; Möller, M.; Hoal, E.G.; Salie, M. TLR1, 2, 4, 6 and 9 Variants Associated with Tuberculosis Susceptibility: A Systematic Review and Meta-Analysis. *PLoS ONE* **2015**, *10*, e0139711. [CrossRef]
42. Zhao, L.; Liu, K.; Kong, X.; Tao, Z.; Wang, Y.; Liu, Y. Association of polymorphisms in toll-like receptors 4 and 9 with risk of pulmonary Tuberculosis: A meta-analysis. *Med. Sci. Monit.* **2015**, *21*, 1097–1106.
43. Richard, K.; Piepenbrink, K.H.; Shirey, K.A.; Gopalakrishnan, A.; Nallar, S.; Prantner, D.J.; Perkins, D.J.; Lai, W.; Vlk, A.; Toshchakov, V.Y.; et al. A mouse model of human TLR4 D299G/T399I SNPs reveals mechanisms of altered LPS and pathogen responses. *J. Exp. Med.* **2021**, *218*, e20200675. [CrossRef]
44. Bösl, K.; Giambelluca, M.; Haug, M.; Bugge, M.; Espevik, T.; Kandasamy, R.K.; Bergstrøm, B. Coactivation of TLR2 and TLR8 in Primary Human Monocytes Triggers a Distinct Inflammatory Signaling Response. *Front. Physiol.* **2018**, *9*, 1–13. [CrossRef]
45. Stewart, C.R.; Stuart, L.M.; Wilkinson, K.; van Gils, J.M.; Deng, J.; Halle, A.; Rayner, K.J.; Boyer, L.; Zhong, R.; Frazier, W.A.; et al. CD36 ligands promote sterile inflammation through assembly of a Toll-like receptor 4 and 6 heterodimer. *Nat. Immunol.* **2010**, *11*, 155–161. [CrossRef] [PubMed]
46. Perkins, D.J.; Richard, K.; Hansen, A.M.; Lai, W.; Nallar, S.; Koller, B.; Vogel, S.N. Autocrine–paracrine prostaglandin E 2 signaling restricts TLR4 internalization and TRIF signaling. *Nat. Immunol.* **2018**, *19*, 1309–1318. [CrossRef]
47. World Health Organization. *WHO | WHO End TB Strategy*; World Health Organization: Geneva, Switzerland, 2015.
48. Moreno-Eutimio, M.A.; López-Macías, C.; Pastelin-Palacios, R. Bioinformatic analysis and identification of single-stranded RNA sequences recognized by TLR7/8 in the SARS-CoV-2, SARS-CoV, and MERS-CoV genomes. *Microbes Infect.* **2020**, *22*, 226–229. [CrossRef]
49. Choudhury, A.; Mukherjee, S. In silico studies on the comparative characterization of the interactions of SARS-CoV-2 spike glycoprotein with ACE-2 receptor homologs and human TLRs. *J. Med. Virol.* **2020**, *92*, 2105–2113. [CrossRef]
50. Brandão, S.C.S.; Ramos, J.d.O.X.; Dompieri, L.T.; Godoi, E.T.A.M.; Figueiredo, J.L.; Sarinho, E.S.C.; Chelvanambi, S.; Aikawa, M. Is Toll-like receptor 4 involved in the severity of COVID-19 pathology in patients with cardiometabolic comorbidities? *Cytokine Growth Factor Rev.* **2020**. [CrossRef]
51. Imai, Y.; Kuba, K.; Neely, G.G.; Yaghubian-Malhami, R.; Perkmann, T.; van Loo, G.; Ermolaeva, M.; Veldhuizen, R.; Leung, Y.H.C.; Wang, H.; et al. Identification of Oxidative Stress and Toll-like Receptor 4 Signaling as a Key Pathway of Acute Lung Injury. *Cell* **2008**, *133*, 235–249. [CrossRef]
52. Oh, D.-Y.; Taube, S.; Hamouda, O.; Kücherer, C.; Poggensee, G.; Jessen, H.; Eckert, J.K.; Neumann, K.; Storek, A.; Pouliot, M.; et al. A functional toll-like receptor 8 variant is associated with HIV disease restriction. *J. Infect. Dis.* **2008**, *198*, 701–709. [CrossRef]
53. Sali, A.; Blundell, T.L. Comparative protein modelling by satisfaction of spatial restraints. *J. Mol. Biol.* **1993**, *234*, 779–815. [CrossRef]
54. Kaplan, W.; Littlejohn, T.G. Swiss-PDB Viewer (Deep View). *Brief. Bioinform.* **2001**, *2*, 195–197. [CrossRef] [PubMed]
55. Schneidman-Duhovny, D.; Inbar, Y.; Nussinov, R.; Wolfson, H.J. PatchDock and SymmDock: Servers for rigid and symmetric docking. *Nucleic Acids Res.* **2005**, *33*, W363–W367. [CrossRef] [PubMed]
56. Mashiach, E.; Schneidman-Duhovny, D.; Andrusier, N.; Nussinov, R.; Wolfson, H.J. FireDock: A web server for fast interaction refinement in molecular docking. *Nucleic Acids Res.* **2008**, *36*, W229–W232. [CrossRef]
57. Kamentsky, L.; Jones, T.R.; Fraser, A.; Bray, M.A.; Logan, D.J.; Madden, K.L.; Ljosa, V.; Rueden, C.; Eliceiri, K.W.; Carpenter, A.E. Improved structure, function and compatibility for cellprofiler: Modular high-throughput image analysis software. *Bioinformatics* **2011**, *27*, 1179–1180. [CrossRef]
58. Wiśniewski, J.R.; Zougman, A.; Nagaraj, N.; Mann, M. Universal sample preparation method for proteome analysis. *Nat. Methods* **2009**, *6*, 359–362. [CrossRef]

59. Cox, J.; Mann, M. MaxQuant enables high peptide identification rates, individualized p.p.b.-range mass accuracies and proteome-wide protein quantification. *Nat. Biotechnol.* **2008**, *26*, 1367–1372. [CrossRef]
60. Tyanova, S.; Temu, T.; Sinitcyn, P.; Carlson, A.; Hein, M.Y.; Geiger, T.; Mann, M.; Cox, J. The Perseus computational platform for comprehensive analysis of (prote)omics data. *Nat. Methods* **2016**, *13*, 731. [CrossRef] [PubMed]

11. Publikation 3: Thada et al. (2020)

Thada S, Burkert S, Sivangala R, Hussain A, Sur S, Dittrich N, Conrad ML, Slevogt H, Latha Gaddam S, Schumann RR. A SNP upstream of the cyclic GMP-AMP synthase (cGAS) gene protects from relapse and extra-pulmonary TB and relates to BCG vaccination status in an Indian cohort. *Genes Immun*. 2020;21(1):13-26. https://doi.org/10.1038/s41435-019-0080-1

Thada S, Burkert S, Sivangala R, Hussain A, Sur S, Dittrich N, Conrad ML, Slevogt H, Latha Gaddam S, Schumann RR. A SNP upstream of the cyclic GMP-AMP synthase (cGAS) gene protects from relapse and extra-pulmonary TB and relates to BCG vaccination status in an Indian cohort. *Genes Immun*. 2020;21(1):13-26. https://doi.org/10.1038/s41435-019-0080-1

Thada S, Burkert S, Sivangala R, Hussain A, Sur S, Dittrich N, Conrad ML, Slevogt H, Latha Gaddam S, Schumann RR. A SNP upstream of the cyclic GMP-AMP synthase (cGAS) gene protects from relapse and extra-pulmonary TB and relates to BCG vaccination status in an Indian cohort. *Genes Immun*. 2020;21(1):13-26. https://doi.org/10.1038/s41435-019-0080-1

Thada S, Burkert S, Sivangala R, Hussain A, Sur S, Dittrich N, Conrad ML, Slevogt H, Latha Gaddam S, Schumann RR. A SNP upstream of the cyclic GMP-AMP synthase (cGAS) gene protects from relapse and extra-pulmonary TB and relates to BCG vaccination status in an Indian cohort. *Genes Immun*. 2020;21(1):13-26. https://doi.org/10.1038/s41435-019-0080-1

Thada S, Burkert S, Sivangala R, Hussain A, Sur S, Dittrich N, Conrad ML, Slevogt H, Latha Gaddam S, Schumann RR. A SNP upstream of the cyclic GMP-AMP synthase (cGAS) gene protects from relapse and extra-pulmonary TB and relates to BCG vaccination status in an Indian cohort. *Genes Immun*. 2020;21(1):13-26. https://doi.org/10.1038/s41435-019-0080-1

Thada S, Burkert S, Sivangala R, Hussain A, Sur S, Dittrich N, Conrad ML, Slevogt H, Latha Gaddam S, Schumann RR. A SNP upstream of the cyclic GMP-AMP synthase (cGAS) gene protects from relapse and extra-pulmonary TB and relates to BCG vaccination status in an Indian cohort. *Genes Immun*. 2020;21(1):13-26. https://doi.org/10.1038/s41435-019-0080-1

Thada S, Burkert S, Sivangala R, Hussain A, Sur S, Dittrich N, Conrad ML, Slevogt H, Latha Gaddam S, Schumann RR. A SNP upstream of the cyclic GMP-AMP synthase (cGAS) gene protects from relapse and extra-pulmonary TB and relates to BCG vaccination status in an Indian cohort. *Genes Immun*. 2020;21(1):13-26. https://doi.org/10.1038/s41435-019-0080-1

Thada S, Burkert S, Sivangala R, Hussain A, Sur S, Dittrich N, Conrad ML, Slevogt H, Latha Gaddam S, Schumann RR. A SNP upstream of the cyclic GMP-AMP synthase (cGAS) gene protects from relapse and extra-pulmonary TB and relates to BCG vaccination status in an Indian cohort. *Genes Immun*. 2020;21(1):13-26. https://doi.org/10.1038/s41435-019-0080-1

Thada S, Burkert S, Sivangala R, Hussain A, Sur S, Dittrich N, Conrad ML, Slevogt H, Latha Gaddam S, Schumann RR. A SNP upstream of the cyclic GMP-AMP synthase (cGAS) gene protects from relapse and extra-pulmonary TB and relates to BCG vaccination status in an Indian cohort. *Genes Immun*. 2020;21(1):13-26. https://doi.org/10.1038/s41435-019-0080-1

Thada S, Burkert S, Sivangala R, Hussain A, Sur S, Dittrich N, Conrad ML, Slevogt H, Latha Gaddam S, Schumann RR. A SNP upstream of the cyclic GMP-AMP synthase (cGAS) gene protects from relapse and extra-pulmonary TB and relates to BCG vaccination status in an Indian cohort. *Genes Immun*. 2020;21(1):13-26. https://doi.org/10.1038/s41435-019-0080-1

Thada S, Burkert S, Sivangala R, Hussain A, Sur S, Dittrich N, Conrad ML, Slevogt H, Latha Gaddam S, Schumann RR. A SNP upstream of the cyclic GMP-AMP synthase (cGAS) gene protects from relapse and extra-pulmonary TB and relates to BCG vaccination status in an Indian cohort. *Genes Immun*. 2020;21(1):13-26. https://doi.org/10.1038/s41435-019-0080-1

Thada S, Burkert S, Sivangala R, Hussain A, Sur S, Dittrich N, Conrad ML, Slevogt H, Latha Gaddam S, Schumann RR. A SNP upstream of the cyclic GMP-AMP synthase (cGAS) gene protects from relapse and extra-pulmonary TB and relates to BCG vaccination status in an Indian cohort. *Genes Immun*. 2020;21(1):13-26. https://doi.org/10.1038/s41435-019-0080-1

Thada S, Burkert S, Sivangala R, Hussain A, Sur S, Dittrich N, Conrad ML, Slevogt H, Latha Gaddam S, Schumann RR. A SNP upstream of the cyclic GMP-AMP synthase (cGAS) gene protects from relapse and extra-pulmonary TB and relates to BCG vaccination status in an Indian cohort. *Genes Immun*. 2020;21(1):13-26. https://doi.org/10.1038/s41435-019-0080-1

Thada S, Burkert S, Sivangala R, Hussain A, Sur S, Dittrich N, Conrad ML, Slevogt H, Latha Gaddam S, Schumann RR. A SNP upstream of the cyclic GMP-AMP synthase (cGAS) gene protects from relapse and extra-pulmonary TB and relates to BCG vaccination status in an Indian cohort. *Genes Immun*. 2020;21(1):13-26. https://doi.org/10.1038/s41435-019-0080-1

12. Publikation 4: Dittrich et al. (2015)

Dittrich N, Berrocal-Almanza LC, Thada S, Goyal S, Slevogt H, Sumanlatha G, Hussain A, Sur S, Burkert S, Oh D-Y, Valluri V, Schumann RR, Conrad ML. Toll-like receptor 1 variations influence susceptibility and immune response to Mycobacterium tuberculosis. *Tuberculosis (Edinb)*. 2015;95(3):328-335. https://doi.org/10.1016/j.tube.2015.02.045.

Dittrich N, Berrocal-Almanza LC, Thada S, Goyal S, Slevogt H, Sumanlatha G, Hussain A, Sur S, Burkert S, Oh D-Y, Valluri V, Schumann RR, Conrad ML. Toll-like receptor 1 variations influence susceptibility and immune response to Mycobacterium tuberculosis. *Tuberculosis (Edinb)*. 2015;95(3):328-335. https://doi.org/0.1016/j.tube.2015.02.045.

Dittrich N, Berrocal-Almanza LC, Thada S, Goyal S, Slevogt H, Sumanlatha G, Hussain A, Sur S, Burkert S, Oh D-Y, Valluri V, Schumann RR, Conrad ML. Toll-like receptor 1 variations influence susceptibility and immune response to Mycobacterium tuberculosis. *Tuberculosis (Edinb)*. 2015;95(3):328-335. https://doi.org/0.1016/j.tube.2015.02.045.

Dittrich N, Berrocal-Almanza LC, Thada S, Goyal S, Slevogt H, Sumanlatha G, Hussain A, Sur S, Burkert S, Oh D-Y, Valluri V, Schumann RR, Conrad ML. Toll-like receptor 1 variations influence susceptibility and immune response to Mycobacterium tuberculosis. *Tuberculosis (Edinb)*. 2015;95(3):328-335. https://doi.org/0.1016/j.tube.2015.02.045.

Dittrich N, Berrocal-Almanza LC, Thada S, Goyal S, Slevogt H, Sumanlatha G, Hussain A, Sur S, Burkert S, Oh D-Y, Valluri V, Schumann RR, Conrad ML. Toll-like receptor 1 variations influence susceptibility and immune response to Mycobacterium tuberculosis. *Tuberculosis (Edinb)*. 2015;95(3):328-335. https://doi.org/0.1016/j.tube.2015.02.045.

Dittrich N, Berrocal-Almanza LC, Thada S, Goyal S, Slevogt H, Sumanlatha G, Hussain A, Sur S, Burkert S, Oh D-Y, Valluri V, Schumann RR, Conrad ML. Toll-like receptor 1 variations influence susceptibility and immune response to Mycobacterium tuberculosis. *Tuberculosis (Edinb)*. 2015;95(3):328-335. https://doi.org/0.1016/j.tube.2015.02.045.

Dittrich N, Berrocal-Almanza LC, Thada S, Goyal S, Slevogt H, Sumanlatha G, Hussain A, Sur S, Burkert S, Oh D-Y, Valluri V, Schumann RR, Conrad ML. Toll-like receptor 1 variations influence susceptibility and immune response to Mycobacterium tuberculosis. *Tuberculosis (Edinb)*. 2015;95(3):328-335. https://doi.org/0.1016/j.tube.2015.02.045.

Dittrich N, Berrocal-Almanza LC, Thada S, Goyal S, Slevogt H, Sumanlatha G, Hussain A, Sur S, Burkert S, Oh D-Y, Valluri V, Schumann RR, Conrad ML. Toll-like receptor 1 variations influence susceptibility and immune response to Mycobacterium tuberculosis. *Tuberculosis (Edinb)*. 2015;95(3):328-335. https://doi.org/0.1016/j.tube.2015.02.045.

13. Lebenslauf

"Mein Lebenslauf wird aus datenschutzrechtlichen Gründen in der elektronischen Version meiner Arbeit nicht veröffentlicht."

14. Vollständige Publikationsliste

1. Peters L, **Burkert S**, Dinse-Lambracht A, Peifer J, Grüner B. COVID-19: Ambulante oder stationäre Betreuung? – Risikoscore zur prospektiven Differenzierung leichter und schwerer Verläufe. *Der Notarzt*. 2021 Apr 09. doi: 10.1055/a-1438-2019
Impact Factor: 0,43

2. Thada S, Horvath GL, Müller MM, Dittrich N, Conrad ML, Sur S, Hussain A, Pelka K, Gaddam SL, Latz E, Slevogt H, Schumann RR*, **Burkert S***. Interaction of TLR4 and TLR8 in the Innate Immune Response against Mycobacterium Tuberculosis. *Int J Mol Sci*. 2021;22(4):1560. doi: 10.3390/ijms22041560 *equal contribution
Impact factor: 4,556

3. Peters L*, **Burkert S***, Grüner B. Parasites of the Liver -epidemiology, diagnosis and clinical management in the European context. *J Hepatol*. 2021 Feb 23:S0168-8278(21)00115-X. doi: 10.1016/j.jhep.2021.02.015. Epub ahead of print. *equal contribution
Impact factor: 14,679

4. Thada S, **Burkert S**, Sivangala R, Hussain A, Sur S, Dittrich N, Conrad ML, Slevogt H, Latha Gaddam S, Schumann RR. A SNP upstream of the cyclic GMP-AMP synthase (cGAS) gene protects from relapse and extra-pulmonary TB and relates to BCG vaccination status in an Indian cohort. *Genes Immun*. 2020;21(1):13-26. doi: 10.1038/s41435-019-0080-1
Impact factor: 2,339

5. **Burkert S**, Schumann RR. RNA Sensing of Mycobacterium tuberculosis and Its Impact on TB Vaccination Strategies. *Vaccines*. 2020;8(1):67. doi: 10.3390/vaccines8010067.
Impact factor: 4,760

6. Ugolini M*, Gerhard J*, **Burkert S***, Jensen KJ, Georg P, Ebner F, Volkers SM, Thada S, Dietert K, Bauer L, Schäfer A, Helbig ET, Opitz B, Kurth F, Sur S, Dittrich N, Gaddam S, Conrad ML, Benn CS, Blohm U, Gruber AD, Hutloff A, Hartmann S, Boekschoten M V., Müller M, Jungersen G, Schumann RR, Suttorp N, Sander LE. Recognition of microbial viability via TLR8 drives TFH cell differentiation and vaccine responses. *Nat Immunol*. 2018;19(4):386-396. doi: 10.1038/s41590-018-0068-4. * equal contribution
Impact factor: 20,479

7. Dittrich N, Berrocal-Almanza LC, Thada S, Goyal S, Slevogt H, Sumanlatha G, Hussain A, Sur S, **Burkert S**, Oh D-Y, Valluri V, Schumann RR, Conrad ML. Toll-like receptor 1 variations influence susceptibility and immune response to Mycobacterium tuberculosis. *Tuberculosis (Edinb)*. 2015;95(3):328-335. doi: 0.1016/j.tube.2015.02.045.
Impact factor: 2,576

15. Danksagung

Allen voran möchte ich mich für die langjährige Unterstützung bei meinem Doktorvater Prof. Ralf Schumann bedanken.

Des Weiteren möchte ich mich für die gute und konstruktive Zusammenarbeit innerhalb des Graduiertenkollegs mit Shruthi Thada, Nickel Dittrich, Luis Berrocal-Almanza, Surbhi Goyal, Melanie Conrad und Prof. Slevogt bedanken, sowie bei den medizinisch-technischen Assistenten Fränzi, Diana und Inga. Für die Unterstützung in Hyderabad möchte ich Dr. Gaddam Suman Latha danken. Prof. Leif Sander, Matteo Ugolini und Jenny Steele gilt Dank für die gelungene Kooperation und gemeinsame Publikation.

Persönlich möchte ich mich bei meiner Familie und meinen Freunden für die mentale Unterstützung, ohne welche der Abschluss dieser Arbeit wohl nicht möglich gewesen wäre, bedanken.